SANDIA REPORT
SAND2026-18395
Printed March 2026

Sandia National Laboratories

Improbability of Post-Closure Criticality in Compacted Criticality Control Overpacks after Room Closure at Waste Isolation Pilot Plant

Rob P. Rechard, Brad A. Day,
Benjamin Reedlunn, James E. Bean, Jr.

Prepared by
Sandia National Laboratories
Albuquerque, New Mexico
87185 and Livermore,
California 94550

Issued by Sandia National Laboratories, operated for the United States Department of Energy by National Technology & Engineering Solutions of Sandia, LLC.

NOTICE: This report was prepared as an account of work sponsored by an agency of the United States Government. Neither the United States Government, nor any agency thereof, nor any of their employees, nor any of their contractors, subcontractors, or their employees, make any warranty, express or implied, or assume any legal liability or responsibility for the accuracy, completeness, or usefulness of any information, apparatus, product, or process disclosed, or represent that its use would not infringe privately owned rights. Reference herein to any specific commercial product, process, or service by trade name, trademark, manufacturer, or otherwise, does not necessarily constitute or imply its endorsement, recommendation, or favoring by the United States Government, any agency thereof, or any of their contractors or subcontractors. The views and opinions expressed herein do not necessarily state or reflect those of the United States Government, any agency thereof, or any of their contractors.

Printed in the United States of America. This report has been reproduced directly from the best available copy.

Available to DOE and DOE contractors from

U.S. Department of Energy
Office of Scientific and Technical Information
P.O. Box 62
Oak Ridge, TN 37831

Telephone: (865) 576-8401
Facsimile: (865) 576-5728
E-Mail: reports@osti.gov
Online ordering: http://www.osti.gov/scitech

Available to the public from

U.S. Department of Commerce
National Technical Information Service
5301 Shawnee Rd
Alexandria, VA 22312

Telephone: (800) 553-6847
Facsimile: (703) 605-6900
E-Mail: orders@ntis.gov
Online order: https://classic.ntis.gov/help/order-methods/


DEPARTMENT OF ENERGY
UNITED STATES OF AMERICA
NNSA
National Nuclear Security Administration

Improbability of Post-Closure Criticality in Compacted Criticality Control Overpacks after Room Closure at Waste Isolation Pilot Plant

Rob P. Rechard
Applied Systems Analysis and Research Department 8844
Sandia National Laboratories,
Albuquerque, New Mexico 87185-0747

Brad A. Day
Piru Associates, Inc.
Carlsbad, New Mexico

Benjamin Reedlunn
Materials and Failure Modeling Department 1558
Sandia National Laboratories
Albuquerque, New Mexico 87185-0840

James E. Bean, Jr.
Solid Mechanics Department 1554
Sandia National Laboratories
Albuquerque, New Mexico 87185-0840

ABSTRACT

As part of its periodic re-certification of the Waste Isolation Pilot Plant (WIPP), an operating repository in bedded salt for the disposal of transuranic (TRU) waste from atomic energy defense activities, the United States Environmental Protection Agency expects a re-evaluation of features, events, and processes, such as post-closure nuclear criticality. Although salt creep beneficially encapsulates the TRU waste in the closed WIPP repository, the spacing between an array of waste packages is disrupted as the salt creep closes disposal rooms and containers lose structural integrity. For most TRU waste, the possibility of post-closure criticality is exceedingly small either because the salt neutronically isolates TRU waste canisters or because closure of a disposal room from salt creep does not sufficiently compact the low mass of fissile material. The criticality evaluation was updated, however, because of the introduction of criticality control overpack (CCO) containers, which may dispose up to 380 fissile gram equivalent plutonium-239 in each container. The criticality potential is evaluated through high-fidelity geomechanical modeling of a disposal room filled with CCO containers during two representative conditions: (1) large salt block fall, and (2) gradual disposal room closure from salt creep. Geomechanical models of roof fall demonstrate three tiers of CCO containers are not greatly disrupted. Geomechanical models of gradual room closure from salt creep (without brine seepage and subsequent gas generation to permit maximum room closure) were used to predict irregular arrays of closely packed CCOs after 1000 years, when room closure has asymptotically approached maximum compaction. Models of spheres or cylinders with 380 fissile gram equivalent of plutonium (as oxide) at the predicted irregular compacted spacing demonstrate that an array of CCO containers is not critical when surrounded by salt and magnesium oxide, provided the mass of hydrogenous material shipped in CCO containers (usually plastics) is controlled or boron carbide (a neutron poison) is mixed with the fissile contents.

Keywords: post-closure criticality evaluation; features, events, and processes screening; transuranic radioactive waste disposal; safety assessment; performance assessment; Waste Isolation Pilot Plant

FOREWARD

The nuclear criticality calculations referenced within this document were originally published by Oak Ridge National Laboratory (ORNL) to meet the requirements of the US Environmental Protection Agency's (EPA) implementing regulation, 40 CFR §194.32(e)(3). The ORNL calculations are relied on to justify the exclusion of nuclear criticality impacting the Waste Isolation Pilot Plant (WIPP) disposal system during the post-closure regulatory timeframe. This justification is performed in accordance with EPA "reasonable expectation" standard of proof given in 40 CFR §191.13(b) for the post-closure timeframe. This report is being issued outside of Sandia National Laboratories' Nuclear Criticality Safety Program that is governed under 10 CFR 830 and US Department of Energy (DOE) Order 420.1C, Chg. 3 without receiving that program's concurrence or dissension of the conclusions within.

PREFACE

EPA has regulatory authority for certifying the performance of WIPP in isolating radionuclides over the next 10 000 years against its long-term environmental standard specified in 40 CFR 191. DOE is not self-regulating when evaluating WIPP performance after closure. DOE has assigned Sandia National Laboratories (Sandia) as responsible for evaluating WIPP post-closure performance for EPA certification. Part of the performance assessment includes a formal analysis of all features, events, and processes (FEPs) that may impact WIPP isolation.

EPA does not designate the post-closure criticality FEP for special consideration in 40 CFR 191. Rather, criticality is considered like all other FEPs. The EPA Standard, 40 CFR 191, is probabilistic and Sandia has developed a probabilistic rationale that criticality is improbable in the post-closure timeframe when humans are absent, using EPA exclusion criteria specified in its implementing regulation, 40 CFR 194, at §194.32(e)(3). Also in 40 CFR 194, EPA requires compliance evaluations for WIPP about every 5 years. Thus, the screening rationale for omitting the post-closure criticality FEP is periodically documented in certification applications to EPA, along with the compliance evaluation. The first application to EPA was in 1996. The most recent Compliance Recertification Application was in 2019. This report supports the 2026 Compliance Recertification Application.

We refer to the analysis underlying the rationale as a post-closure criticality evaluation. Estimates of mean criticality behavior are used for this post-closure criticality evaluation, not worst-case behavior, in keeping with the concept of reasonable expectation invoked by EPA as the standard of proof for demonstrating compliance with 40 CFR 191. We use the term nuclear criticality safety analysis when referring to analysis performed to show criticality is incredible when humans are present during operations or transporting transuranic waste to WIPP. Furthermore, we avoid referring to the criticality screening as a credibility argument because the term connotes a rule-based approach that estimates worst-case behavior and uses great care in conservatively defining an upper subcriticality limit.

The criticality control overpack (CCO) evaluated here was designed by the WIPP management and operating (M&O) contractor for the US Department of Energy (DOE). The M&O is responsible for the nuclear criticality safety analysis in the Safety Analysis Report to the US Nuclear Regulatory Commission (NRC) that has shown criticality is incredible in CCOs under normal and accident conditions. NRC has certified use of CCOs in TRUPACT-II packages for transporting transuranic waste to WIPP. Furthermore, the M&O has shown criticality in CCOs is incredible during normal and accident conditions at the WIPP facility prior to closure in the Design Safety Analysis report to DOE.

This report supersedes report SAND2022-0952, *Improbability of Nuclear Criticality in Compacted Criticality Control Overpacks after Room Closure by Salt Creep at Waste Isolation Pilot Plant*. No additional criticality calculations or CCO compaction simulations were conducted; rather, the update ensures applicability to the 2026 Compliance Recertification Application and coordinates with companion reports.

ACKNOWLEDGEMENTS

The authors thank Sandi Larson of 21Consulting Group for providing an overall technical/programmatic review of the criticality approach in SAND2022-0952, which is repeated herein. Sandi Larson is the nuclear criticality safety engineer for SIMCO (M&O for DOE Carlsbad Field Office overseeing WIPP). Mariah Garcia of Sandia conducted the internal technical review. Paul E. Shoemaker, retired Sandian, and Ronald Livingston, Omega Technical Services, provided guidance and review as this work progressed. G. Ross Kirkes, Piru Associates, provided insight on screening the post-closure criticality scenario. Bret Brickner and his team from Oak Ridge National Laboratory, conducted the criticality calculations from which the figures here and in SAND2022-0952 were created. Their work is documented in B.D. Brickner, R. Cumberland, R. Reed. 2022. *Post-closure nuclear criticality safety evaluations for disposition of criticality control overpacks at the Waste Isolation Pilot Plant,* ORNL/TM-2021/2046. The criticality evaluation uses geomechanical simulations to determine spacing for the criticality calculations. Sandia provided the simulations, which is documented in several reports between 2018 and 2024; the most complete report is B. Reedlunn, J.E. Bean, Jr., J. Wilkes, J. Bignell. 2023. *Simulations of criticality control overpack container compaction at the Waste Isolation Pilot Plant*, SAND2023-10477.

CONTENTS

I. Introduction 11
I.A. Criticality Control Overpack 11
I.B. Approach for Screening Post-Closure Criticality in CCOs 12
II. Screening Criticality Scenario 12
II.A. Low Probability Criteria for Screening 12
II.B. Studies of Post-Closure Criticality Applicable to WIPP 13
III. Modeling of Roof Fall 15
III.A. Conceptual Model of Roof Fall 15
III.B. Roof Fall Results 17
IV. Modeling of Room Closure From Salt Creep 17
IV.A. Conceptual Model of Room Closure 17
IV.A.1. Salt Stratigraphy 17
IV.A.2. CCO Configuration 17
IV.B. Deformed Irregular Array 18
IV.C. Mid-Height and Mid-Width Room Closure Measure 21
IV.C.1. Room Closure at 1000 years 21
IV.C.2. Room Closure in Previous CCO and POC Simulations 21
IV.C.3. Closure of Room Filled with Mix of CCOs and other Containers 23
IV.D. CCO Concentration Measure 23
IV.D.1. Concentration of CCOs at 1000 years 23
IV.D.2. Relative Weighted Concentration 24
IV.D.3. Concentration at 1000 years for Containers with Different Strengths 25
IV.E. Consistency of Room Closure and CCO Concentration 26
V. Criticality Evaluation of Compacted Arrays Without Boron Carbide 27
V.A. Computational Tool 27
V.B. Upper Subcriticality Limit in Criticality Modeling 27
V.B.1. Nuclear Criticality Safety in Current Timeframe 27
V.B.2. Approximation of Mean Probability of Criticality after WIPP Closure 28
V.C. CCO Conceptual Model for Criticality Evaluation 28
V.C.1 Plutonium, Waste Form, Volume, and Mass 29
V.C.2. Material Mixed with Pu Waste 29
V.C.3. Material Surrounding Individual CCCs 30
V.C.4. Geometry: Irregular CCO Array Configuration 30
V.C.5. Geometry: Idealized Uniform Array 31
V.C.6. Geometry: Fissile Shape 31
V.D. Room Reactivity with and without Filler Material in Fissile Region 32
V.D.1. Carbon and Cement Filler 32
V.D.3. Mixing of Pu, Moderator, and Filler 34
V.D.4. Influence of Spherical and Cylindrical Fissile Region on Reactivity 34
VI. Influence of other Parameters on Room Reactivity without B_4C 36
VI.A. Room Reactivity with Material in Fissile Region 36
VI.A.1. Water and Polyethylene Moderator 36
VI.A.2. Density and Salt/MgO Proportion 37
VI.A.3. Beryllium Influence 37
VI.B. CCC Stainless Steel around Fissile Region 38
VI.C. Uncertainty from Geologic Strata Arrangement 40
VI.D. Minor Reactivity Differences between Hexagonal and Triangular Arrays 40
VI.E. Reduced Reactivity when Brine Enters Room 41
VI.F. Reactivity Changes as Room Creeps Closed 41
VI.G. Correlation of CCO Concentration with Neutron Flux 41
VII. Criticality Evaluation of Compacted Arrays with Boron Carbide 45
VII.A. CCO Conceptual Model with B_4C 45

VII.B. Results with B_4C 45
VII.C. Comparison with Previous B_4C Analysis....45
VII.C. Longevity of B_4C in Disposal Room....46
VII.C.1 Insolubility of B_4C....46
VII.C.2. B_4C Consumption in Radiation Field....46
VIII. WIPP Waste Acceptance Criteria....46
VIII.A. Conservative Bias in Supplemental WAC Limits for CCOs....46
VIII.B. Supplemental WAC Limits for CCOs....46
VIII.C. Use of Acceptable Knowledge....47
IX. Summary of Low-Probability of Criticality in Compacted CCO....48
IX.A. Roof Fall in Room Filled with CCOs....48
IX.B. Compaction of CCOs from Salt Creep....49
IX.C. Criticality Evaluation of Compacted Arrays without Boron Carbide....49
IX.C.1. Allowable Hydrogenous Moderator with and without Filler in Fissile Region....49
IX.C.2. Other Material in Fissile Region....50
IX.C.3. CCC Stainless Steel Around Fissile Region....50
IX.C.4 Uncertainty from Geologic Strata....50
IX.C.5. Minor Influence of Initial CCO Configuration and Boundary Conditions....50
IX.C.6. Reduced Reactivity from Brine around Fissile Region....50
IX.D. Criticality Evaluation of Compacted Arrays with Boron Carbide....50
IX.E. Uniform Array Analysis Provides Additional Understanding....50
References....53
Distribution....57

FIGURES

1. Criticality control container (CCC), and criticality control overpack (CCO); two convenience handling containers used for conditioned surplus Pu (dimensions in cm).[1;17, Figs. 2-7,2-8&Table 2-1;18,pp. 8,30;19, App. C] 12
2. Conceptual model of large trapezoidal-shaped salt block that detaches at Clay G seam and falls onto CCOs...15
3. Roof fall onto CCOs emplaced in a hexagonal array in lower repository horizon (a) mostly flat roof fall; (b) rotating roof fall. Brown discs represent top and bottom plywood stabilizer for blue stainless steel CCCs inside 55-gallon CCO shell (which is hidden for visualization).[68, Fig. 5] 16
4. Idealized stratigraphy near WIPP disposal rooms in lower and upper horizon. Elevations referenced to Clay G, which is at elevation 386 m, 652 m below surface at 17
5. Hexagonal and triangular model emplacement schemes for CCOs in WIPP disposal room segment.[65, Figs. 4&6] .18
6. Plan and side view of undeformed coordinate positions emplaced as a triangular array in 10.06 m wide, 3.96 m tall, and 2.08 m thick room segment in upper horizon relative to ultra-conservative positions of CCC fissile centers used in 2018 criticality evaluation and more realistic deformed coordinate positions in current analysis.[62, Fig. B-13;74, Fig. 12] 18
7. Salt compaction in room segment with CCOs emplaced in triangular array with most inner CCCs on their side by 200 years; outer CCO shell and bedded salt stratigraphy included in analysis but removed in visualization; brown elements represent plywood stabilizing CCC, which are deleted when splintered and failed.[68, Fig. 9] 19
8. Deformed centerlines of CCCs at 1000 years when initially emplaced as triangular array. 20
9. Horizontal and vertical closure at room mid-height and mid-width, respectively, for CCOs initially emplaced as triangular and hexagonal arrays in upper and lower repository horizons.[19, Fig. 3-4;64;65, Fig. 10;68, Fig. 7] 21
10. CCO compaction in hexagonal array in upper horizon has more column buckling when friction coefficient set at 0.5 for Clay F and Clay G layers.[65, Fig. 21] 22
11. Horizontal and vertical closure of upper and lower horizon rooms filled with CCOs and POCs initially emplaced in triangular and hexagonal arrays with different clay friction coefficients (μ), where room closure in Fig. 10 shown as gray lines.[65, Fig. 18] 22
12. Distribution of simple and relative CCO concentration about each CCC center at initial condition and at 1000 years.[65, Fig. 11] 23
13. Weighting in sphere of influence for uniformly weighted (simple) and point-source (relative-weighted) concentration in one-half of room [65, Fig. 8] 25
14. Change in distribution of container concentration at 1000 years with change in clay friction coefficient (μ), change in CCC stainless-steel strength, and change in POC container; unlabeled curves same as Fig. 12.[65, Fig. 19] 26
15. Although critical asymptote greatly decreases, Pu critical mass in carbon does not change much for porosity between 5% and 80% filled with water or WIPP brines.[14, Fig. 11] 30
16. Critical limits of ^{239}Pu in CCO cement mixture similar to those in carbon/graphite mixture in Salado brine at 20% porosity.[14, Fig. 15;89, Fig. 17b] 30
17. Three material regions of criticality model where dimensions of Region 2 defined by maximum extent of the coordinates for CCO centers, which change somewhat per geomechanical simulation; dimensions shown for CCOs in upper horizon initially as triangular array. 30
18. Room closure of uniform array of CCOs.[65] 31
19. Range of horizontal room closure in modeled irregular and idealized uniformly compacted CCO arrays initially emplaced as triangular and hexagonal arrays in upper and lower repository horizons.[65, Fig. 10] 31
20. Adding 2-kg graphite or cement filler to fissile region moderately reduces reactivity of irregular, non-uniformly compacted CCO array; similar trend observed for more reactive regular, uniformly compacted CCO array (data from criticality calculations described by Brickner et al.[24]). 33
21. Adding 4 kg filler reduces reactivity somewhat more for irregular non-uniformly and regular uniformly compacted CCO arrays (data from Brickner et al.[24]). 33
22. Stainless steel material from handling canisters mixed in fissile region reduces reactivity of uniform array and irregular CCO array (data from Brickner et al.[24]). 34
23. Cylindrical representation most reactive if fissile region constrained by 7.7 cm radius of CCC in both irregular, non-uniformly compacted and regular, uniformly compacted CCO array (data from Brickner et al.[24]). 34
24. Unconstrained spherical fissile region slightly more reactive than cylindrical fissile region for irregular, non-uniformly compacted CCO array (data from Brickner et al.[24]). 35
25. Cylindrical representation of fissile region for 50% and 25% uniformly compacted array remains more reactive than unconstrained sphere (data from Brickner et al.[24]). 35

26. Largest reactivity of irregular, non-uniformly compacted CCO array with cylindrical fissile region changes from smallest radius at low moderation to largest radius at high moderation; behavior is similar for uniformly compacted CCO array but the transition to the largest radius occurs at lower moderation (data from Brickner et al.[24]). 36
27. CCO array with water moderator less reactive than polyethylene moderator for irregular array; uniform array follows a similar trend (data from Brickner et al.[24]). 36
28. Influence of changes in MgO in Region 2 on system reactivity is noticeable but small (data from Brickner et al.[24, App. L] 37
29. Adding 0.585 kg Be/BeO has little influence on reactivity for k_{eff} near unity but does slightly reduce reactivity below and above k_{eff} of unity (data from Brickner et al.[24]). 38
30. Stainless-steel reflector, twice thickness of CCC, slightly changes the reactivity of irregular and uniformly compacted CCO arrays (data from Brickner et al.[24]). 39
31. Reactivity of irregular CCO array in upper horizon greater than in lower horizon of repository when initially emplaced in hexagonal array (data from Brickner et al.[24]). 40
32. Reactivity of irregular compacted array emplaced in hexagonal configuration is similar to irregular compacted array emplaced in triangular configuration (data from Brickner et al.[24]).....40
33. Presence of brine in Region 2 greatly reduces room reactivity filled with CCOs (data from Brickner et al.[24]). .41
34. General monotonic increase of reactivity as room creeps closed in upper repository horizon filled with CCOs that include stainless steel CCC reflector, 100% polyethylene moderator, and no filler or beryllium (data from Brickner et al.[24]). 41
35. Plan and side view of spatial distribution of simple concentration within 75-cm radius sphere at 1000 years for CCOs emplaced in a hexagonal array in lower repository horizon; maximum neutron flux overlays maximum simple concentration. 43
36. Plan and side view of spatial distribution of relative weighted concentration at 1000 years for CCOs emplaced in a hexagonal array in lower repository horizon; maximum neutron flux overlays maximum relative weighted concentration.[65, Fig. 27] 43
37. Plan and side view of spatial distribution of simple concentration at 1000 years for CCOs emplaced in a hexagonal array in upper repository horizon; maximum neutron flux at edge of region with highest simple concentration. 44
38. Plan and side view of the spatial distribution of relative weighted concentration at 1000 years for CCOs emplaced in a hexagonal array in upper repository horizon; maximum neutron flux at edge of region with high relative weighted concentration.[65, Fig. 29] 44
39. Reactivity of irregular array with between 10 g and 50 g B_4C and up to 6 kg moderator (data from Brickner et al. [24]). 45

TABLES

I. Studies of Post-Closure Criticality at WIPP and Related Events....14
II. Allowable Moderator Mass per CCO with Non-Hydrogenous Filler and Metal Mixed in Fissile Region with Subcriticality Limit of Unity 33
III. Supplemental WIPP Waste Acceptance Criteria for CCO[1;20] 47
IV. Rationale that rockfall and salt-creep compaction of CCO containers has low probability of causing criticality at WIPP. 52

ACRONYMS AND INITIALISMS

CCA	Compliance Certification Application
CCC	criticality control container
CCO	criticality control overpack (container)
CFR	Code of Federal Regulations
CRA	Compliance Re-certification Application
DOE	US Department of Energy
EPA	US Environmental Protection Agency
FEP	features, events (natural and anthropogenic phenomena of short duration), and processes (natural phenomena of long duration)
FGE	fissile gram equivalent
HalfPACT	Half Transuranic Package Transporter
LANL	Los Alamos National Laboratory
MCNP	Monte Carlo N-Particle transport code
NRC	US Nuclear Regulatory Commission
ORNL	Oak Ridge National Laboratory
PA	performance assessment; the process of assessing whether a system or component meets a set of performance criteria; for US, the process is a stochastic simulation; the system is a deep geologic repository disposal system; the performance criteria are the long-term measures in the EPA post-closure environmental standard 40 CFR 191
POC	pipe overpack container
RPPCR	replacement panels planned change request (PA analysis)
SCALE	Standardized Computer Analysis for Licensing Evaluation neutron transport code system.
SPD	Surplus Plutonium Disposition
TRU	transuranic (radionuclide waste)
TRUPACT-II	Transuranic Package Transporter Model 2 packaging
US	United States
USL	upper subcriticality limit
WAC	waste acceptance criteria
WIPP	Waste Isolation Pilot Plant (repository in southeastern New Mexico for TRU waste from atomic energy defense activities)

I. INTRODUCTION

To certify the post-closure compliance of a geologic repository for disposing of radioactive waste, the United States (US) Environmental Protection Agency (EPA), who has regulatory authority over post-closure standards, requires estimates of the range of future behavior through models that capture essential features, events, and processes (FEPs) of the disposal system as it evolves after closure. One potential FEP is the possibility of sufficient fissile mass and concentration causing a self-sustained neutron chain reaction (hereafter, succinctly referred to as criticality) when spacing between containers decreases as the salt creep closes disposal rooms and containers lose structural integrity. Concern about criticality in waste disposed at the Waste Isolation Pilot Plant (WIPP), an operating repository in bedded salt for disposal of wastes containing transuranic (TRU) radioisotopes from atomic energy defense activities, is generally negligible because of (1) the low initial concentration and mass of fissile material (mostly plutonium—Pu) in contact-handled containers (e.g., 325 fissile gram equivalent—FGE—^{239}Pu in each bundle of seven standard drums transported to WIPP), (2) the neutronic isolation of remote-handled containers by salt, and (3) the natural tendency of fissile solute to disperse after release from degraded containers.[1-3]

However, the periodic re-evaluation of features, events, and processes described here has included an updated post-closure criticality evaluation[a] because waste destined for WIPP now includes additional contact-handled TRU waste streams from surplus plutonium disposition (SPD). Specifically, the US Department of Energy (DOE) decided to dispose 6 t of surplus non-pit Pu waste as contact-handled TRU at WIPP (in the 2010 SPD Supplemental Environmental Impact Statement and 2016 Record of Decision).[4] The 6-t contact-handled TRU waste was added to the 2019 WIPP Compliance Re-certification Application to EPA (CRA-2019).[5;6] An additional 7.1-t SPD, which could in part be accommodated within 2 replacement panels, is included in the 2023 Replacement Panels Planned Change Request (RPPCR-2023) to EPA.[7] Finally, DOE has decided to dispose an additional 26.9 t SPD at WIPP,[8;9] instead of converting the Pu to mixed-oxide fuel as originally planned in 1997.[10] DOE will propose, in a Supplemental Environmental Impact Statement, to add 7 additional panels to the WIPP disposal area to accommodate the additional waste.

This report in combination with companion reports[11-15] demonstrates that the possibility of criticality is still remote in a geologic setting. Hence, post-closure criticality was omitted from the performance assessments for CRA-2019[5;6] and CRA-2026[b] to EPA.

I.A. Criticality Control Overpack

In anticipation of transporting 6-t of surplus Pu waste to WIPP, DOE asked the WIPP Management and Operations contractor in 2010 to design and license the criticality control overpack (CCO) container, which could transport almost double the amount of fissile mass authorized for the previously used pipe overpack container (POC). About 26 800 POCs have been used to ship 3.2 t of SPD waste (Pu residues and scraps from Rocky Flats Plant) to WIPP in the early 2000s.[11, Fig. 6]

The CCO consists of a standard 55-gallon carbon-steel drum shell that overpacks a criticality control container (CCC), composed of 304L stainless steel (Fig. 1). The CCC, with a flange on the top and bottom, is held in place by top and bottom plywood spacers. Nothing is placed in the space between the CCC and CCO (i.e., no impact absorbing fiberboard, and no polyethylene liner in contrast to the POC).[11,Fig. 5] Various handling canisters may be used inside the CCC to facilitate loading of the TRU waste.

In 2012, the US Nuclear Regulatory Commission (NRC), who has regulatory authority over containers used to ship TRU waste to WIPP, certified the new criticality control overpacks (CCOs). Like POCs, CCOs can maintain fissile separation during a transportation accident. Thus, each CCO in a shipment is authorized to transport 380 ^{239}Pu FGE. Specifically, 2660 FGE ^{239}Pu can be shipped in a 7-pack bundle of CCOs for the HalfPACT Type B package and 5320 FGE ^{239}Pu in two 7-packs bundles of CCOs for the TRUPACT-II Type B package.[16] Hence, CCOs provide a significant cost advantage for shipping waste streams with surplus Pu and improved use of disposal space in comparison to POCs.

[a] We refer to the analysis here as a criticality evaluation to show the improbability for criticality in the post-closure timeframe when humans are absent (i.e., post-closure criticality evaluation). We use the term nuclear criticality safety analysis when we wish to connote a rule-based approach to show criticality is incredible when humans are present during operations, as more fully discussed in §V.B.

[b] The 2026 analysis conducted a PA for an interim state repository with 2 additional panels in the disposal area (12 panels total), designated CRA-26-12P, and conducted a PA for the final state repository with 9 additional panels (19 panels total), designated CRA-26-19P. The evaluation reported here is for post-closure criticality in a disposal room filled with CCOs at their maximum fissile mass and so is unaffected by the total inventory and number of panels, so herein we refer to CRA-2026 inclusively.

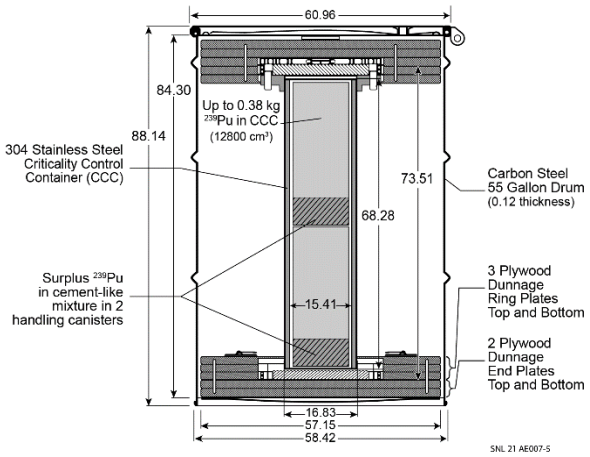

Fig. 1. Criticality control container (CCC), and criticality control overpack (CCO); two convenience handling containers used for conditioned surplus Pu (dimensions in cm).[1;17, Figs. 2-7,2-8&Table 2-1;18,pp. 8,30;19, App. C]

I.B. Approach for Screening Post-Closure Criticality in CCOs

The analysis herein supports the development of supplemental criteria for CCOs in the WIPP Waste Acceptance Criteria (WAC) to complete authorization of CCOs at WIPP. Two types of criticality evaluation are performed to support screening out post-closure criticality in CCOs: (1) criticality evaluation with B_4C mixed with CCO fissile contents, and (2) criticality evaluation without B_4C but with several options for managing moderator mass in CCO contents. The analysis without B_4C examines the potential for criticality in CCOs disposing TRU wastes defined by (1) mass limits on hydrogenous material (primarily water and plastics) and miscellaneous filler material, and (2) general conditions of transport (e.g., 380 FGE ^{239}Pu compacted waste). The materials mixed with the Pu are varied over a wide range, and the findings are translated into constraints for the 2022 WIPP WAC, Revision 11.[20]

A manufactured waste form, such as used when disposing surplus Pu, readily defines the conditions for a criticality evaluation. However, an unspecified, generic waste form is evaluated here to support authorizing use of CCOs for a broader range of contents.

The criticality evaluation follows the methodology used for evaluating the improbability of criticality in POCs for CRA-2019.[11] As with POCs, the concern for criticality with CCOs is not necessarily that the waste inside the pipes is compacted to a critical concentration (since each CCO can only contain 380 FGE) but that the space between CCOs decreases such that neutrons interact as a critical array.

Support for a low-probability rationale in the closed WIPP repository depends upon constraints developed from two types of quantitative modeling: geomechanical phenomenological modeling and neutron/photon transport modeling. For the evaluation, Sandia National Laboratories (Sandia) has conducted geomechanical modeling, using the Sierra/Solid Mechanics finite-element code system,[21] to predict coordinate positions of CCOs after compaction from salt creep closure of the disposal room.[22]

In turn, Oak Ridge National Laboratory (ORNL) has conducted criticality modeling using the SCALE (Standardized Computer Analysis for Licensing Evaluation) neutron transport code system.[23] A sphere or cylinder of fissile material is placed at the final coordinate position of each CCO in the compacted irregular array (or a bounding regular uniformly compacted array) to determine whether the CCO compacted array is sufficient to promote criticality, and, if so, what constraints on moderating hydrogenous material are necessary, including constraints coupled with the presence of filler materials or B_4C neutron poison.[24]

The WIPP Project uses administrative controls for (a) the safe movement of TRU waste within the WIPP facility, (b) positioning of TRU waste containers in the disposal room, (c) placement of the magnesium oxide (MgO) engineered barrier above the waste containers, and (d) recording the emplacement location of TRU containers for auditing and potential retrieval. Conceivably, administrative controls could also be specified for CCO placement in the repository. However, administrative controls on CCO proximity could complicate CCO disposal if a large campaign of CCOs must be stored while waiting for other waste streams to mix within a room. Hence, the geomechanical analysis and subsequent criticality evaluation evaluates the possibility of a room filled entirely with CCOs.

II. SCREENING CRITICALITY SCENARIO

Steps taken to ensure the incredibility of critical event during transport, such as required spacing between fissile material as controlled by TRU waste containers, do not necessarily remain applicable after repository closure when room closure from salt creep compacts and encapsulates containers or confinement of fissile material within the containers is lost due to compaction damage or corrosion degradation.

II.A. Low Probability Criteria for Screening

A post-closure criticality scenario evaluation occurs within the probabilistic regulatory framework for radioactive waste disposal defined by EPA. EPA promulgated radiation protection standards for spent nuclear fuel, high-level waste, and TRU waste disposal under Title 40 Code of Federal Regulations Part 191 (40

CFR 191) in response to the *Nuclear Waste Policy Act of 1982*.[25, §121;26;27 28]

In 40 CFR 191, EPA defines the process of assessing whether the WIPP radioactive waste disposal system meets its regulatory performance criteria as a performance assessment (PA).[26, §191.12 (q)] The PA answers three basic questions:[29] What FEPs and scenarios formed from these FEPs may occur in the disposal system? What is the probability of each FEP or scenario? What are the consequences in terms of the performance criteria of each FEP or scenario?[c]

In 40 CFR 191 and the WIPP implementing regulation, 40 CFR 194, EPA set the guiding philosophy for FEP selection and provides three criteria for excluding FEPs and scenarios, such as criticality, from the PA:[30,§194.32] (1) regulatory fiat; (2) low consequence; and (3) low probability of occurring. Regarding the latter probability criterion, EPA states "…performance assessments need not consider categories of events or processes that are estimated to have less than one chance in 10,000 of occurring over 10,000 years." Yet, direct estimation of a numerical probability is not required; EPA also accepts reasoned qualitative discussion that argues against the likelihood of a FEP.

The approach here develops a qualitative low-probability rationale to exclude criticality in the closed, underground facility based on arguments that compaction cannot sufficiently concentrate ^{239}Pu.[d]

II.B. Studies of Post-Closure Criticality Applicable to WIPP

Like other nuclear facilities, the possibility of criticality has been considered since inception of WIPP. In the preparation for the first environmental impact statement (EIS) of the WIPP facility, FEPs were identified in 1976 that had not been eliminated through WIPP site selection (Table I).[28] The list included post-closure criticality,[33;34] but it was dismissed in supporting documentation and not included in the 1979 draft and 1980 final EIS.[35] When the option to place high-level waste and spent nuclear fuel at WIPP was blocked by Congress in 1979,[36] concern for criticality greatly diminished because of the low initial concentrations in typical TRU waste. Nevertheless, FEP screening efforts retained criticality for more thorough investigation in 1989, 1992, and 1996.[37-39]

The criticality scenario was evaluated and omitted for the compliance certification application to EPA in 1996 (CCA-1996).[2;40] The emphasis was on geochemical deposition outside disposal region but compaction of standard drums inside the disposal region was considered (Table I).

Since authorization in 1979,[36] the WIPP mission has been to dispose of TRU waste produced from the nation's atomic energy defense activities. Traditionally, the majority of TRU waste has consisted of waste streams with debris contaminated with TRU radionuclides (usually Pu), including organics (e.g., cellulose material—such as paper, cardboard, laboratory tissues, wood, cloth—rubber, and plastics), and inorganics (e.g., iron and aluminum alloys, equipment, glass, firebrick, ceramics, cement, and soils). However, surplus Pu waste streams have been added.

To elaborate, DOE declared ~50 t of Pu as surplus to defense needs in various stages of manufacturing at several sites within the DOE Complex in response to 1991 Strategic Arms Reduction Treaty (START I) with Russia. In a 1996 Programmatic EIS, DOE identified disposal options for the ~50 t (identified as 51.4 t below). Although DOE preferred to directly dispose this excess Pu, the US relented and decided in the 1997 Record of Decision to convert ~33 t non-pit metal Pu into mixed oxide (MOX) fuel for use in several US commercial nuclear reactors (eventually identified as ~34 t in 2003) to be consistent with plans in Russia.[10] The other ~17.4 t to be dispositioned included (a) 3.2 t Pu residues and scraps already disposed in POCs as contact-handled at WIPP, (b) 1.1 t of miscellaneous Pu to dispose at WIPP, (c) 7.1 t of Pu from weapon pits, and (d) 6.0 t non-pit Pu unsuitable for producing MOX fuel. Disposition of the MOX spent fuel, 7.1-t pit Pu, and 6.0-t non-pit Pu were included in the 2008 license application for the proposed Yucca Mountain repository.[41]

In 2007, DOE began construction of a mixed oxide Fuel Fabrication Facility for processing 34 t at Savannah River Site, but it encountered substantial schedule delays and cost overruns.[42, p.4] Furthermore, the Yucca Mountain repository was suspended in 2010. In 2014, DOE re-assessed disposition options and proposed to dilute the 34 t of surplus Pu, and dispose it at WIPP in CCOs,[43] using the process already being evaluated for disposal of the non-pit 6.0 t.[44;45] However, stakeholders challenged the logical viability and noted that rough estimates showed a potential for post-closure criticality.[46, p.11]

[c] Within the WIPP Project, a scenario is a set of FEPs that outlines a possible future condition for the WIPP disposal system but does not include the timing or order of events and processes. Once a mathematical model of the disposal system is developed, timing and order of events and processes is introduced.

[d] EPA does not designate post-closure criticality FEP for special consideration in 40 CFR 191. In the later 2008 site-specific standard for the proposed Yucca Mountain repository (40 CFR 197),[31;32] EPA again did not set criticality apart even though EPA had the opportunity to do so when EPA used criticality as a FEP screening example in the preamble.

Table I. Studies of Post-Closure Criticality at WIPP and Related Events

Date	Study	Description
1973	Operational Safety Analysis at Hanford	Hanford evaluates and dismisses the potential for criticality in radioactive waste disposed in trenches on Hanford Reservation.[47]
1979/ 1980	WIPP EIS	Post-closure criticality scenario listed in documents supporting WIPP EIS; emphasis on mobilization in disposal room and deposition elsewhere;[33;34] geochemical constraints on accumulating fissile material used to dismiss criticality.[35]
1980	Operational Design Safety Analysis at WIPP	First design safety analysis for operations dismisses potential for criticality event in array of contact-handled TRU standard drums on surface and in disposal room;[48;49] updates to the operational nuclear criticality safety analysis occur periodically.[17]
1983	Nuclear explosion in waste trenches dismissed	Los Alamos National Laboratory (LANL) dismisses speculation that explosion in waste trenches in the Russia Ural Mountains was nuclear.[50]
1989	FEP construction for 1989 WIPP PA	Criticality scenario listed when identifying universe of FEPs and scenarios for the first WIPP PA.[37]
1992	FEP construction for 1995 preliminary CCA	Criticality scenario listed and retained for more thorough investigation for 1992 WIPP PA and 1995 preliminary CCA.[38]
1995	Autocatalytic critical event in fractures at Yucca Mt. speculated	News articles draw attention to Bowman and Venneri (of LANL) speculation that autocatalytic critical event possible in ^{239}Pu deposited in fractured tuff below proposed repository for commercial spent nuclear fuel at Yucca Mountain.[51;52]
1996	Conditions for autocatalytic assembly dismissed	Numerous articles argue geochemical constraints on deposition prevent assembling sufficient ^{239}Pu in condition necessary for autocatalytic behavior in tuff fractures (and, by analogy, fractures in WIPP disposal system, particularly Culebra).[53-57]
1996	FEP construction and screening for CCA-1996 submission	Criticality scenario dismissed in CCA-1996;[58, App. SCR] qualitative reasoning emphases lack of geochemical processes capable of causing deposition of sufficient quantities of fissile material in WIPP disposal system; room porosity evaluation shows maximum fissile density inside drum far below asymptotic critical concentration for water.[2] Low heat, low fission, and low damage consequences are also reported.[40;59]
2005	Supplemental analysis for CRA-2004	Sandia conducts supplemental evaluation of compaction of other containers, such as POCs, on room porosity for 1st Compliance Recertification Application (CRA-2004).[60]
2015	Stakeholder challenges criticality screening of surplus Pu disposal	Stakeholder scoping analysis shows a uniform array of 21 CCOs compacted 30% with MgO reflector has potential for criticality;[42;61] analysis demonstrates an update to post-closure criticality scenario screening is needed that includes CCO compaction.
2017-2018	Efficacy of B_4C in preventing criticality in CCO demonstrated	ORNL concludes criticality is unlikely for unrealistic, extremely uniformly compacted array of CCOs with fissile material touching when hydrogenous material limited and 50-g boron carbide (B_4C) added to dilute-and-dispose waste form of the Surplus Plutonium Disposition Program.[62]
2018-2019	Geomechanical studies of empty and CCO-filled rooms	With advances in computational geomechanics of salt creep,[63] Sandia improves modeling of disposal room closure when empty[64] and when filled with CCOs emplaced as hexagonal array in ~2-m room segment.[19;65, Table 1]
2019	4th Compliance Re-certification Application (CRA-2019)[6] includes demonstration compacted POCs not critical	Sandia updates post-closure criticality screening for CRA-2019 that includes 6-t surplus Pu (as contact-handled TRU waste).[12] Sandia models compaction of 6-inch and 12-inch POCs emplaced as a hexagonal array after roof fall and while gradually closing from salt creep.[22] ORNL places 0.2-kg ^{239}Pu spheres at centroids of deformed POC array in three different hydrologic regimes to show compacted assembly not critical.[11;66]
2020	Efficacy of B_4C in CCOs updated	ORNL updates criticality evaluation for unrealistic, extremely compacted uniform array of CCOs and shows limits on hydrogenous material unnecessary if 50-g B_4C included.[67]
2021-2022	Criticality FEP updated and WAC revised to include options on constraining hydrogenous material in addition to including B_4C	Sandia expands CCO disposal options for the 2022 WAC revision, in addition to the B_4C option. The geomechanical analysis determines realistic CCO configuration after CCO compacted from salt creep when initially emplaced as hexagonal and triangular arrays.[65;68] In the criticality evaluation, ORNL places 0.38-kg ^{239}Pu cylinders and spheres of generic wastes at center of deformed CCOs in a dry hydrologic regime to define constraints on water/plastic to ensure subcriticality after WIPP closure.[24]
2023-2026	WIPP PA updated with 2 replacement panels; also, PA updated to include full 34-t surplus Pu for CRA-2026	RPPCR-2023 PA includes 2 replacement panels to west of current panels and 7.1-t surplus plutonium waste streams;[7] CRA-2026, the 5th Compliance Recertification Application, builds upon RPPCR-2023 but with additional 26.9-t surplus Pu (as contact-handled TRU waste).[20] For CRA-2026, Sandia updates the post-closure criticality FEP screening to include CCO disposal options specified in 2022 WAC update.

In FY17, Congress authorized $15 million for DOE planning, which was completed in 2018,[42, p.5;69] and for examination of the disposal option viability by the National Academies, which was completed in 2020.[61] Re-evaluating the potential for post-closure criticality in compacted CCOs was coordinated by Sandia with ORNL providing criticality modeling. In 2018, ORNL concluded that criticality was highly unlikely in CCOs with limited hydrogenous material (primarily, moisture and plastics) if boron carbide (B_4C—a highly insoluble, nonhazardous neutron poison) is added to the mixture of oxidized surplus Pu and adulterant. The adulterant is added to reduce the level of attractiveness of the disposed Pu to adversaries.[62] In 2020, ORNL showed that limiting hydrogenous materials in CCOs was unnecessary if 50-g B_4C was included in each CCO.[67]

As part of WIPP's fourth compliance re-certification application to EPA in 2019 (CRA-2019), Sandia updated the rationale excluding criticality from the performance assessment.[6, App. SCR-2019;11;12;15] One focus of the criticality screening was the criticality potential of 3.2 t of surplus Pu in POCs already disposed at WIPP as contact handled TRU waste. High-fidelity salt-creep modeling in combination with the criticality evaluation showed criticality in POCs was improbable (Table I).[11] For the CCOs disposing 6.0 t of surplus non-pit Pu, CRA-2019 adopted the option to add 50-g B_4C to the Pu waste form to exclude consideration of criticality.[6, App. SCR-2019;11] The final report from the National Academies acknowledged this option.[61]

In the Replacement Panel Planned Change Request PA (RPPCR-2023),[7] Sandia included 7.1-t of the 34-t of surplus non-pit Pu (not to be confused with 7.1 t of pit Pu discussed above) which could in part be accommodated within 2 replacement panels to the west of original disposal region (Table I).[70] The 2 replacement panels account for disposal areas abandoned because of radiation contamination in 2014 and past disposal inefficiency.[71] The expansion does not change the maximum TRU waste volume of 175 546 m^3 authorized in 1992 *Waste Isolation Pilot Plant Land Withdrawal Act.*[72]

Sandia built upon RPPCR-2023 for the fifth re-certification application to EPA in 2026 (CRA-2026), which includes an additional 26.9-t surplus plutonium disposition in CCOs (for a total of 34 t non-pit Pu). In support of CRA-2026, this report updates the post-closure criticality FEPs to consider additional CCO disposal options besides B_4C to provide flexibility when using CCOs.[20] Sandia will build upon CRA-2026 to support a WIPP supplemental EIS on including 9 additional panels in the disposal area.

III. MODELING OF ROOF FALL

To establish a reasonable CCO configuration after compaction, high-fidelity geomechanical simulations were conducted for a slice of a room segment filled with discrete CCOs.[19;68] Two phases of post-closure repository conditions are envisioned: (1) roof fall in the first 20 years or so, and (2) gradual compaction of containers from salt creep to the maximum extent at 1000 years without brine present (thus, avoiding gas generation by metal corrosion and cellulose degradation and subsequent room pressurization which impedes room compaction). The geomechanical modeling of CCOs for these two phases is similar to the geomechanical modeling of POCs conducted for CRA-2019, which used the Sierra/Solid Mechanics finite-element code system.[22]

III.A. Conceptual Model of Roof Fall

During the first 20 years or so after sealing a panel of disposal rooms, salt roof fall and room closure from salt creep mostly fills the room void space (Fig. 2). Discrete roof fall models were constructed to evaluate the potential of roof fall scattering and clustering CCOs and, thereby, potentially producing a reactive CCO configuration prior to full compaction from salt creep.

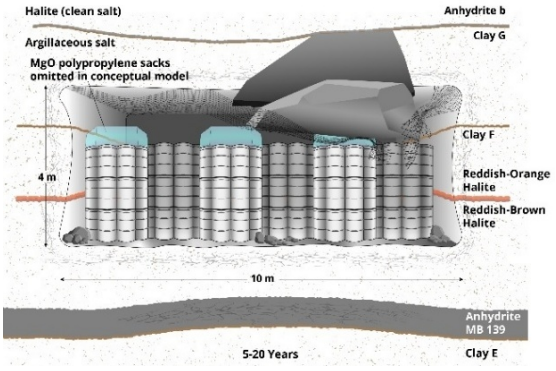

Fig. 2. Conceptual model of large trapezoidal-shaped salt block that detaches at Clay G seam and falls onto CCOs.

A trapezoidal-shaped salt block was chosen to match the Panel 7, Room 4 roof fall, which is the biggest roof fall that has occurred in a disposal room at WIPP.[11] The WIPP disposal panels are located in two different horizons (elevations) of the geologic strata of the Salado Formation. Panel 7 is in the lower horizon with 2-m distance to Clay G seam, from where the salt block separated. Larger salt blocks that separate above Clay G seam are not anticipated (Fig. 2).

Two rock-fall models are developed. In the first roof-fall simulation, the entire length of the trapezoidal salt block detaches from the roof at once (Fig. 3a). In the

second roof-fall simulation, the salt block progressively detaches from the roof, to impart rotation (Fig. 3b).

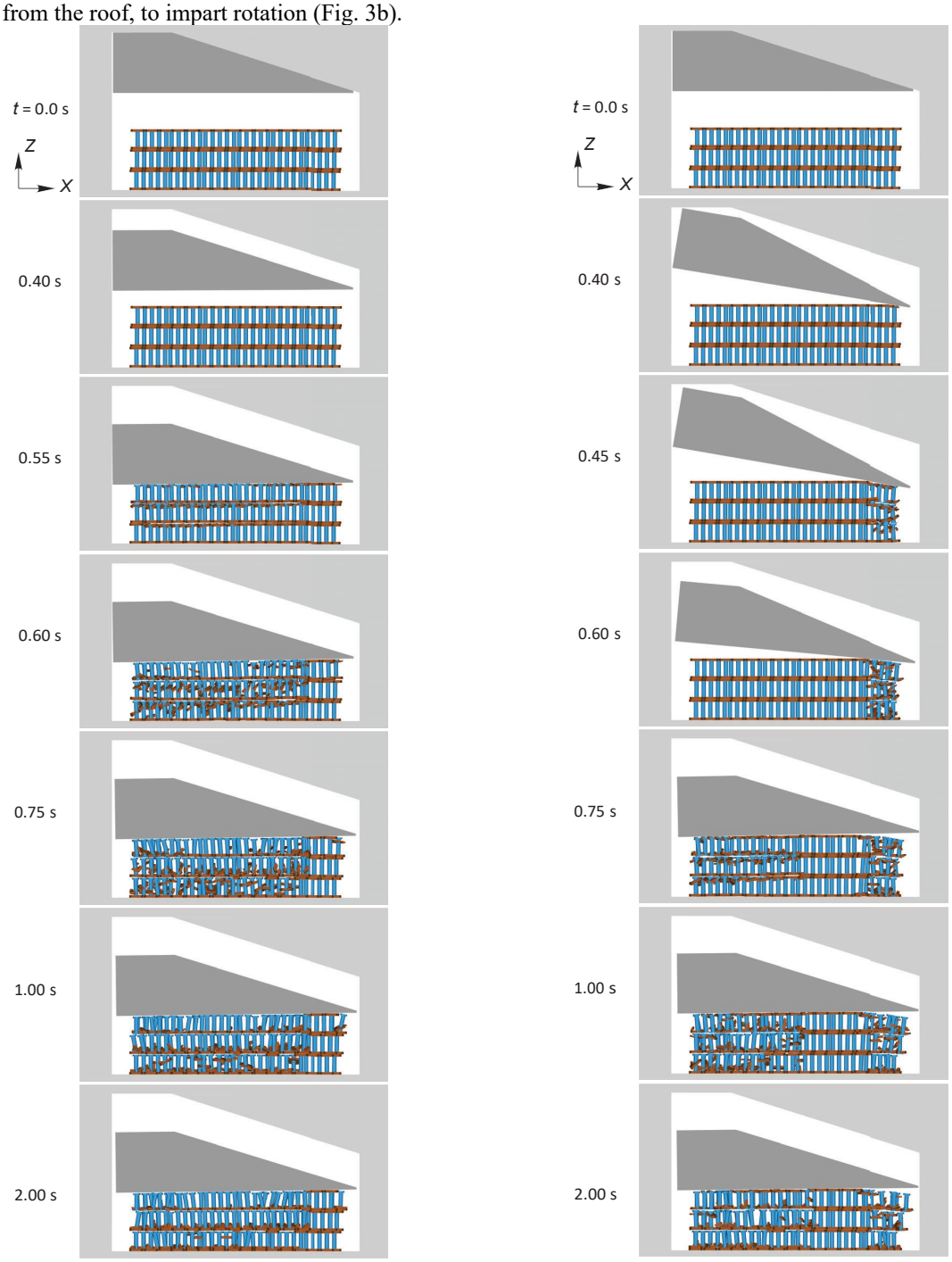

(a) Mostly flat roof fall (b) Rotating roof fall

Fig. 3. Roof fall onto CCOs emplaced in a hexagonal array in lower repository horizon (a) mostly flat roof fall; (b) rotating roof fall. Brown discs represent top and bottom plywood stabilizer for blue stainless steel CCCs inside 55-gallon CCO shell (which is hidden for visualization).[68, Fig. 5]

III.B. Roof Fall Results

When the entire block length detaches simultaneously (Fig. 3a), the trapezoidal shape imparts some rotation, but the salt block lands almost flat and settles on top of the drum ensemble. The impact breaks the top plywood layers (in brown), dents some of the outer 55-gallon drums (not shown), and causes the CCCs to sway back and forth slightly (blue pipes); but CCOs mostly return to the initial arrangement.

When the salt block progressively detaches (Fig. 3b), the CCOs are jostled more such that not all the CCOs return to a neat arrangement, but still no clustering or noticeable deformation of CCCs occurs. Hence, salt block falls after CCO disposal are not likely to cause extensive deformation, collapse, or clustering and, thereby, do not produce a critical assembly of CCOs prior to room closure from salt creep.

IV. MODELING OF ROOM CLOSURE FROM SALT CREEP

IV.A. Conceptual Model of Room Closure

An array of CCOs compacts as the disposal room in the bedded salt naturally closes and beneficially encapsulates the CCOs. Salt creeps in the presence of shear stress, and a large void space within a geologic salt formation, such as a room, causes large shear stresses. As the salt creeps inward, it contacts and gradually compacts the containers. The containers provide little crushing resistance at first, but they slowly become stiffer and stronger. Eventually, the container resistance balances the salt crushing pressure, the salt shear stresses become negligible, and the room closure asymptotically comes to a halt.

IV.A.1. Salt Stratigraphy

The geomechanical model adopted an idealized stratigraphy of the salt formation that included salt, anhydrite, and clay seams. The idealized stratigraphy is the same as used for POC analysis.[11] A portion of this stratigraphy around the repository room horizon is shown in Fig. 4.[73]

The salt/anhydrite constitutive models were based on laboratory measurements of their mechanical behavior. Sliding along the clay seams was modeled using Coulomb friction with a friction coefficient (μ) of 0.2. This friction coefficient has not been directly measured, but μ of 0.2 produces reasonable room closure rates that agree with underground measurements.[73]

The model represents the 10.06-m wide (*x*-direction), 4-m high (*z*-direction), and ~ 2-m slice (*y*-direction) of Room 4 (middle of a panel of 7 rooms) halfway down a 91-m room segment where the ratio of horizontal to vertical room closure is likely the greatest.[e] The room closure analysis models a disposal room segment in both repository salt horizons to estimate the influence of differing arrangements of geologic strata (Fig. 4).[19;68]

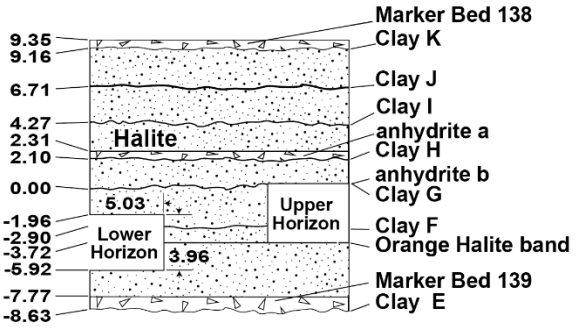

Fig. 4. Idealized stratigraphy near WIPP disposal rooms in lower and upper horizon. Elevations referenced to Clay G, which is at elevation 386 m, 652 m below surface at

IV.A.2. CCO Configuration

The geomechanical analysis examined CCO arrays starting in two different configurations: (1) hexagonal array, and (2) triangular array. A hexagonal, 7-pack bundle array is the approximate emplacement scheme for CCOs (Fig. 5). With a disposal room filled with 7-pack hexagon CCO bundles, any room slice cuts 12 CCOs in half. In a 2.15-m room segment, the hexagonal array has 51 whole and 12 half CCOs in a tier (3.52 kg $^{239}Pu/m^2$ for 57 whole CCOs at 380 FGE per CCO).

For modeling with a mirror boundary condition, the 12 half CCOs must be eliminated because half CCOs cannot buckle in the direction of the mirror boundary, which, in turn, causes numerical difficulties with shell elements, as used here. When 12 one-half CCOs are eliminated in a tier (3.15 kg $^{239}Pu/m^2$), a total of 153 CCOs are in three tiers in 2.15-m room segment. Reducing the material in the room permits slightly more room closure.

The 7-packs of CCOs are held together with plastic wrapping, which could allow CCOs to shift into an approximate triangular array once the walls contact the CCOs. In the more compact triangular array, 14 CCOs are modeled per row in a 8.607-m width and 2.08-m segment with mirror boundary conditions. The triangular array with 168 CCOs has a slightly higher fissile areal

[e] A disposal room consists of a straight 91.4-m long segment and a portion of the drift on either end to form a square bracket. Although this definition is important for tracking disposal room contents, most salt-creep analysis only models the straight 91.4 m segment to avoid three-dimensional effects. Herein, we are referring to the straight room segment rather than an entire disposal room.

density of 3.57 kg $^{239}Pu/m^2$ compared to the hexagon modeled density of 3.15 kg/$^{239}Pu/m^2$ (Fig. 5).

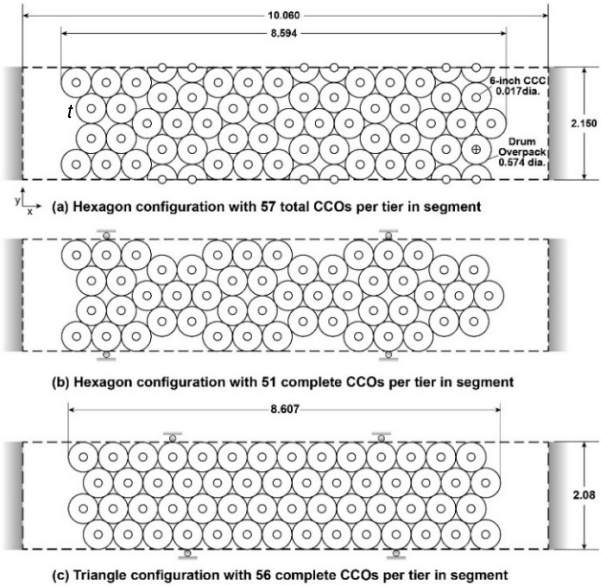

Fig. 5. Hexagonal and triangular model emplacement schemes for CCOs in WIPP disposal room segment.[65, Figs. 4&6]

In the analysis (and like the roof fall simulations), three CCO components (CCC stainless-steel pipe, the plywood stabilizer on the top and bottom, and outer 55-gallon carbon-steel CCO shell—Fig. 1) use separate elastic-plastic-failure material constitutive equations.

IV.B. Deformed Irregular Array

The 2018 criticality evaluation, which first set the 50-g boron carbide requirement in CCOs defined an ultra-conservative configuration of fissile regions in which each CCC was touching (not just the CCOs themselves) and added sufficient rows of CCOs to fill the room segment (Fig. 6). The high-fidelity, salt-creep simulations of this report show much greater spacing of CCC fissile centers and, thus, remove the excessive conservatism of the 2018 criticality evaluation.[62]

The salt-creep simulations predict the outer CCO shell crumples, and the plywood rapidly fails shortly after the room ceiling contacts the CCO drums (in the room center by ~35 years and along the entire length after ~60 years—Fig. 7). By 100 years, the CCCs have begun to topple over. By 200 years, most CCOs are on their side, which allows for substantial compaction.

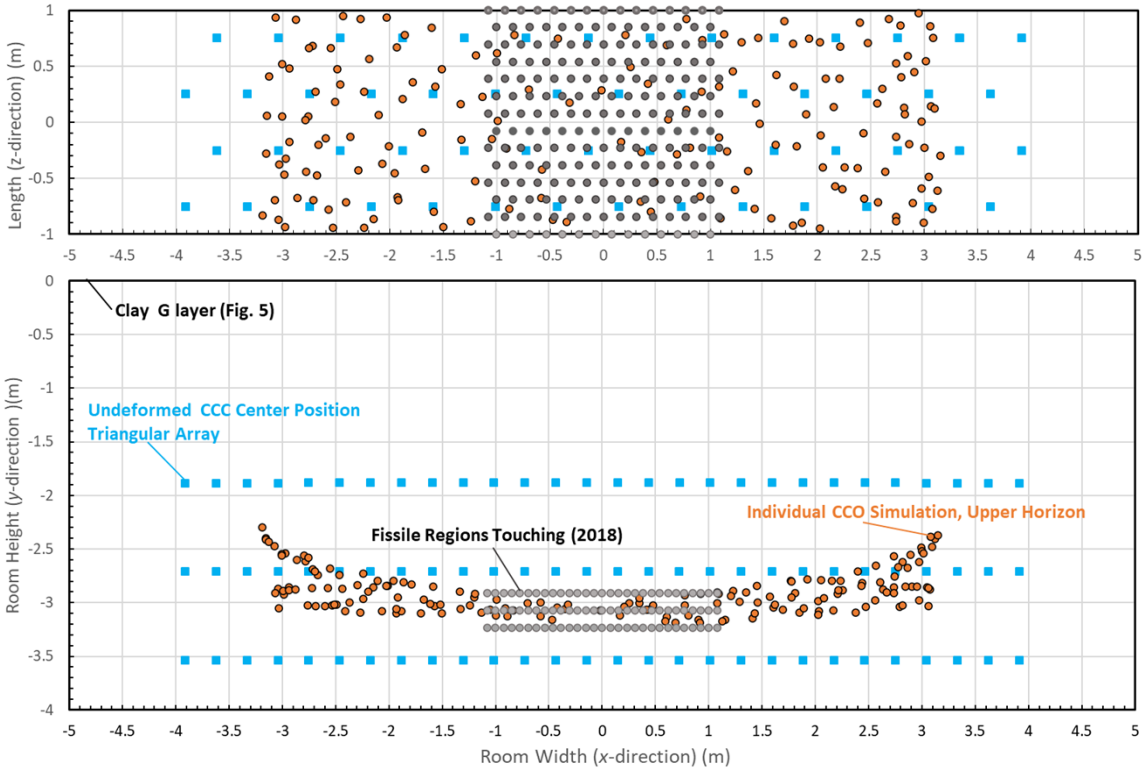

Fig. 6. Plan and side view of undeformed coordinate positions emplaced as a triangular array in 10.06 m wide, 3.96 m tall, and 2.08 m thick room segment in upper horizon relative to ultra-conservative positions of CCC fissile centers used in 2018 criticality evaluation and more realistic deformed coordinate positions in current analysis.[62, Fig. B-13;74, Fig. 12]

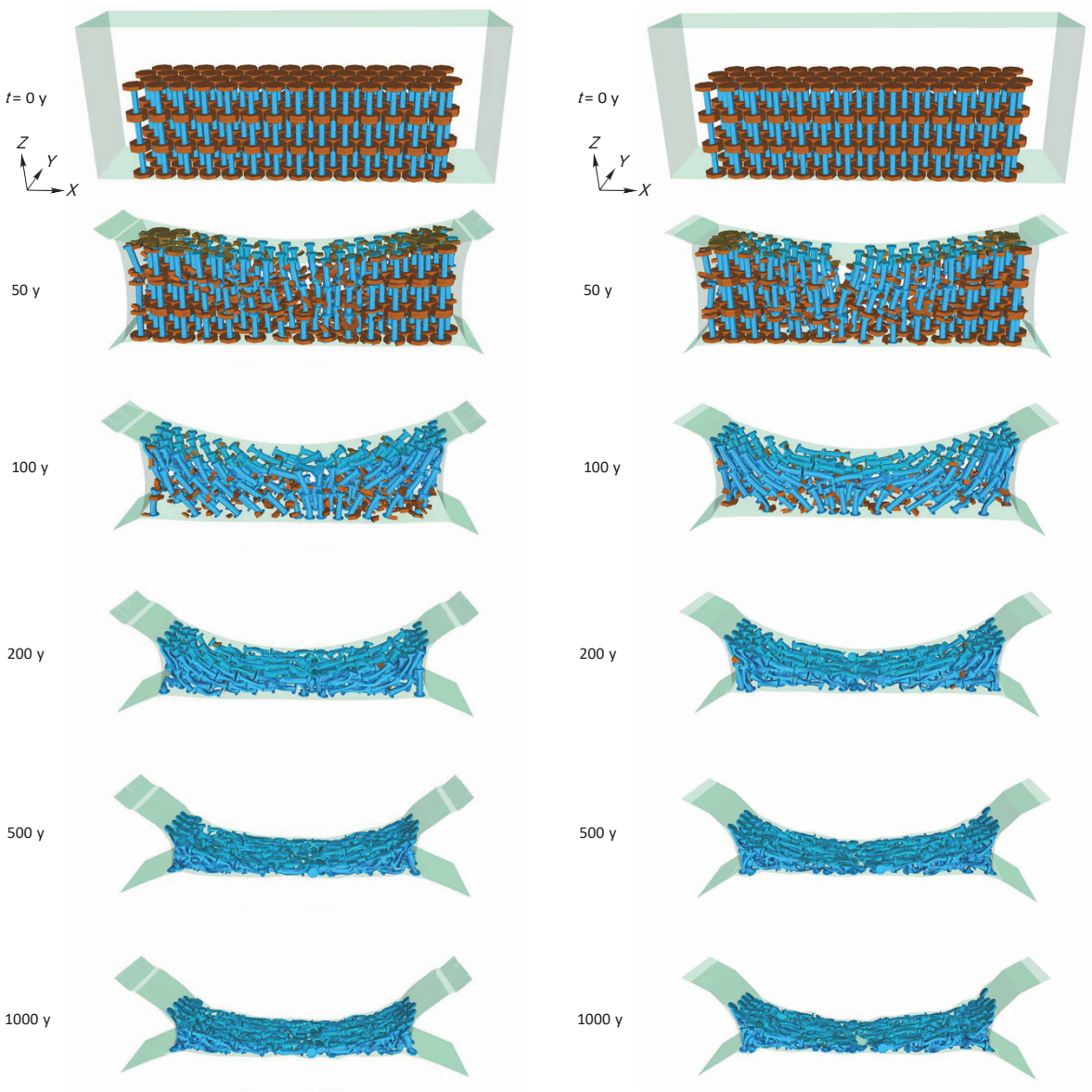

(a) Lower horizon in northern portion of repository (b) Upper horizon in southern portion of repository

Fig. 7. Salt compaction in room segment with CCOs emplaced in triangular array with most inner CCCs on their side by 200 years; outer CCO shell and bedded salt stratigraphy included in analysis but removed in visualization; brown elements represent plywood stabilizing CCC, which are deleted when splintered and failed.[68, Fig. 9]

A more revealing perspective of CCO compaction is the plan and side view of CCC centerlines (Fig. 8). At emplacement (t=0), the model has CCOs touching each other; thus, a 0.83-m gap exists between the CCO drum and room wall (and a 1.12 m gap exists between the CCC centerline and the room wall). Normally, the slipsheets and plastic wrap for the 7-pack CCO bundles prevent such a tight spacing. Regardless, CCOs are always >20 cm from a room wall at emplacement.[11, Fig. 8;75, p. 26]

At 1000 years, clearly most CCOs are on their side. The greater closure at the room center displaces much of the top tier of CCOs (green, yellow-green, and brown centerlines) toward the room walls. The second tier of CCOs (deep blue, burgundy, and pink) is also displaced toward the room walls but not nearly as much. The center is mostly a single layer, which consists primarily of the bottom tier of CCOs (orange, light blue, and red). The CCOs are not noticeably clumped or bunched together down the axis of the room segment in the y-direction. The final coordinate positions of CCC centers are used in subsequent criticality calculations (Fig. 6 and Fig. 8).

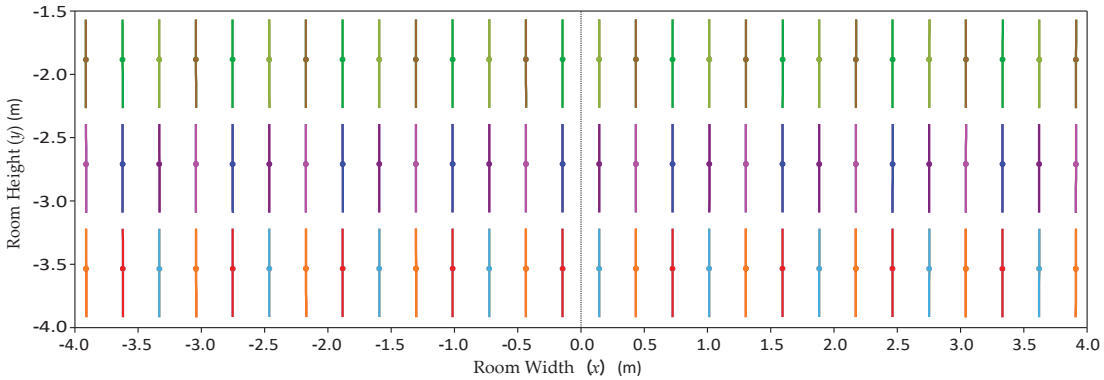

(a) CCC triangular array in side view at 0 years[65, Fig. 7]

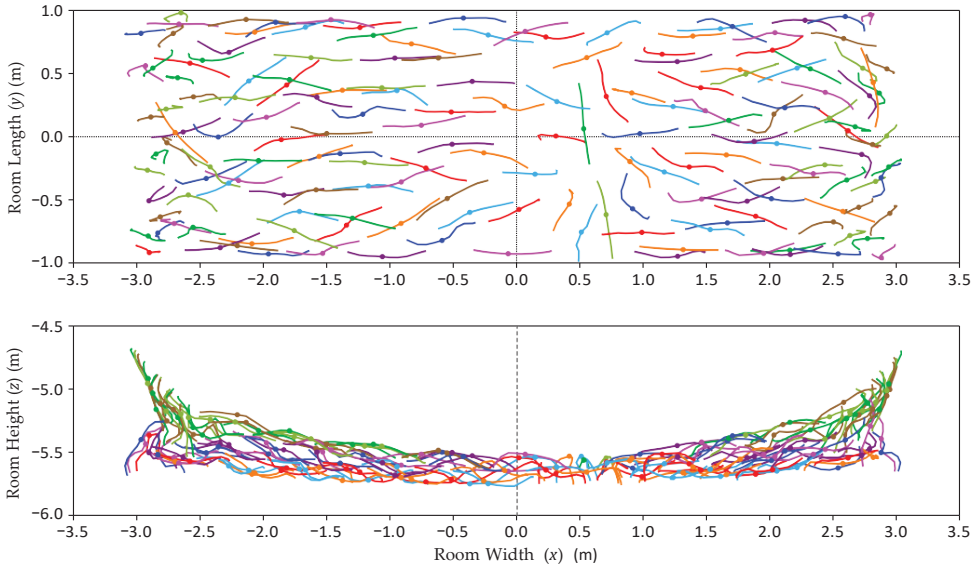

(b) Lower horizon plan (*x*-*y* direction) and side view (*x*-*z* direction) at 1000 years[65, Fig. 31]

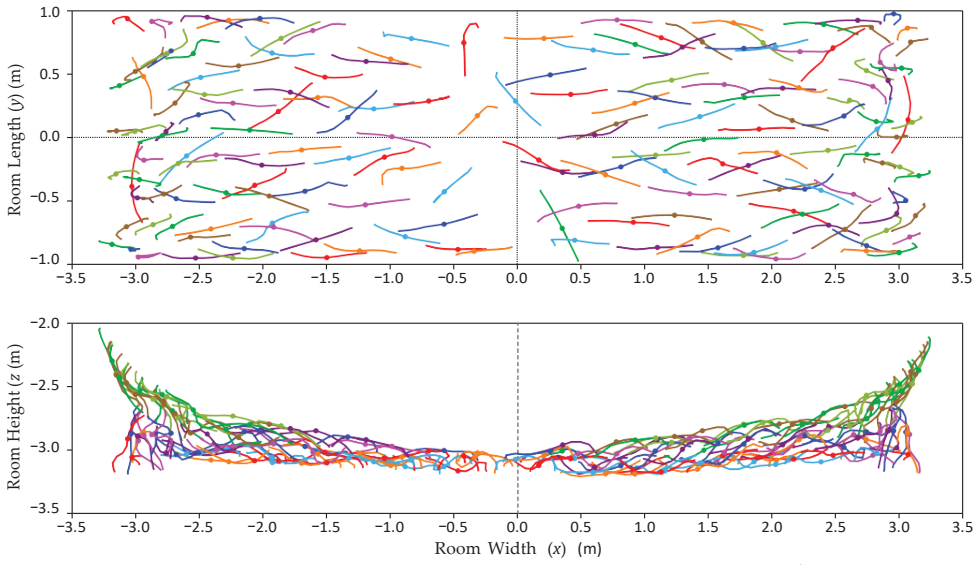

(c) Upper horizon plan and side view at 1000 years[65, Fig.33]

Fig. 8. Deformed centerlines of CCCs at 1000 years when initially emplaced as triangular array.

IV.C. Mid-Height and Mid-Width Room Closure Measure

To quantitatively compare geomechanical model results and thereby determine the influence of input parameters and starting conditions, two measures are considered (1) room closure at the disposal room mid-height and mid-width, and (2) the distribution of CCO concentration within the room to determine the extent of CCO clustering.

IV.C.1. Room Closure at 1000 years

Most room closure occurs by 300 years; yet the room continues to close and approaches a maximum at ~1000 years (Fig. 9). The smallest horizontal closure at the room mid-height at 1000-years occurs for the triangular array in the upper repository horizon: 39.0% of the original 10.06 m width. The largest horizontal room closure occurs in the lower horizon for the hexagonal array: 42.5%.

The smallest vertical closure at the room mid-width occurs for the hexagonal array in the lower horizon 93.9% of the original 3.96 m height (Fig. 9). The largest vertical compaction occurs for the hexagonal array in the upper horizon: 97.3%. Understandably, a room filled with 168 CCOs in the triangular array generally compacts less than 153 CCOs in the hexagonal array, but the difference is not great. That is, changes in the initial emplacement configuration influence the progression of room closure between 100 and 400 years but cause only minor changes in final room closure at 1000 years.

Comparing closure results of an empty room and a room full of CCOs room shows that containers weaker than CCOs (or POCs) will only somewhat increase room closure.

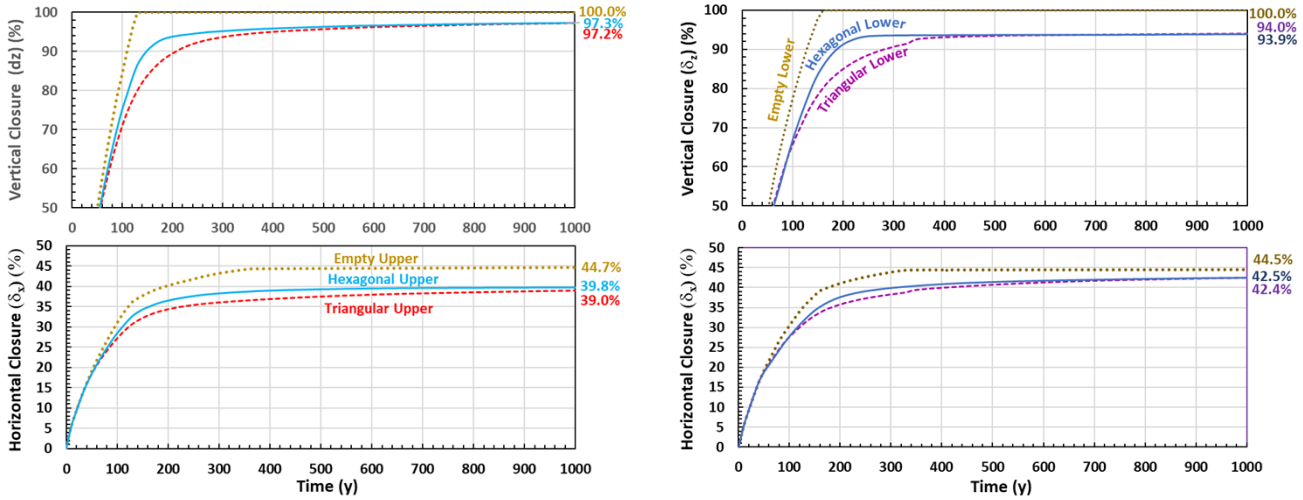

(a) Upper horizon (b) Lower horizon

Fig. 9. Horizontal and vertical closure at room mid-height and mid-width, respectively, for CCOs initially emplaced as triangular and hexagonal arrays in upper and lower repository horizons.[19, Fig. 3-4;64;65, Fig. 10;68, Fig. 7]

IV.C.2. Room Closure in Previous CCO and POC Simulations

In 2018, several preliminary simulations of room closure were conducted with CCOs in a hexagonal array in the upper horizon with a friction coefficient of 0.5 for Clay F and Clay G seams (Fig. 4).[65, Fig. 21] A friction coefficient (μ) of 0.5 reduces clay slippage such that the room closes slightly slower. In turn, more CCCs are pinned first and then column buckle. Because the CCCs are pinned in place, the CCCs are not segregated into layers as before (Fig. 10 versus Fig. 8). A friction coefficient (μ) of 0.2 allows slightly faster closure such that more CCCs toppled over with the top tier shoved to the sides.[65;76]

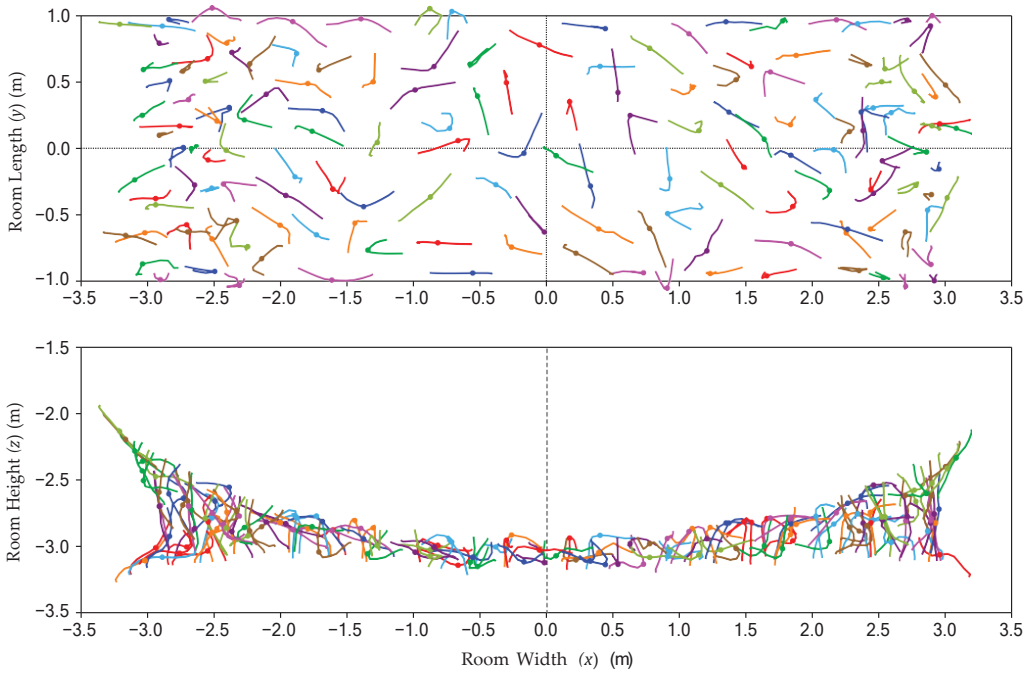

Fig. 10. CCO compaction in hexagonal array in upper horizon has more column buckling when friction coefficient set at 0.5 for Clay F and Clay G layers.[65, Fig. 21]

To make additional comparisons, 6-inch and 12-inch POC simulations were repeated with the CCO modeling assumptions.[68] The final horizontal and vertical closure of a room filled with 6-inch POCs initially emplaced in hexagonal arrays remains similar to room closure of CCOs, but the progression of room closure differs somewhat since the internal construction differs (Fig. 11).

The progression of vertical closure for CCOs with four times nominal material strength is somewhat like the stronger 12-inch POC (stronger because of geometrical shape), but the geometrical difference is such that the final vertical closure of the 12-inch POC is noticeably less than for the CCO (Fig. 11).

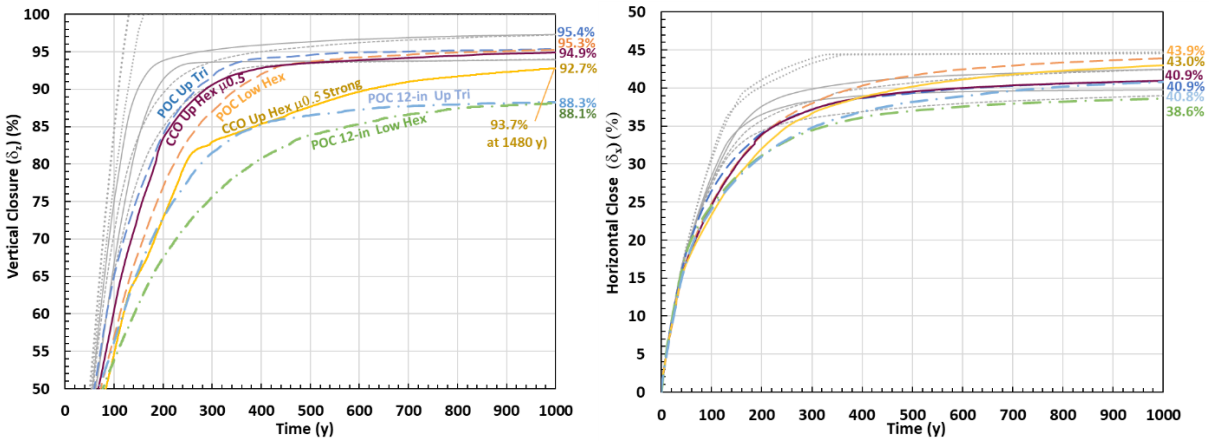

Fig. 11. Horizontal and vertical closure of upper and lower horizon rooms filled with CCOs and POCs initially emplaced in triangular and hexagonal arrays with different clay friction coefficients (μ), where room closure in Fig. 10 shown as gray lines.[65, Fig. 18]

IV.C.3. Closure of Room Filled with Mix of CCOs and other Containers

All the CCO simulations assume the disposal room is filled with CCOs, which will be reasonable for large shipment campaigns. However, WIPP disposal rooms are typically filled with a mixture of mostly standard 55-gallon TRU drums (54% global average), standard 12-inch POCs (15%), 100-gallon drums (20%), some TRU waste boxes (8%), and miscellaneous other containers, usually stacked 3 high.[11, Table V] Mixing the most common types of containers in a disposal room mostly filled with CCOs would not likely substantially change the final extent of compaction. For example, the initial yield strength of the stainless steel CCCs has been varied between zero (like empty room) to a factor of four greater than nominal material strength; yet, the final vertical room closure is similar (Fig. 11).[19] Only the time to reach asymptotic closure varies. An empty room vertically closes by 150 years; a room with CCOs initially emplaced in hexagonal array closes by 250 years; CCOs and 6-inch POCs initially emplaced in triangular array close by 350 years; 6-inch POCs initially emplaced in hexagonal array close by 450 years; and a CCO with 4 times nominal strength in 1480 years (Fig. 11). For most containers, the initial container strength is too small to provide resistance to the lithostatic pressure (~15 MPa).[68] Only when the containers become significantly compacted are they able to resist the overburden pressure.

The container strength of 100-gallon drums filled with super-compacted waste (compressed with ~60 MPa) could resist the lithostatic pressure and a cluster would prop up a small portion of a disposal room, which could allow greater horizontal compaction in another portion of a room, However, super compacted waste containers are not allowed to be located next to each other.[11;68] Super compacted waste containers randomly distributed throughout the room would likely shield the weaker CCO containers; thus, CCO compaction would likely be less than observed in simulations here (e.g., Fig. 8 and Fig. 10).[11;22]

IV.D. CCO Concentration Measure

IV.D.1. Concentration of CCOs at 1000 years

A more direct measure of the CCO compaction is a uniformly weighted CCO concentration ($c_{uniform}$) defined as

$$c_{uniform} = n_{CCO} / V_{sphere} \quad (1)$$

where n_{CCO} is the number of CCOs in a sphere volume V_{sphere} calculated as $4\pi(r_{sphere})^3/3$ based on a defined sphere radius r_{sphere}. The sphere radius relates to the distance neutrons interact between CCOs through the interstitial material, here modeled as a 1:1 mixture of salt and MgO. As explained in the next section (§V.D.2), the neutron flux is reduced by <2 orders of magnitude in 75 cm from an ideal point source; hence, the sphere radius was set at 75 cm. The concentration for the irregular array is calculated for periodic boundary conditions to avoid artificially increasing the concentration when a CCO is near a boundary.

At 1000 years, CCO concentration has a mean between 10.9 and 11.9 CCO/m^3 and maximum between 15.3 and 18.1 CCO/m^3, where the minor variation is caused by the initial emplacement configuration, either hexagonal or triangular, and the stratigraphic variation is represented by the upper and lower repository horizons (Fig. 12). For 0.38 kg/CCO, the corresponding mean fissile concentration is between 4.1 and 4.5 kg Pu/m^3 and the maximum is between 5.8 and 6.8 kg Pu /m^3).

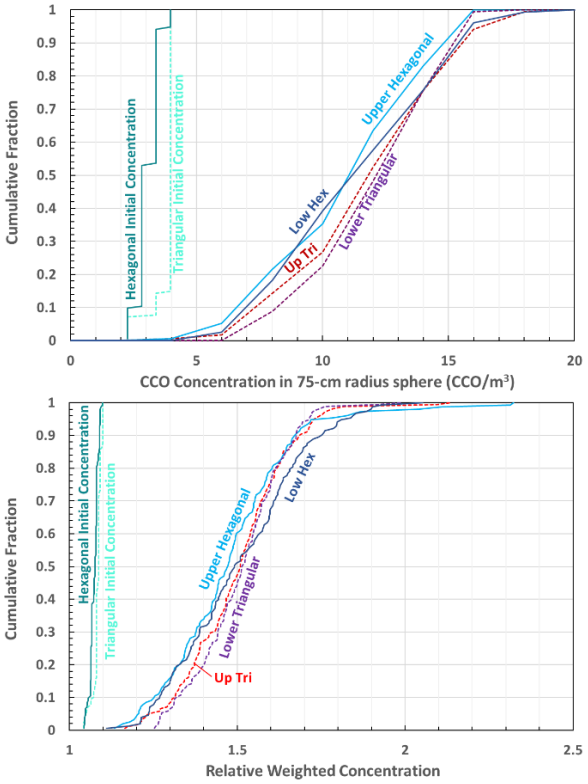

Fig. 12. Distribution of simple and relative CCO concentration about each CCC center at initial condition and at 1000 years.[65, Fig. 11]

IV.D.2. Relative Weighted Concentration

In salt, the neutron flux (ϕ) rapidly attenuates with increasing radial distance.[f] This rapid decrease in ϕ is not

[f] Neutron flux is the neutron density per unit volume multiplied by the neutron velocity. Neutron velocity varies over a wide spectrum. Neutrons released during fission of a fissile atom typically have high energy/high speed (average of 2 MeV).

captured well by a calculating a CCO concentration that uniformly weights all CCOs within a specified radius (e.g., 75 cm). Thus, an alternative weighted concentration (c_{weight}) has been defined:[65]

$$c_{weight} = \frac{\sum_{n=1}^{N} w(r_n)}{\int_{V_{sphere}} w(r)dV} \quad (2)$$

where $w(r)$ is the weighting function that varies with radial distance r, and r_n is the radial distance corresponding to CCO center n. Eq. (2) reduces to Eq. (1) if $w(r)$ is a constant.

A reference weighted concentration for one CCO can also be defined as[65]

$$c_0 = \frac{\sum_{n=1}^{N} w(0)}{\int_{V_{sphere}} w(r)dV} \quad (3)$$

and a relative weighted concentration can be defined as

$$\hat{c} = \frac{c_{weight}}{c_0} = \sum_{n-1}^{N} \frac{w(r_n)}{w(0)} \quad (4)$$

To be consistent with the physics of the criticality evaluation, the weighting function is chosen to resemble the attenuation of neutron flux from an ideal steady source, which can be approximated as a radial diffusion process. The one-dimensional, steady-state diffusion equation for ϕ emanating from a point source of strength S_0 is

$$\frac{D_{diff}}{r^2}\frac{\partial}{\partial r}\left(r^2\frac{\partial \phi}{\partial r}\right) - K_{abs}\phi = 0 \quad (5)$$

where D_{diff} and K_{abs} are the neutron diffusion and absorption constants, respectively, of the salt/MgO mixture surrounding the point source. The solution to this equation with the boundary conditions of $\lim_{r\to 0}(-4\pi r^2 D_{diff} d\phi / dr) = S_0$ and $\lim_{r\to\infty}\phi = 0$ is

$$\phi = \frac{A}{r}\exp\left(\frac{-r}{r_{char}}\right) \quad (5)$$

where the characteristic radius r_{char} is $\sqrt{D_{diff} / K_{abs}}$ and the constant A is $S_0 / 4\pi D_{diff}$.

The weighting function $w(r)$ is based on Eq. (5) but a limit is placed on $w(r)$ for arbitrary small r_{limit} because at the source with r of zero, the neutron flux is infinite. Consequently, $w(r)$ is set at unity for $r < r_{limit}$. A limit is also placed on $w(r)$ for large r to avoid evaluating the weighting at infinite radii. With these constraints, the point source weighting function is

$$w(r) = \begin{cases} 1 & \text{for } 0 \le r \le r_{limit} \\ \frac{r_{limit}}{r}\exp\left(\frac{r_{limit} - r}{r_{char}}\right) & \text{for } r_{limit} < r \le r_{max} \\ 0 & \text{for r} > r_{max} \end{cases} \quad (6)$$

This point source weighting function values of r_{limit}, r_{char}, and r_{max} were calibrated against neutron flux results of a model built with waste set in a 0.05-m radius sphere surrounded by 1:1 mixture of WIPP salt and MgO of infinite extent using the MAVERIC module in SCALE, as evaluated by ORNL.[65] In general, the neutron flux drops 2 orders of magnitude in 0.7-m radial distance (i.e., ϕ / ϕ_0 =0.01 for r >0.7 m)[g] (Fig. 13).

Both the uniformly weighted (simple) and relative-weighted concentration measures after 1000-year room closure (Fig. 12) reinforce the earlier conclusion (Fig. 9) that changing the repository horizon or the emplacement configuration has only a subtle impact on the final arrangement of CCOs in a compacted room.

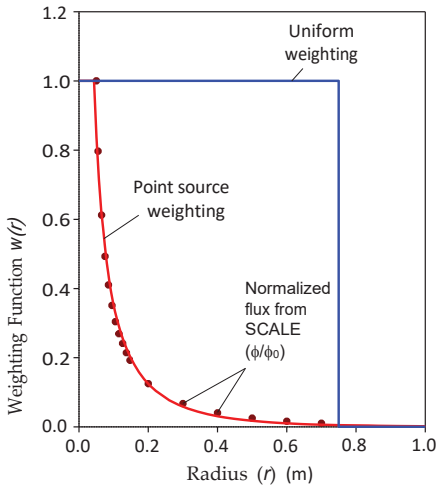

(a) Difference in weighting function profiles

High energy/fast neutrons have a small probability of being absorbed by the nucleus of another fissile atom. In contrast, low energy/slow neutrons (i.e., those with thermal energy ~0.025 eV) have a much greater probability of being absorbed by an atom and causing fission. Neutron interaction with other matter can moderate or reduce the neutron energy through inelastic impacts with heavy nuclei and elastic impacts with light nuclei.

[g] In pure salt, the decrease is ~4 orders of magnitude.[11, Fig. 31]

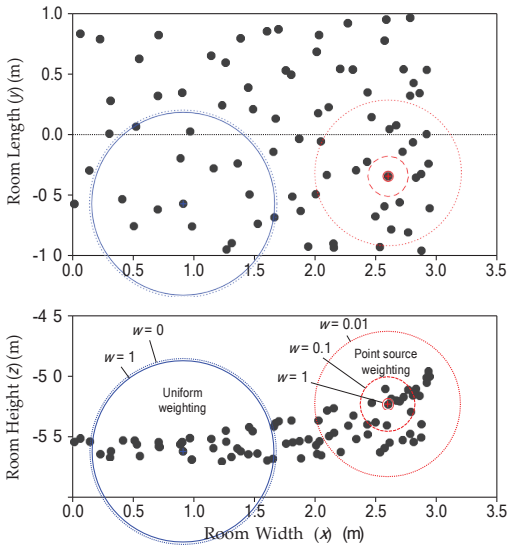

(b) Spheres of influence

Fig. 13. Weighting in sphere of influence for uniformly weighted (simple) and point-source (relative-weighted) concentration in one-half of room [65, Fig. 8]

IV.D.3. Concentration at 1000 years for Containers with Different Strengths

The simple concentration distributions remain similar for (1) CCOs with high strength (4 times nominal strength); (2) 6-inch POC with its different construction and, thus, compaction strength; and (3) 6-inch POCs in strata with clay friction coefficient (μ) of 0.5 (Fig. 14). In particular, the means of the simple concentration are similar. Furthermore, the distribution tails of the simple concentration are remarkably similar at high concentration values between 13 and 18.7 containers/m^3 (cumulative fraction above 0.75 m.

The means of the relative-weighted concentration also remain similar for CCO with high strength and 6-inch POCs.[h] In contrast, however, the relative weighted concentration have increased variation at high values. That is, the relative weighted concentration is more discerning in identifying differences in the final arrangement of containers at the distribution tail of high concentrations.

A room filled with 12-inch POCs has similar minimum concentration values (Fig. 14). However, the 12-inch POC with roughly twice the stainless-steel inner pipe mass and, thus, the structural strength, significantly reduces the maximum and the mean concentration.

[h] Six-inch POC arrays have a similar geometric concentration as CCO arrays, but the fissile concentration is less because POCs contain 0.2 kg Pu/POC (e.g., POC fissile mean of 2.3 kg Pu/m^3 versus CCO fissile mean of 4.4 Pu/m^3 when emplaced in triangular arrays at geometric mean concentration of 11.7 containers/m^3 in upper horizon).

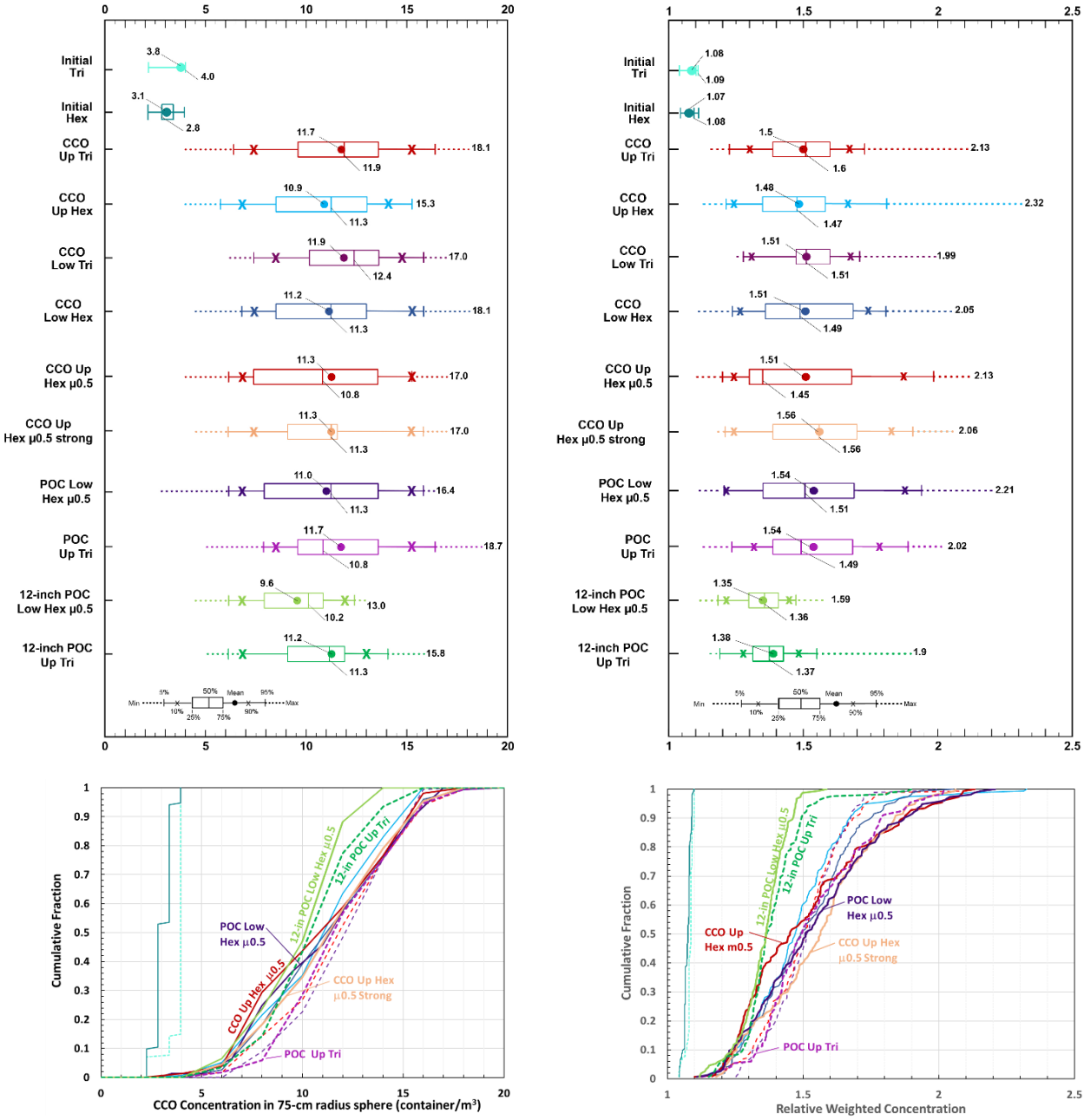

Fig. 14. Change in distribution of container concentration at 1000 years with change in clay friction coefficient (µ), change in CCC stainless-steel strength, and change in POC container; unlabeled curves same as Fig. 12.[65, Fig. 19]

IV.E. Consistency of Room Closure and CCO Concentration

The geomechanical compaction analysis evaluated the influence of changes in (1) repository horizon and, thereby, changes arrangement of clay strata; (2) clay friction coefficient; (3) emplacement configuration (triangular and hexagonal); (4) change to 12-inch POC sizes and mass (i.e., twice the stainless steel mass); and (5) strength of CCC (a) directly through increase of yield strength by four times, and (b) indirectly through analysis of empty room and changing to 6-inch POC construction (Fig. 9, Fig. 11, Fig. 12, and Fig. 14). Except for 12-inch POC, these variations cause only minor changes in final room closure. Furthermore, the variations all produced a wide variety of deformed

spacing between CCOs, as measured by the distribution of CCO concentration. Yet, the distribution shape and range of the simple and more complicated relative weighted CCO concentration measures remain stable. Consequently, the coordinate positions of CCCs for the four cases of the irregular, non-uniformly compacted array reasonably represent conditions in the WIPP disposal room for subsequent criticality calculations.

V. CRITICALITY EVALUATION OF COMPACTED ARRAYS WITHOUT BORON CARBIDE

V.A. Computational Tool

To evaluate the post-closure criticality potential of compacted rooms, a series of models were developed and analyzed with SCALE developed by Oak Ridge National Laboratory [23] Version 6.2.3 was predominately used;[24, §3] however, version 6.2.4 was also used for validation analysis.[24, App. H]

Oak Ridge National Laboratory conducted hundreds of thousands of criticality calculations from which the report figures were created. Their work is documented in a separate report.[24] Within SCALE, the Monte Carlo module, KENO-VI (Criticality Safety Analysis Sequence Six—CSAS6), was used to calculate neutron multiplication factors (k_∞ or k_{eff}).[24, §3] That is, the integral neutron and photon transport equations are solved with Monte Carlo techniques. The distance between interactions, the fissions that occur, and the neutron loss by capture or leakage are characterized by parameters such as, the mean free path lengths between interactions, the distribution describing scattering, the distribution of neutron energy, and the reaction cross-section of the atoms of each material. All analysis started with the 238 group Evaluated Nuclear Data File/B Version 7.1 (ENDF/B-VII.1) criticality library of tabulated cross-sections, which is provided in the standard release of SCALE, and used CENTRM module to provide analysis-dependent multigroup cross-sections.[24, §3;67]

V.B. Upper Subcriticality Limit in Criticality Modeling

At the WIPP facility, the evaluation of criticality occurs in two timeframes: (1) post-closure timeframe when humans are absent and (2) current timeframe when humans are present. Two aspects are pertinent to current timeframe: transportation of CCOs to WIPP and operational handling of CCOs at WIPP facility. Regulatory authority differs for each situation. As described in the 1992 *Waste Isolation Pilot Plant Land Withdrawal Act,*[72] EPA has regulatory authority for certifying WIPP repository performance in post-closure timeframe, NRC has regulatory authority for certifying transportation containers such as CCOs in the current timeframe, and the US Department of Transportation regulates transportation routes. DOE is self-regulating only for current WIPP facility operations.

V.B.1. Nuclear Criticality Safety in Current Timeframe

The approach for showing to NRC that criticality is incredible during waste transport is rule-based (10 CFR §71.55, §71.59 and NRC regulatory guidance documents).[77;78] Similarly, the approach that DOE takes to show that criticality is incredible during WIPP operations is also rule-based based on DOE Standard 5506 and related DOE orders, which implement 10 CFR 810.[i]

SCALE can be used in both timeframes but the upper subcriticality limit (USL) at which a fissile configuration is considered critical differs for current and post-closure times. In an engineered system on the surface with humans present, great care is taken to conservatively define USL on the index of criticality (k_{eff}).[j] The USL is derived from the bias and uncertainties associated with SCALE, the underlying nuclear data, and the modeling fidelity.

Benchmark experiments that are similar to the case under evaluation are used to determine the bias in the SCALE criticality model and the bias uncertainty. In addition, an administrative factor is often added (i.e., USL = 1– (code bias + bias uncertainty + administrative factor) where only unfavorable code bias and bias uncertainty is considered, and 0.05 administrative factor applied when analyzing transportation events. For example, the USL is 0.9382 rather than unity for nuclear criticality safety analysis of TRUPACT-II package transporting CCOs.[81, Ch 6]

---

[i] Underlying these rules is the ANSI/ANS-8.1-2014 (*An American National Standard for Nuclear Criticality Safety in Operations with Fissionable Materials Outside Reactors*). As the title of the standard suggests, it describes rules for evaluating nuclear criticality safety during transportation or facility operations, not after closure of a geologic disposal system.[79]

[j] A fissile system is critical when a nuclear chain reaction is sustained, which is described by a neutron multiplication factor (k) of unity. Traditionally, k_∞ denotes a homogenous system of infinite extent and k_{eff} denotes a multiplication factor for a system of finite extent.[80, pp. 75-84] We also speak generally about the system reactivity (ρ^{crit}), which is related to k_{eff} (i.e., $\rho^{crit} = (k_{eff} - 1) / k_{eff}$). ANSI/ANS-8.1-2014 describes k_{eff} as "the ratio of the total number of neutrons produced during a time interval…to the total number of neutrons lost by absorption and leakage during the same interval."[79] This definition is conceptually useful here because neutron absorption and leakage play an important role in explaining behavior of a deformed CCO array.

Furthermore, worst-case scenarios of assembling fissile material are developed for the engineered systems (e.g., very conservative assumptions are made to fashion worst-case final accident configurations for transportation). These worst-case scenarios may be the result of unrealistic combinations of imagined events such as optimal moderation with water, polyethylene, and beryllium (even though the transport container must not leak in NRC impact tests). Furthermore, the fissile contents of each payload container may be unrealistically assembled after an accident. Otherwise, the payload container must maintain sufficient fissile separation with other payload containers in the transport accident. By showing that the calculated k_{eff} from nuclear criticality safety analysis of worst-case scenarios plus any Monte Carlo calculation uncertainty ($k_{eff} + 2\overline{\sigma}_{SCALE}$) is less than a conservatively defined USL, an analyst demonstrates that scenario does not result in criticality and, thereby, ensures safety when humans may be nearby.

V.B.2. Approximation of Mean Probability of Criticality after WIPP Closure

After closure of the WIPP geologic disposal system, EPA has regulatory authority and its standard 40 CFR 191 and implementing regulation 40 CFR 194 apply. Phenomenological modeling, such as salt-creep modeling described above in §IV, is necessary to predict a range of reasonable fissile configurations as natural processes cause the disposal system to evolve. Much uncertainty exists as to the plausible configurations. The factors that determine the uncertainty in reasonable configurations, such as variation in initial conditions of waste, variation in host rock characteristics (e.g., porosity, saturation, and host rock composition), and arrangement of geologic layers (e.g., position of clay layers and influence on salt creep) have similar or more influence on whether the system is critical than calculational biases and uncertainties in neutron/photon transport codes. (i.e., the uncertainty in specifying the physical state of the assembly after 1000 or more years, using Sierra/Solid Mechanics finite-element code system, is larger than the calculation uncertainty and bias in codes like SCALE). Furthermore, applicable criticality experiments are lacking.

EPA guidance implies that the mean of the probability of criticality provides an adequate estimate for screening a FEP such as criticality.[k] To elaborate, EPA invoked "reasonable expectation" as the standard of proof for compliance with the Containment Requirements specified in 40 CFR §191.13(a)). Reasonable expectation connotes a flexible standard of proof and use of central estimates when encountering unknowns. Furthermore, in the implementing regulations, EPA stated "Finally, the CCA [compliance certification application] must demonstrate that the mean of the population of CCDFs [complementary cumulative distributions functions] meets the containment requirements of §191.13…" Consequently, the WIPP Project does not develop worse-case scenarios that combine unrealistic combinations of imagined events to assemble fissile material for evaluating the potential for criticality after WIPP closure.[l]

This use of mean values for evaluating the probability of criticality after disposal and closure of the repository when personnel are absent, and the nearest humans are separated by 654 m of geologic strata such that consequences are minimal, differs substantially to screening criticality during TRU waste transportation and WIPP operations when humans may be nearby and consequences severe, as described above in §V.B.1.[17;83]

Although the mean is formally evaluated in PA, the mean is usually approximated in screening FEPs and scenarios (and we use the term representative to acknowledge this approximation). For example, we use a reasonable, representative configuration of compacted CCOs for disposal options, not the worst imaginable condition. We do not use extreme conditions of criticality from a uniformly compacted array for evaluating the criticality potential after closure of WIPP facility. Rather the conditions modeled using the uniformly compacted arrays provide assurance that the trends observed for representative irregular array do not dramatically change at extremes.

Granted, mildly conservative estimates of some parameters are used, and conservative initial and boundary conditions are set, but these parameters are not set at extremes. The purpose is not to produce a worse case but rather to ensure that the conditions will indeed bound a reasonable estimate of mean behavior.

V.C. CCO Conceptual Model for Criticality Evaluation

Whether a fissile assembly is critical depends upon the generation and interaction of neutrons with matter within and outside the assembly, which depends upon four general categories of parameters: (1) type, enrichment, mass, and form of fissile material; (2) material mixed with the fissile material and its overall concentration; (3) nearby material and its concentration

[k] The use of the mean probability for screening FEPs is emphasized by NRC in the Yucca Mountain Review Plan:[82, 2.2-14] "…the mean of the distribution range is to be used to screen an event from the performance assessment…"

[l] We avoid referring to this screening approach as a credibility argument herein because in nuclear criticality safety analysis for operating engineered systems the term connotes a rule-based approach with worst-case scenarios to demonstrate that the criticality scenario is incredible.

outside the fissile array, and (4) individual or array shape of fissile assembly (and thereby neutron leakage). In the criticality evaluation here, the parameters in the first category are fixed and parameters in the latter three categories varied to determine relative importance.

V.C.1 Plutonium, Waste Form, Volume, and Mass

Here, we are most interested in ^{239}Pu from atomic energy defense activities, in general, and surplus ^{239}Pu, in particular. In general, the contact-handled TRU waste disposed at WIPP is ~90% enriched in ^{239}Pu (and remote-handled TRU waste, 78% enriched).[11, Table I;84;85] However, some of the surplus Pu may have higher enrichment (e.g., >93%) and may dominate when disposed at WIPP. Other isotopes mixed with ^{239}Pu, such as ^{240}Pu, influence criticality. Thus, the transportation limit is set at 380 FGE of ^{239}Pu, rather than ^{239}Pu. The Pu FGE is the mass of ^{239}Pu plus a factor for other fissionable masses:[86] specifically, 0.113·^{238}Pu, 0.0225·^{240}Pu, 2.25·^{241}Pu, 0.00750·^{242}Pu, 0.900·^{233}U, 0.643·^{235}U, 0.0150·^{237}Np, 0.0187·^{241}Am, 34.6·^{242m}Am, 0.0129·^{243}Am, 15.0·^{245}Cm, 0.500·^{247}Cm, 45.0·^{245}Cf, and 90.0·^{251}Cf. This approach for the fissile content bounds isotopic influences including changes with the decay over the 10^4-y regulatory period. Hence, for criticality evaluation, the fissile content is modeled as 100% ^{239}Pu. The Pu mass is set at the transportation maximum of 380 ^{239}Pu FGE per CCO. The volume of TRU waste disposed at WIPP in CCOs is the inner 0.0128-m^3 volume of the CCC.

For the surplus Pu that may come to WIPP, ~6.4 t is already oxidized, the remainder will also be oxidized to plutonium dioxide (PuO_2). Granted some generic Pu waste forms that use the CCO may be metallic Pu or Pu with water of hydration or hydroxyl groups (i.e., $PuO_2(OH)_2{\cdot}H_2O$ or $Pu(OH)_4$), but the mineral form only influences criticality limits when the mixture is severely under moderated for highly enriched ^{239}Pu.[15, Fig. 8] The CCO array must be fairly well moderated to be critical. The CCO array is far from critical when severely under moderated (see §V.B.1). Therefore, all Pu is modeled as PuO_2.

V.C.2. Material Mixed with Pu Waste

V.C.2.a. Hydrogenous Material

The POC analysis for CRA-2019 examined three hydrologic regimes: (1) dry conditions exterior to the container up to 1000 years, (2) a transitional phase with influx of some brine that partially saturates pores and initiates some container corrosion up to 2000 years; and (3) a final phase with influx of sufficient brine to saturate containers and complete container corrosion after 2000 years. The hydrologic regime of the fissile region (Region 1) and the reflector (Region 2) surrounding the fissile region change to reflect the room evolution through the three regimes. The POC analysis clearly showed that introduction of brine into the disposal room reduced k_{eff} in the second regime, and greatly reduced k_{eff} in the third regime.[11]

Hence, the CCC criticality evaluation here focuses on the first hydrologic regime with dry conditions outside the CCC in a disposal room (during initial salt compaction) with water and polyethylene only inside the CCC in the fissile region. However, brine (density of 1160 kg/m^3) inside and outside the CCC is also considered in one case.

For most simulations, the criticality evaluation includes up to 3 kg of 100% water or 100% polyethylene (CH_2) moderator inside the fissile region, but for a few simulations the evaluation also includes up to 6 kg of moderator. Water is only present as adsorbed water because the WIPP WAC limits free water to ≤ 1 wt. % to prevent (a) spillage contaminating the repository during operations and (b) undue container corrosion prior to salt creep entombing the containers. Polyethylene (CH_2) is generally only present in CCCs as thin bagging material for Pu and Pu-contaminated articles and cannot reasonably exceed 25% of the available volume. Polyethylene is a slightly better moderator than water and lowers the critical mass.[87] Other hydrocarbons and polymer compounds are usually bound by polyethylene.[88]

V.C.2.b. Beryllium

Previous sensitivity studies with POCs showed only a small influence of beryllium (Be—density of 1848 kg/m^3) or beryllium oxide (BeO) regardless of whether mixed with the fissile material or around the fissile assembly in geologic systems;[11;66] however, Be/BeO may act as a special moderator when the system is highly under moderated with hydrogenous material and so it is included here. The contents of a CCO is not authorized to contain >1 wt. % of Be/BeO,[11, Table VI;86] which translates to 0.545 kg as follows: the CCO empty mass is 104.3 kg; the maximum gross mass is 158.8 kg; thus, the maximum waste mass is 54.5 kg; hence, the maximum authorized Be/BeO content is 0.545 kg. For the criticality evaluation, a slightly larger 0.585-kg per CCO is used (7% increase).

V.C.2.c. Carbon/Graphite Filler

The criticality evaluation examines the influence of other materials on the allowable mass of hydrogenous material in CCCs. As a surrogate for other material, carbon/graphite filler (density of 2300 kg/m^3) is included in the Pu fissile region in some studies. Other material present within the CCC often increases the minimum critical mass. However, adding graphite to the Pu-water-polyethylene mixture likely has only a small influence on the minimum critical mass and, thus, thought to be bounding, based on a Pu-carbon-fluid ideal system (Fig. 15).

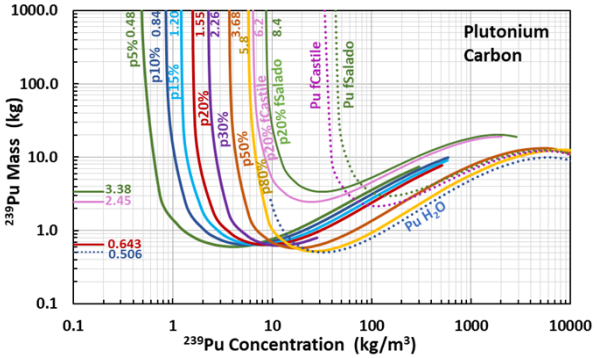

Fig. 15. Although critical asymptote greatly decreases, Pu critical mass in carbon does not change much for porosity between 5% and 80% filled with water or WIPP brines.[14, Fig. 11]

V.C.2.d. Cement Filler Material

In past analysis of surplus plutonium waste, a cement material has been used to bound criticality behavior of the adulterant that will actually be mixed with Pu in the fissile region to prevent ready diversion of the Pu for nefarious purposes.[62] The cement filler material is composed of 58.5 wt.% SiO_2, 19.8 wt.% MgO, 11.7 wt.% Al_2O_3 and 10 wt.% H_2O with density of 2400 kg/m^3.[62, App A] The cement filler minimum ^{239}Pu mass in the cement filler is greater than in carbon/graphite when water is the fluid (i.e., 0.95 kg—Fig. 16—versus 0.643 kg—Fig. 15). However, carbon/graphite and the cement filler have a similar influence on the system reactivity in Salado brine (e.g., 3.2 kg versus 3.38 kg minimum ^{239}Pu in cement filler and carbon/graphite, respectively). Likewise, carbon/graphite and the cement filler have similar influence on reactivity of compacted CCO array in WIPP brine, as discussed in §V.D.

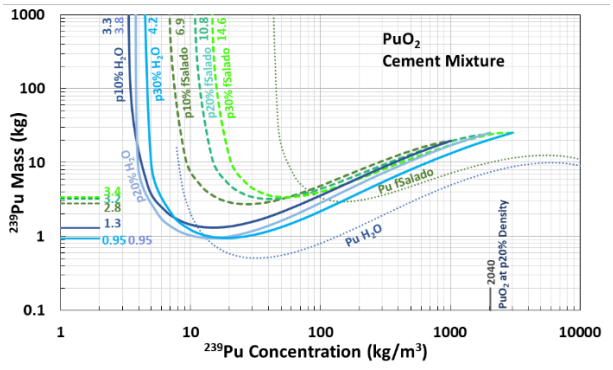

Fig. 16. Critical limits of ^{239}Pu in CCO cement mixture similar to those in carbon/graphite mixture in Salado brine at 20% porosity.[14, Fig. 15;89, Fig. 17b]

V.C.3. Material Surrounding Individual CCCs

Material in between individual CCCs and surrounding the fissile assembly may either reflect neutrons back into the fissile mass assembly or absorb neutrons and, thereby, promote or suppress criticality, respectively. In the criticality evaluation, the fissile material (Region 1) inside the CCC is surrounded by reflecting/absorbing material (Region 2). A 10-m layer of salt (modeled as pure NaCl—density of 2165 kg/m^3) is around the reflecting material (Region 3—Fig. 17).

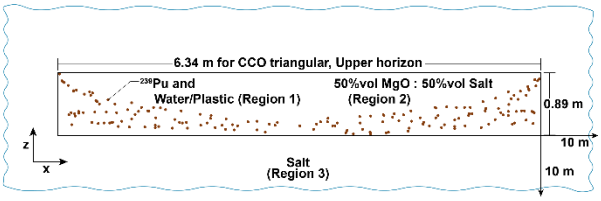

Fig. 17. Three material regions of criticality model where dimensions of Region 2 defined by maximum extent of the coordinates for CCO centers, which change somewhat per geomechanical simulation; dimensions shown for CCOs in upper horizon initially as triangular array.

One reflecting/absorbing material is 304L stainless steel (Schedule 40) of the CCC. Stainless-steel handling cans inside the CCC and the CCO carbon-steel overpack drum are not usually included with the discrete reflector of the CCC. The 4 end plates and 6 ring plates of ¾-inch plywood spacers are also not included (~15.2 kg plywood per CCO if plywood density is ~387 kg/m^3).

A second reflector material is magnesium oxide (MgO—density of 1450 kg/m^3), which is placed on the top tier of containers in polypropylene bags. As the room closes, MgO filters down between the CCOs. MgO is an engineered barrier placed in the disposal rooms to combine with any CO_2 formed during degradation of organic matter such that highly soluble Pu carbonate species are not formed.[11] In the criticality evaluation, MgO is usually mixed with salt in Region 2 in a volume ratio of 1:1 (with calculated density of 1737 kg/m^3);[24, §4] however, sensitivity analysis with 100% salt shows that the influence of MgO to reactivity is not large (as discussed in §VI.A.2).

V.C.4. Geometry: Irregular CCO Array Configuration

The coordinate positions of CCCs for the irregular, non-uniformly compacted array is used in the criticality evaluation. The dimensions of Region 2 are defined by the maximum extent of the coordinate positions of the corresponding simulation (e.g., CCO emplaced in upper horizon as triangular array—Fig. 17). The ~2-m slice uses periodic boundary conditions to represent a room segment of infinite extent down its axis (*y*-direction), but also examines the influence of mirror boundary conditions.[66, Table E-1]

V.C.5. Geometry: Idealized Uniform Array

A criticality evaluation of an idealized regular, uniformly compacted CCO array is also conducted to more fully explain behavior observed in the irregular, non-uniformly compacted array. This supporting uniform analysis assumes that the CCO array remains intact (i.e., CCOs remain vertical and in three tiers); only the spacing between the CCC decreases. The CCOs are placed in a triangular array with alternating 17 and 18 CCOs per row when uniformly spaced.

The uniform criticality evaluation uses both a 25% and 50% reduction in uniform horizontal spacing. The 50% reduction corresponds to the early ORNL criticality evaluation using uniformly compacted CCO arrays (Table I).[62;67] A 50% reduction corresponds to 28.6-cm diameter decrease of the CCO inner 57.15-cm radius (Fig. 1). The 50% reduction bounds the observed range for the irregular array (i.e., between 39.0% and 42.4% horizontal closure (Fig. 19).

The reasonableness of the 25% lower bound of overall compaction observed at the center of the room is explained as follows. Although the decrease in vertical spacing could follow a similar idealized adjustment, the criticality evaluation sets the CCC collapse to the height of the waste inside the CCC.

The width of the gap between the salt wall and CCOs is (Fig. 18)[65]

$$L_x^{gap} = L_x^{room} - L_x^{array} \tag{7}$$

where

$$L_x^{array} = n_x^{CCO} L_x^{CCO}$$

and n_x^{CCO} is 14 CCO/row.

The total room closure is the sum of the closure on the left and right, and where no closure occurs down the axis of the room segment (i.e., plane strain) (Fig. 18):

$$\delta_x = \delta_x^{left} + \delta_x^{right} \tag{8}$$

$$\delta_y = 0 \tag{9}$$

The corresponding compaction of the intact array of CCOs is

$$\delta_x^{array} = \left((\delta_x - L_x^{array}) + \left| \delta_x - L_x^{array} \right| \right) / 2L_x^{array} \tag{10}$$

$$\delta_y^{array} = 0 \tag{11}$$

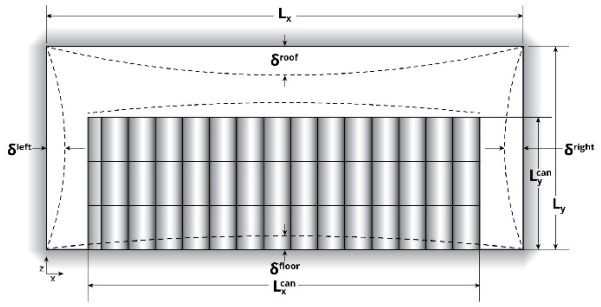

Fig. 18. Room closure of uniform array of CCOs.[65]

The average uniform horizontal compaction of CCCs of all four cases initially arranged in triangular and hexagonal arrays in the upper and lower horizons is 26.85% (Fig. 19) and corresponds to 15.4-cm diameter reduction of the 57.15-cm diameter CCO (Fig. 1). The percentage compaction includes the emplaced void space within the room, which shows as an offset in Fig. 19.

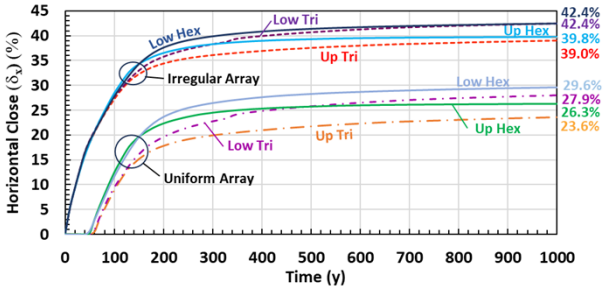

Fig. 19. Range of horizontal room closure in modeled irregular and idealized uniformly compacted CCO arrays initially emplaced as triangular and hexagonal arrays in upper and lower repository horizons.[65, Fig. 10]

V.C.6. Geometry: Fissile Shape

The criticality evaluation places cylinders, bound by the original CCC diameter, or spheres of fissile material at the centers of the deformed CCO arrays. For the cylinders and spheres, the ^{239}Pu waste form in any handling convenience containers is combined and centered in the CCC pipe, since a combined mass of fissile material is more applicable to a generic waste and concentrating the Pu mass is more conservative.

The diameter of the CCC, inside the CCO, constrains the fissile shape until the CCC corrodes. To be consistent with no gas generation and thereby maximum salt-creep compaction, no CCC corrosion is assumed. Yet, a sphere (usually the most reactive shape for criticality evaluation) optimally moderated with hydrogenous material cannot fit inside a 15.4-cm diameter CCC (7.7 cm radius). A sphere with insufficient hydrogenous material is often less reactive than a cylindrical shape. Hence, cylinders of three radii (4.80, 6.25, 7.70 cm) are used, where the cylinder height is

determined by the amount of ^{239}Pu, moderator, and filler in the fissile Region 1. For the criticality evaluation with cylinders, the model uses the final orientation of the CCC.

An *unconstrained* spherical shape for the fissile Region 1 (where the radius is determined by the ^{239}Pu, moderator, and filler in the CCC) is also examined because a spherical shape avoids making assumptions as to the initial distribution of Pu in generic waste forms and the compaction of that material within the CCC from salt creep.

V.D. Room Reactivity with and without Filler Material in Fissile Region

V.D.1. Carbon and Cement Filler

Without any filler homogeneously mixed in the fissile Region 1, the allowable hydrogenous moderator in the CCO at emplacement is ≤1.69 kg for the representative irregular, non-uniformly compacted array (Fig. 20 and Table II). For the more reactive bounding regular, uniformly compacted CCO array, the allowable hydrogenous moderator is ≤0.82 kg. In Fig. 20a, the variation band at each discrete moderator mass is caused by the variation in all other parameters examined in the criticality evaluation besides the presence or absence of 2 kg of filler. The maximums are more readily observed in Fig. 20b.

Including non-hydrogenous homogeneous filler in the fissile region substantially reduces the reactivity of an irregular non-uniformly and regular, uniformly compacted CCO array, whether the filler material is conservatively modeled as graphite or cement material to represent the adulterant material (§V.C.2.c and §V.C.2.d).

For an irregular, nonuniformly compacted array, adding 2 kg of filler decreases k_{eff} by 0.03 near k_{eff} of unity and increases the maximum mass of allowed moderator by 11% from 1.69 kg to 1.88 kg (Fig. 20 and Table II). For a regular, uniformly compacted array, adding 2 kg of either graphite or cement material decreases k_{eff} by 0.08 and increases the maximum allowable moderator mass by 37% from 0.82 kg to 1.12 kg.

For an irregular compacted array, adding 4 kg of filler increases the maximum mass of allowed moderator by 20% (approximately linear increase from 2 kg filler) from 1.69 kg to 2.02 kg (Fig. 21 and Table II). For a uniformly compacted array, adding 4 kg graphite/cement material increases the maximum allowable moderator mass by 76% from 0.82 kg to 1.44 kg (again approximately linear increase from 2 kg filler—Table II).

The maximum k_{eff} in the irregular array for either the 4 kg of cement filler or 4 kg of graphite filler are similar (Fig. 21). The allowable moderator mass is 2.16 for cement filler and 2.02 kg for graphite filler at k_{eff} of unity (7% decrease).The same is true for the uniform array. The allowable moderator mass is 1.49 kg for generic/cement filler and 1.44 kg for graphite filler at k_{eff} of unity (3.4% decrease). The influence of the two fillers is primarily the change in the volume of the fissile region and the corresponding change in neutron leakage. This geometric influence on leakage dominates over the difference in reflection or absorption of neutrons by the two materials.

However, for stainless steel as a filler, the reflection/absorptive of iron have more influence on an irregular array (Table II). For the irregular compacted array, the addition of a 1-kg iron filler (from stainless steel) is about as effective in decreasing reactivity as 2-kg of non-hydrogenous graphite filler. For the regular compacted array, the addition of a 1-kg iron filler is 17% less effective in decreasing reactivity as 2-kg of graphite filler (1.12 kg versus 0.93 kg allowable moderator).

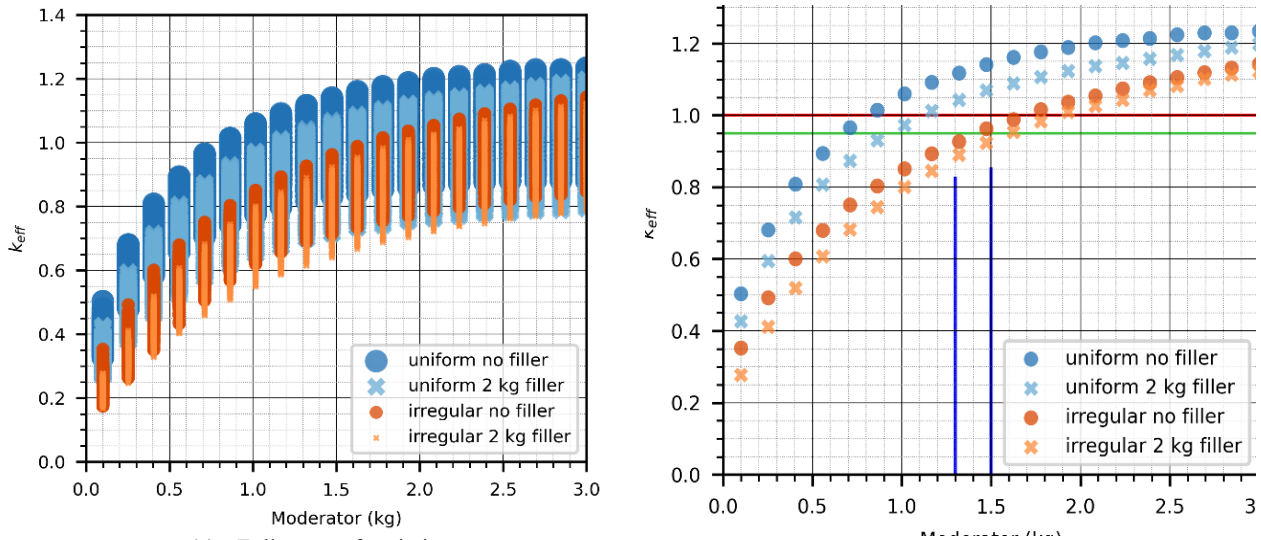

(a) Full range of variation (b) Maximum values

Fig. 20. Adding 2-kg graphite or cement filler to fissile region moderately reduces reactivity of irregular, non-uniformly compacted CCO array; similar trend observed for more reactive regular, uniformly compacted CCO array (data from criticality calculations described by Brickner et al.[24]).

Table II. Allowable Moderator Mass per CCO with Non-Hydrogenous Filler and Metal Mixed in Fissile Region with Subcriticality Limit of Unity

CCO Array	Allowable Moderator Mass per CCO in Upper Horizon (kg)					
	No Filler		Graphite Filler		Cement Filler	Stainless Steel
	Hex	Tri	2 kg	4 kg	4 kg	1 kg Material
Irregular with spheres	1.69	1.74 (3%)	1.88 (11%)	2.02 (20%)	2.16 (28%)	1.86 (10%)
Uniform with cylinders		0.82	1.12 (37%)	1.44 (76%)	1.49 (85%)	0.98 (13%)

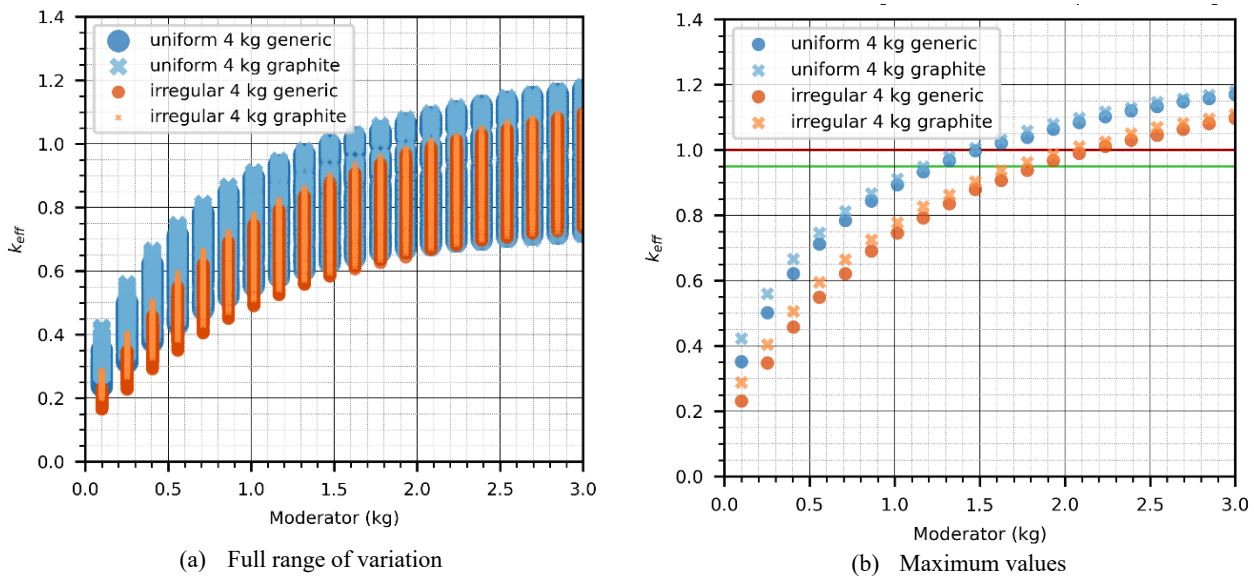

(a) Full range of variation (b) Maximum values

Fig. 21. Adding 4 kg filler reduces reactivity somewhat more for irregular non-uniformly and regular uniformly compacted CCO arrays (data from Brickner et al.[24]).

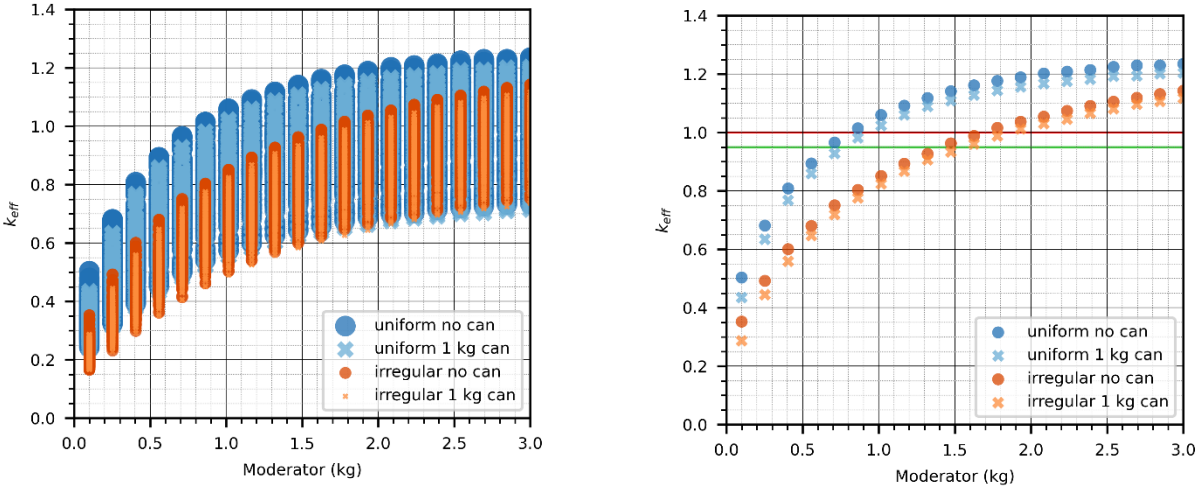

(a) Full range of variation (b) Maximum values

Fig. 22. Stainless steel material from handling canisters mixed in fissile region reduces reactivity of uniform array and irregular CCO array (data from Brickner et al.[24]).

V.D.3. Mixing of Pu, Moderator, and Filler

In most criticality evaluations discussed here, Pu, moderator, and filler in the fissile region is modeled as a homogeneous mixture (with ^{239}Pu mass fixed at 380 g). Homogeneous mixtures of Pu (and U) at high enrichments are more reactive than heterogeneous mixtures.[89, Fig. 23]

V.D.4. Influence of Spherical and Cylindrical Fissile Region on Reactivity

For a fissile region *constrained* by the CCC with a 7.7 cm maximum inside radius, a cylindrical representation is more reactive for both the irregular, non-uniformly compacted and the regular, uniformly compacted CCO array (Fig. 23). The cylindrical representation has a wide range of reactivity because both the radius and height vary.

However, an *unconstrained* spherical representation of the CCO fissile region is slightly more reactive than the cylindrical representation for the irregular CCO array (Fig. 24). This analysis uses the unconstrained spherical representation for the irregular CCO array, as a convenient modeling conservatism, because the difference is small (Δk_{eff} of 0.025 near k_{eff} of unity, which translates into allowable moderator of 1.77 kg for cylinder versus 1.69 kg (5% difference) for unconstrained sphere representation).

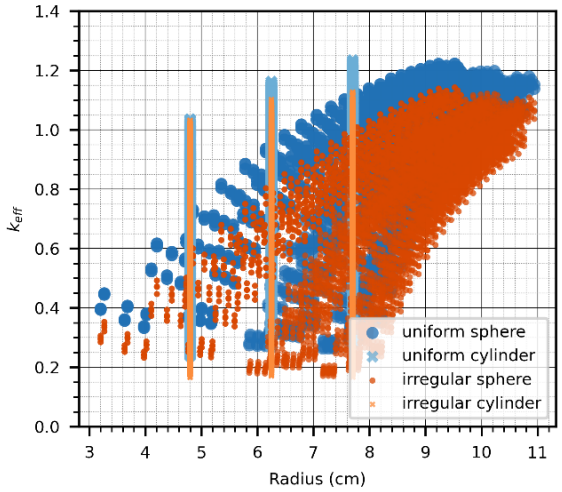

Fig. 23. Cylindrical representation most reactive if fissile region constrained by 7.7 cm radius of CCC in both irregular, non-uniformly compacted and regular, uniformly compacted CCO array (data from Brickner et al.[24]).

For the uniformly compacted array, a cylindrical representation of the fissile region is more reactive than an unconstrained spherical representation (k_{eff} is 0.92 for unconstrained spherical representation versus unity for a cylindrical representation at allowable moderator mass of 0.82 kg—Fig. 25b).

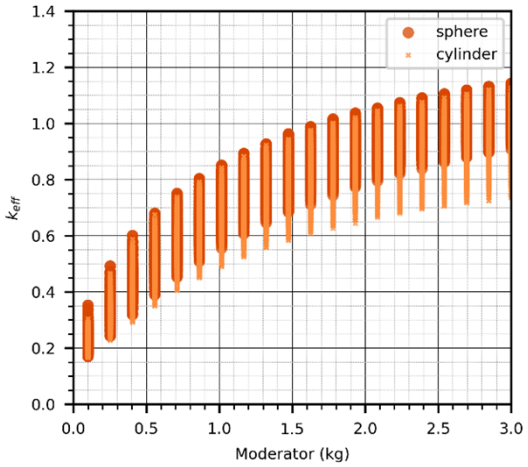

(a) Full range of variation

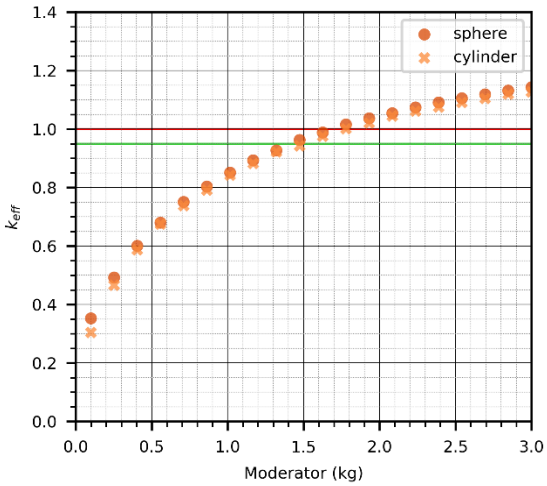

(b) Maximum values

Fig. 24. Unconstrained spherical fissile region slightly more reactive than cylindrical fissile region for irregular, non-uniformly compacted CCO array (data from Brickner et al.[24]).

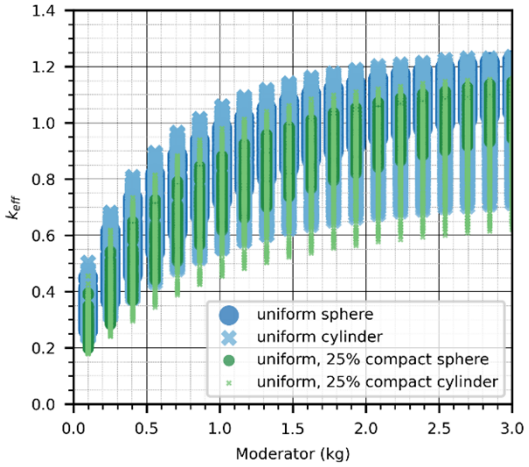

(a) Full range of variation

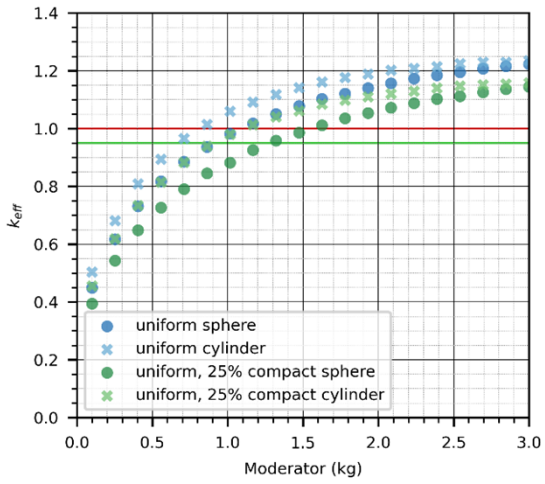

(b) Maximum values

Fig. 25. Cylindrical representation of fissile region for 50% and 25% uniformly compacted array remains more reactive than unconstrained sphere (data from Brickner et al.[24]).

In most analysis with the uniformly compacted array, a bounding horizontal compaction of 50% is used. However, as shown above (§V.C.5) the actual horizontal compaction of a uniformly compacted CCO array is much closer to 25% (Fig. 19). For 25% compaction, the corresponding allowable moderation is 1.1 kg for cylindrical fissile region (Fig. 25), an 35% increase from 0.82 kg (Table II).

For the uniformly compacted array, the most reactive cylindrical CCO array changes from the smallest 4.8-cm radial cylinder at low moderation to the largest 7.7-cm radial cylinder a high moderation (Fig. 26). The behavior is similar for irregular, non-uniformly compacted CCO array but the transition to the largest radius occurs at higher moderation.

The uniformly compacted array results suggest an allowable threshold of 0.82 kg moderator (Table II) when no credit is taken for graphite/cement filler but a large benefit for accounting for the graphite/cement filler (76% increase in moderator mass) whereas the more representative irregular array has a high threshold of allowable 1.69 kg moderator when no credit is taken for graphite/cement filler and modest benefit for accounting for either the graphite/cement filler (18%).

The reason for the stronger influence of the filler for the uniform array is because the disk-like cylinders of the fissile region (which are most reactive for the uniformly compacted array) are stacked on top of each other to form essentially a single stub cylinder (with similar height to diameter ratio) with essentially the ^{239}Pu mass of three CCOs.[90, Fig. 1]

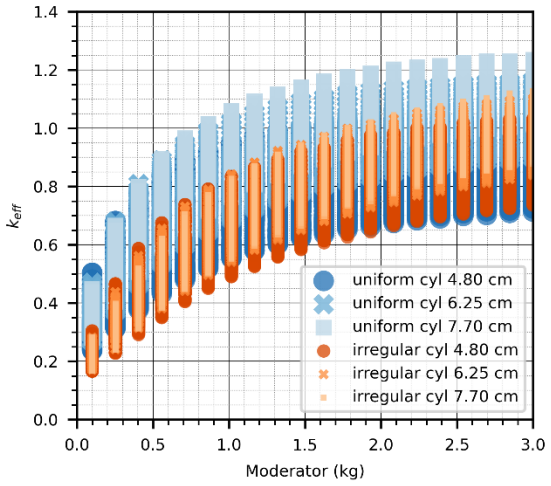

(a) Full range of variation

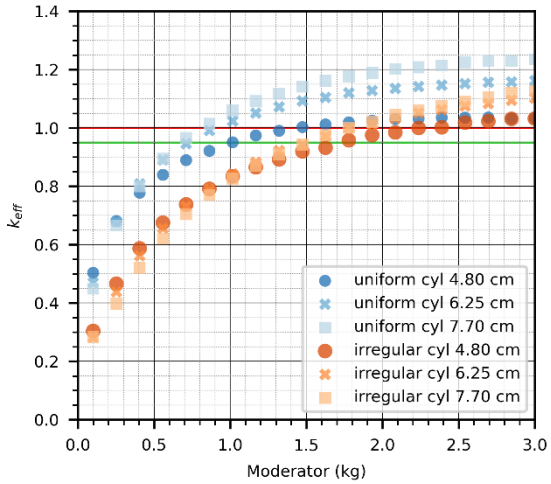

(b) Maximum values

Fig. 26. Largest reactivity of irregular, non-uniformly compacted CCO array with cylindrical fissile region changes from smallest radius at low moderation to largest radius at high moderation; behavior is similar for uniformly compacted CCO array but the transition to the largest radius occurs at lower moderation (data from Brickner et al.[24]).

The reactivity greatly decreases (leakage greatly increases) for the uniformly compacted array as the height of the cylinder is increased to include the graphite/cement filler. To elaborate, the cylindrical fissile region no longer has similar height to diameter ratio because the cylindrical fissile region elongates axially as filler is added since the cylinder cannot expand radially beyond the maximum CCC diameter.

In contrast, the irregular non-uniformly compacted array with spheres is scattered about the room and the reactivity does not change much (i.e., leakage in the system does not greatly increase) as the fissile region radius increases to accommodate the filler.

VI. INFLUENCE OF OTHER PARAMETERS ON ROOM REACTIVITY WITHOUT B_4C

VI.A. Room Reactivity with Material in Fissile Region

VI.A.1. Water and Polyethylene Moderator

As expected, water as the sole moderator in the fissile region is much less reactive than polyethylene as moderator (Fig. 27): k_{eff} is reduced by 0.125 near k_{eff} of unity and the allowable moderator mass increased by ~50% for both the irregular, non-uniformly compacted and regular, uniformly compacted CCO array.

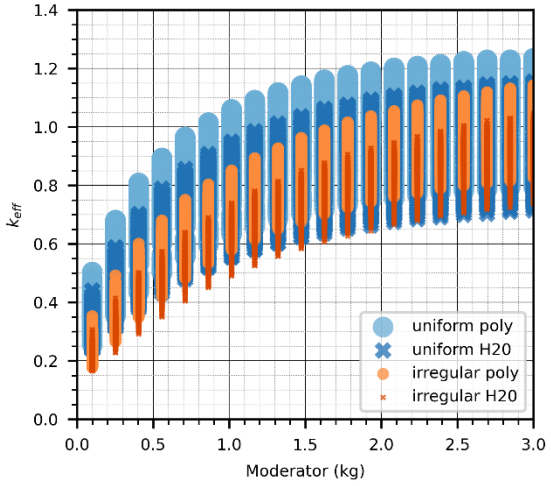

(a) Full range of variation

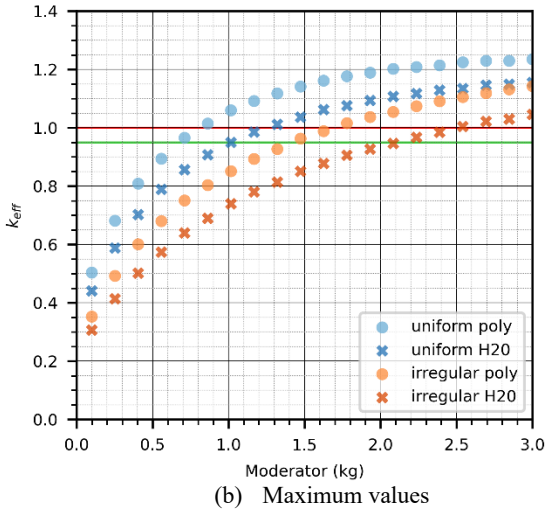

(b) Maximum values

Fig. 27. CCO array with water moderator less reactive than polyethylene moderator for irregular array; uniform array follows a similar trend (data from Brickner et al.[24]).

Specifically, the allowable moderator mass substantially increases from 1.69 kg polyethylene moderator to 2.51 kg water moderator for the irregular CCO array (Fig. 27). For the uniformly compacted CCO array, the allowable moderator mass increases from 0.82 kg polyethylene moderator to 1.26 kg of water.

VI.A.2. Density and Salt/MgO Proportion

In the criticality evaluation model, ~118 kg MgO per CCO is in a disposal room as follows: the volume of the reflector box at 1000 years when modeling 168 CCOs is ~12.4 m^3 (i.e., 6.05-m length, 0.95-m height, and 2.08-m model width—Fig. 17). For MgO with a grain density of 3600 kg/m^3, the MgO mass in one-half of the reflector box is 33 t at the final total room porosity of 0.261 in recent calculations (versus 0.243 in CCA-1996)[11;91, Fig. 3-1, Fig. 3-15] because MgO and salt is mixed in a 1:1 ratio.

The specific amount of MgO in a WIPP disposal room is determined by the container contents and is adjusted for each emplaced container batch. The MgO mass emplaced in a disposal room (m_{MgO}) is calculated based on the disposal room mass of cellulose (m_{cell}), rubber (m_{rub}), and plastics (m_{plstc}) with a safety factor (f_{MgO}^{safety}), and assumes a one-to-one correspondence between CO_2 produced and carbon in (a) cellulose ($C_6H_{10}O_5$) waste, (b) rubber waste, and (c) factor of 1.7 for plastic waste:[92;93]

$$m_{MgO} = 6 f_{MgO}^{safety} \left(m_{cell} + m_{rub} + 1.7 m_{plstc} \right) \bullet \frac{40.3 \text{g/mole MgO}}{162 \text{ g/mole cellulose}} \quad (13)$$

After May 2008,[94] a safety factor of 1.2 is maintained above the estimated amount necessary to react with the cellulose, plastic, and rubber contents in a container.

CCCs containing surplus Pu have only a small amount of plastic used to bag the handling cans (to reduce the possibility of Pu contamination in the packaging facility). For 0.40 kg polyethylene per CCO and 15.2 kg of plywood per CCO, 28.4 kg of MgO per CCO is required (or about one 1905-kg MgO sack on every third 7-pack of CCOs stacked in 3 tiers). For 168 CCOs, 4.8 t is required versus 33 t modeled. Thus, ~7 times more MgO is modeled in a room segment than is necessary.

MgO potentially increases reactivity by reflecting neutrons. Nonetheless, the influence of the MgO at a mixing ratio of 1:1 is small since the reactivity with 100% salt is only slightly less (i.e., k_{eff} decreases by 0.05 near k_{eff} of unity but half or 0.025 of the decrease in k_{eff} is due to the necessary increase in the area of Region 2 to accommodate the changes in material volume—Fig. 28).[m] Reducing the density of MgO/Salt mixture by one-half, assuming salt consolidation is not complete, also has a small influence (i.e., k_{eff} decreases by 0.08 near k_{eff} of unity—Fig. 28).

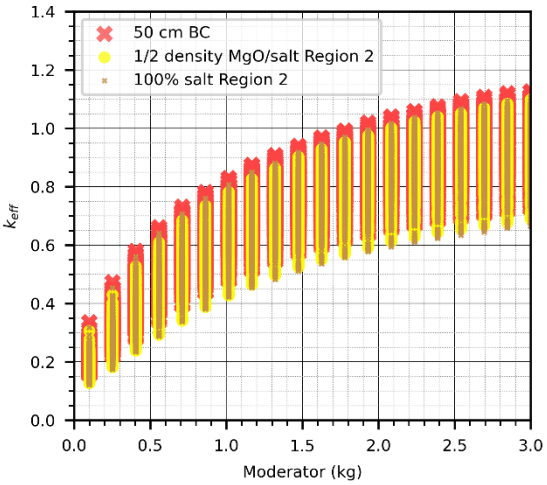

(a) Full range of variation

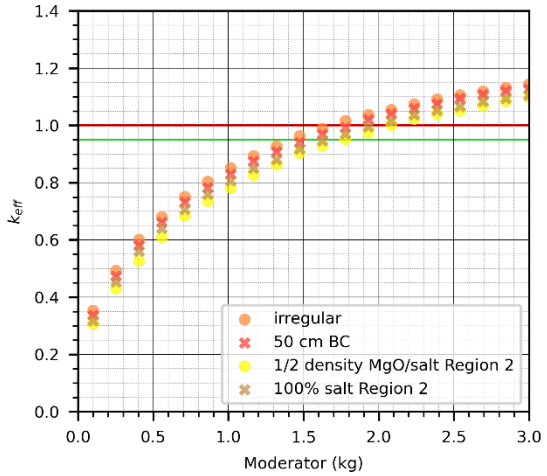

(b) Maximum values

Fig. 28. Influence of changes in MgO in Region 2 on system reactivity is noticeable but small (data from Brickner et al.[24, App. L]

VI.A.3. Beryllium Influence

Excluding Be/BeO special reflector material from the fissile region has little influence on reactivity near k_{eff} of unity (k_{eff} decreases by <0.01 and allowable moderator increases by ~0.03 kg) for both the irregular and uniform CCO array (Fig. 29). However, the influence of Be/BeO is stronger away from a k_{eff} of unity. Excluding Be/BeO

[m] When examining the reactivity difference between salt and MgO, the boundary of Region 2 was enlarged to 50 cm to accommodate changes in material volume. The slight decrease in reactivity from the enlarged boundary condition is displayed in Fig. 28b for a more meaningful comparison to the decrease in reactivity from varying (a) proportion of salt and (b) salt and MgO density.

slightly reduces reactivity at low and high moderation for the uniformly compacted array and reduces reactivity at low moderation for the irregular array.

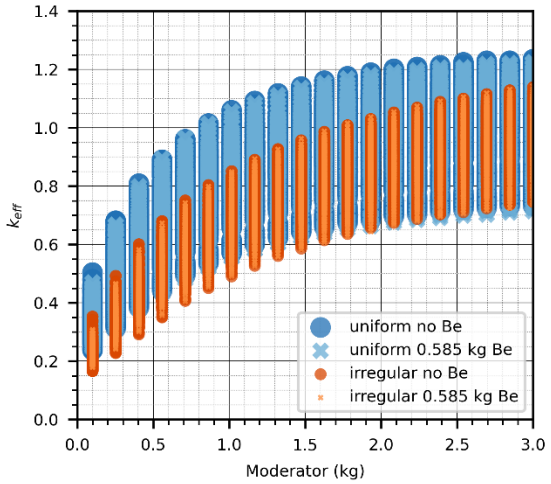

(a) Full range of variation

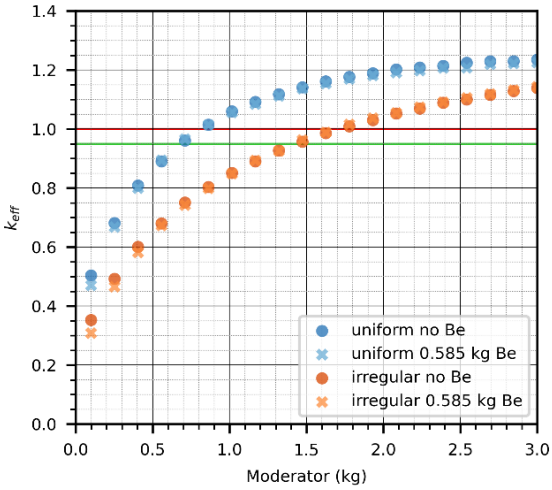

(b) Maximum values

Fig. 29. Adding 0.585 kg Be/BeO has little influence on reactivity for k_{eff} near unity but does slightly reduce reactivity below and above k_{eff} of unity (data from Brickner et al.[24]).

VI.B. CCC Stainless Steel around Fissile Region

For the irregular array base case, a 0.71-cm discrete stainless-steel reflector is set around the fissile Region 1 (Fig. 17), which is the thickness of the CCC. The allowable moderator mass is 1.69 kg for an unconstrained sphere. If the stainless-steel reflector is removed, k_{eff} decreases by 0.05 and the allowable moderator mass increases 11% to 1.87 kg. The stainless-steel reflector increases reactivity by reflecting neutrons back into the fissile region.

If the stainless-steel reflector around the fissile Region 1 is doubled to 1.41 cm to account for the possibly of a handling can inside the CCC, the corresponding allowable moderator mass decreases 5% to 1.61 kg (Fig. 30).[24, App. O] However, a base-case moderator mass of 1.61 kg is not used herein since a handling can is not necessarily used for generic waste. Other conservatisms in the analysis compensate if a handling can or other metal is present in the CCC. For instance, recall a sphere with unconstrained diameter was used in the analysis, which increase moderator mass by ~5% over the more realistic sphere constrained by the CCC diameter (§V.D.4).

When 2 kg of filler is added to the fissile Region 1 for the irregular array with 0.71-cm discrete reflector, the behavior switches: the reactivity decreases and the allowable moderator mass increases 11% to 1.88 kg from 1.69 kg (Table II). With 2-kg filler and a 1.42-cm discrete reflector, the allowable moderator mass increases 12% to 1.81 kg from 1.61 kg (Fig. 30d). Although the presence of a reflector still increases reactivity, the addition of the 2-kg filler dominates the behavior by isolating neutron interactions and so the allowable moderator mass increases overall.

For the uniformly compacted array, a 0.71-cm thick stainless steel CCC around the fissile region slightly decreases k_{eff} by 0.020 at k_{eff} near unity (i.e., decreases reactivity) and increases the allowable moderator mass 7% to 0.88 kg from 0.82 kg with no discrete reflector. [24, App. O] A 1.42-cm thick reflector increases the allowable moderator mass 12% to 0.92 kg, and a 2.13-cm thick reflector further increases the allowable moderator mass 17% to 0.96 kg (Fig. 30b).

The decrease in reactivity from only the reflector contrasts with the irregular array. For the uniform array, adding a stainless-steel reflector increases neutron reflection but the reflector also increases isolation. Between these two competing effects of the reflector, the increased isolation is more important for the uniform array and so the reactivity decreases and the allowable moderator mass increases with the increase in reflector thickness. That is, neutron interactions and reactivity benefits greatly from proximity of fissile regions in the uniformly compacted array. The stainless-steel reflector decreases proximity.

When filler mass is added to the fissile Region 1, neutron isolation is further increased, which is like the behavior of the irregular array. With no reflector, the allowable moderator mass increases 37% from 0.82 kg to 1.22 kg with 2-kg filler (Fig. 30d). With 0.71-cm discrete reflector, the allowable moderator mass increases 30% from 0.88 kg to 1.14 kg with 2-kg filler. With 2.13-cm discrete reflector, the allowable moderator mass increases 25% from 0.96 kg to 1.20 kg with 2-kg filler.

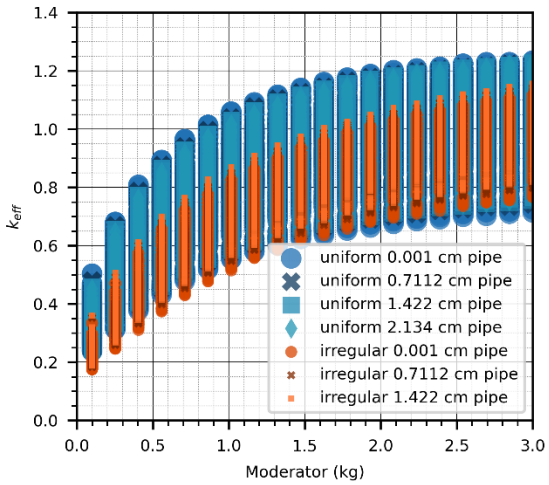

(a) Full range of variation without filler

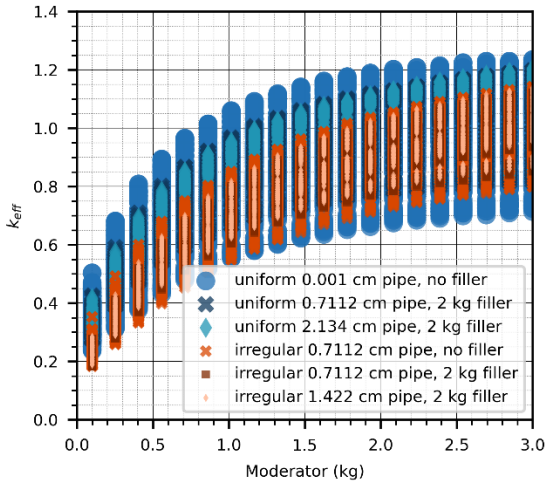

(c) Full range of variation with filler

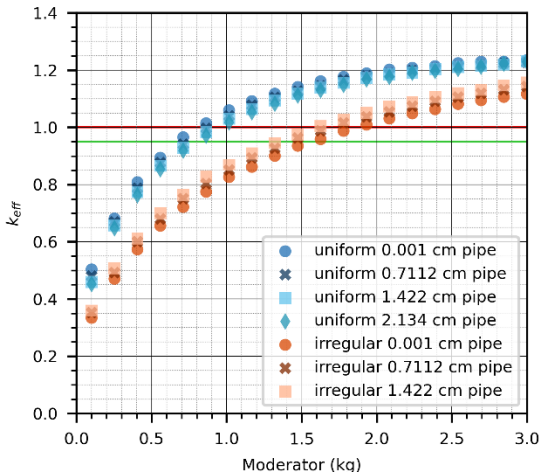

(b) Maximum values without filler

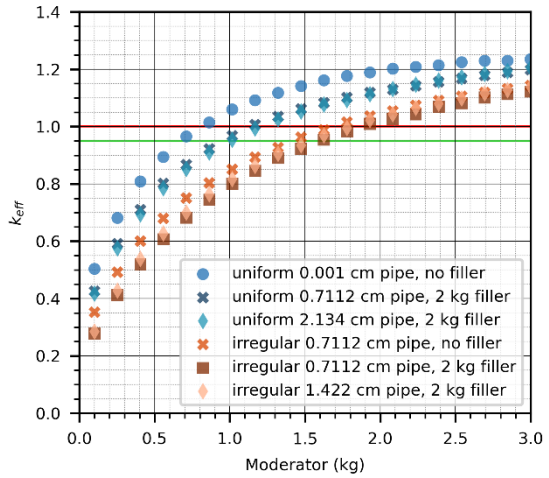

(d) Maximum values with filler

Fig. 30. Stainless-steel reflector, twice thickness of CCC, slightly changes the reactivity of irregular and uniformly compacted CCO arrays (data from Brickner et al.[24]).

VI.C. Uncertainty from Geologic Strata Arrangement

The CCO final configuration in upper horizon is more reactive; k_{eff} is ~0.025 larger in the upper horizon near k_{eff} of unity, which translates to an allowable moderator mass of 1.69 kg for CCOs placed in the upper horizon and 1.85 kg for CCOs in the lower horizon (9% increased moderator mass for lower horizon—Fig. 31 and Table II).

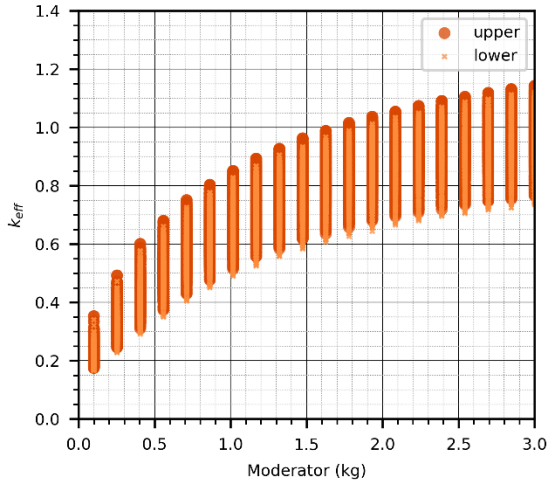

(a) Full range of variation

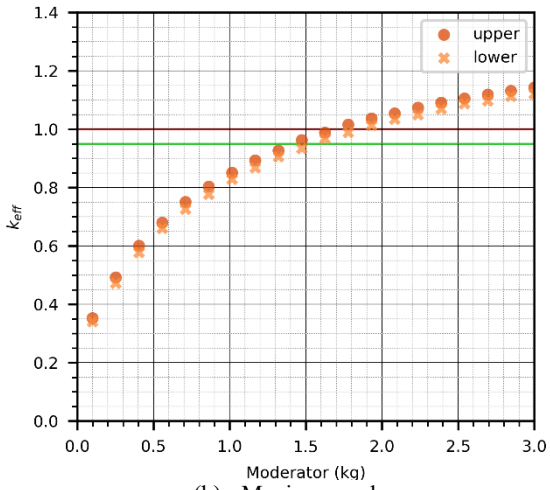

(b) Maximum values

Fig. 31. Reactivity of irregular CCO array in upper horizon greater than in lower horizon of repository when initially emplaced in hexagonal array (data from Brickner et al.[24]).

VI.D. Minor Reactivity Differences between Hexagonal and Triangular Arrays

The slightly wider range in closure and concentration of CCOs initially emplaced in a hexagonal array translates into a slightly wider range of reactivity than CCOs initially emplaced in a triangular array (Fig. 32). In turn, the maximum moderator mass is 1.69 kg for a hexagonal array (§IV.D.1) and slightly increases to 1.74 kg for a triangular array without filler (3% increase—Table II).

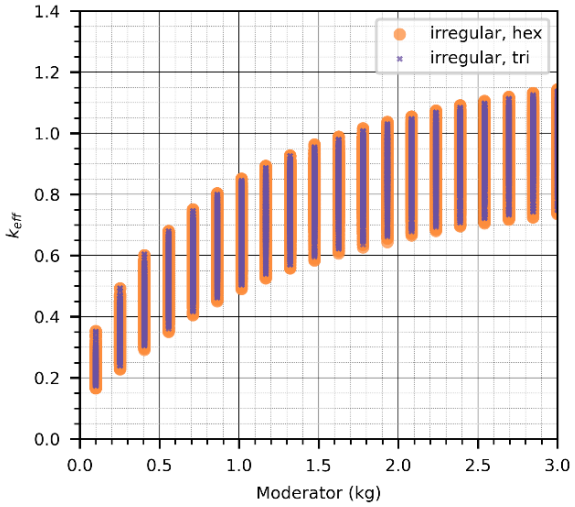

(a) Full range of variation

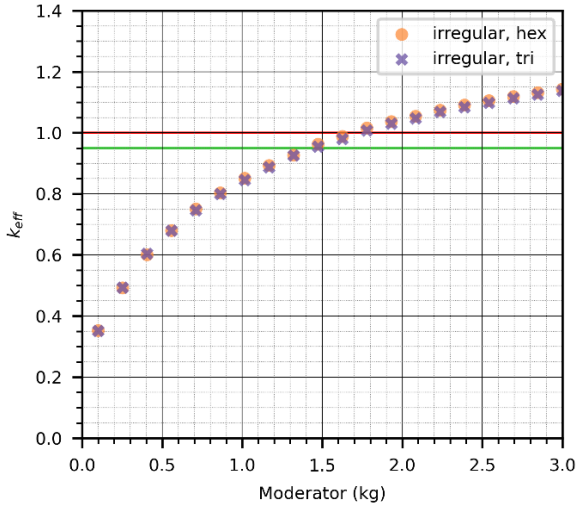

(b) Maximum values

Fig. 32. Reactivity of irregular compacted array emplaced in hexagonal configuration is similar to irregular compacted array emplaced in triangular configuration (data from Brickner et al.[24]).

For the situation with filler, the maximum moderator mass is 2.02 kg for a hexagonal array (§IV.D.1) and slightly increases to 2.08 kg for a triangular array (3% increase). Thus, the room reactivity is only slightly influenced by the (1) initial CCO configuration (hexagonal versus triangular); (2) slight changes in fissile area mass (3.15 kg $^{239}Pu/m^2$ for 153 CCOs initially in hexagonal array versus 3.57 kg $^{239}Pu/m^2$ for 168 CCOs initially in triangular array); and (3) boundary conditions to represent room segment of infinite extend down its axis (mirror boundary conditions

for hexagonal array versus periodic boundary conditions for triangular array).

VI.E. Reduced Reactivity when Brine Enters Room

Some brine may enter a disposal room with creep closure, but on average little brine is present in the undisturbed scenario. However, much brine may enter a disposal room after a hypothetical human intrusion. The presence of brine in Region 2 reduces the room k_{eff} by ~0.15 to the point that 3 kg of moderator per CCO is allowable, which is a factor of 1.8 increase from 1.69 kg (Fig. 33).

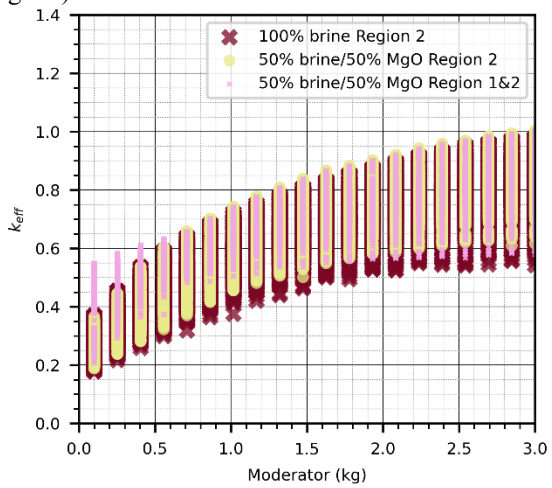

(a) Full range of variation

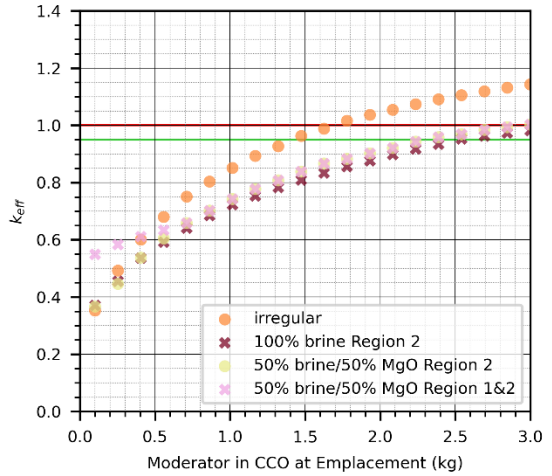

(b) Maximum values

Fig. 33. Presence of brine in Region 2 greatly reduces room reactivity filled with CCOs (data from Brickner et al.[24]).

Previous analysis with POCs also shows that the presence of brine greatly reduces the room reactivity.[11, Fig. 30;66] In contrast, however, brine present in fissile Region 1 (as could occur after extensive corrosion and brine inundation) does not reduce reactivity. In fact, the influx of brine provides some hydrogen and increases reactivity when the CCC has very low initial moderation at emplacement. This influence is somewhat artificial, however, since the hydrogen in the brine is not included in the summed moderator mass on the horizontal axis of Fig. 33).

VI.F. Reactivity Changes as Room Creeps Closed

Although more readily apparent for CCOs uniformly compacted, the reactivity of a room compacted into an irregular array also generally increases as a room creeps closed. That is, the maximum opportunity for criticality generally occurs at maximum room closure at 1000 years because spacing is so important to determining room reactivity (Fig. 34).

However, the reactivity can be driven by local conditions in the irregular array. Between a moderator mass of 1.3 kg and 1.5 kg in the CCC, the reactivity is slightly higher at 600, 800, and 900 years than at 1000 years. The maximum difference between k_{eff} at 1000 years and earlier times is 0.16%.

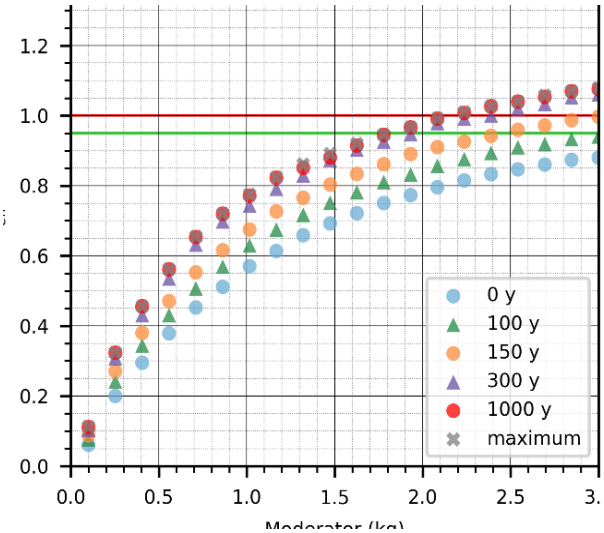

Fig. 34. General monotonic increase of reactivity as room creeps closed in upper repository horizon filled with CCOs that include stainless steel CCC reflector, 100% polyethylene moderator, and no filler or beryllium (data from Brickner et al.[24]).

VI.G. Correlation of CCO Concentration with Neutron Flux

As noted above in §V.C, room reactivity depends upon several parameters, but the individual spacing of fissile regions plays a primary role for a compacted room. The spatial distribution of the simple and relative weighted concentrations for CCOs initially placed in a hexagonal array in the lower and upper horizon show the largest simple and relative-weighted CCO concentrations are on either side of the room near the

collapsed room wall (between 10% and 40% of the distance to the room center) (e.g., Fig. 35).

A neutron flux evaluation considered fluxes in the irregular array with periodic boundary conditions at 1000 years with 585 g Be/BeO. The analysis determined the high flux regions for CCO arrays with/without stainless steel reflector and with/without 2 kg or 4 kg of graphite filler for polyethylene moderator mass of 1.016 kg, 1.168 kg, 1.231 kg, and 3.00 kg (12 cases overall).

For the lower horizon, the neutron flux is dominated by an area on the left side of a room, which correlates with the maximum simple (Fig. 35) and relative-weighted CCO concentration (Fig. 36). In all cases, the highest flux occurred at CCO 117 ({-2.315, 0.191, -5.406} with large star symbol), which overlays the maximum relative-weight flux.[24, App. M] The second highest fluxes were at either CCO 18 or 29 ({-2.160, 0.230, -5.425} or {-2.207, 0.056, -5.459, respectively, with ×`s}—Fig. 35 or Fig. 36).

In solving for the reactivity of the room, generally SCALE focuses on an area with the highest flux and ignores other areas of the room. Hence, the flux analysis also forced SCALE to focus on the right side of the room. In all but 3 cases, the maximum flux on the right side in the lower horizon was at CCO 94 (point {2.496, 0.154, -5.544} with large plus symbol).[24, App. M] Three other points (80, 73, and 74 in rank order are also shown ({1.855, -0.523,-5631}, {2.062, -0.607, -5.490}, and {2.048, -0.458,-5.628} with plus symbols).

In the upper horizon, the simple concentrations are fairly symmetrical on both sides of the room (more so than for the lower horizon—Fig. 35 versus Fig. 37); but, the relative-weighted concentration is asymmetrical with the maximum on the right side (Fig. 38). In all but two cases, however, the highest neutron flux occurred on the opposite left side of the room at CCO 34 ({-2.762, -0.384, -2.832} with large star symbol—Fig. 38).[24, App. M] The second and third highest values on the left were frequently at CCO 7 and CCO 8 ({-2.638, -0.283, -2.840} and {-2.825, -0.309, -3.038}, respectively, with ×`s).

The forced analysis on the right side of the upper horizon did not have a dominant flux area but CCO 96 was the most frequent area in the 12 cases ({2.800, 0.674, -2.882} at large plus symbol). Three other areas in relative rank order were at CCO 88, 82, and 79 ({2.929, 0.577, -2.872}, {2.706, -0.906, -2.781}, and {2.301, -0.374, -2.977}, respectively, with plus symbol). The later point coincides with the maximum relative-weighted concentration.

In summary, the simple concentration suggests general areas on the left and right sides of the room that may have high flux (e.g., general area with many magenta squares); however, the relative-weighted concentration identifies several specific areas on the left and right sides (e.g., red triangles) in these general areas that are more likely to have high flux (i.e., the relative-weighted concentration is better at differentiating high concentrations in the distribution tail, as suggested by Fig. 14 that correspond to high flux areas).

Although the maximum reactivity varied somewhat, the area of maximum flux usually did not change when (a) removing or adding filler, (b) removing or adding the CCC stainless steel reflector, and (c) changing the mass of polyethylene moderator because all CCOs were simultaneously changing. Consequently, the compacted spacing of CCOs plays a very important role in determining room reactivity, and reaffirms the decision to carefully develop representative, compacted CCO configurations with high-fidelity modeling.

.

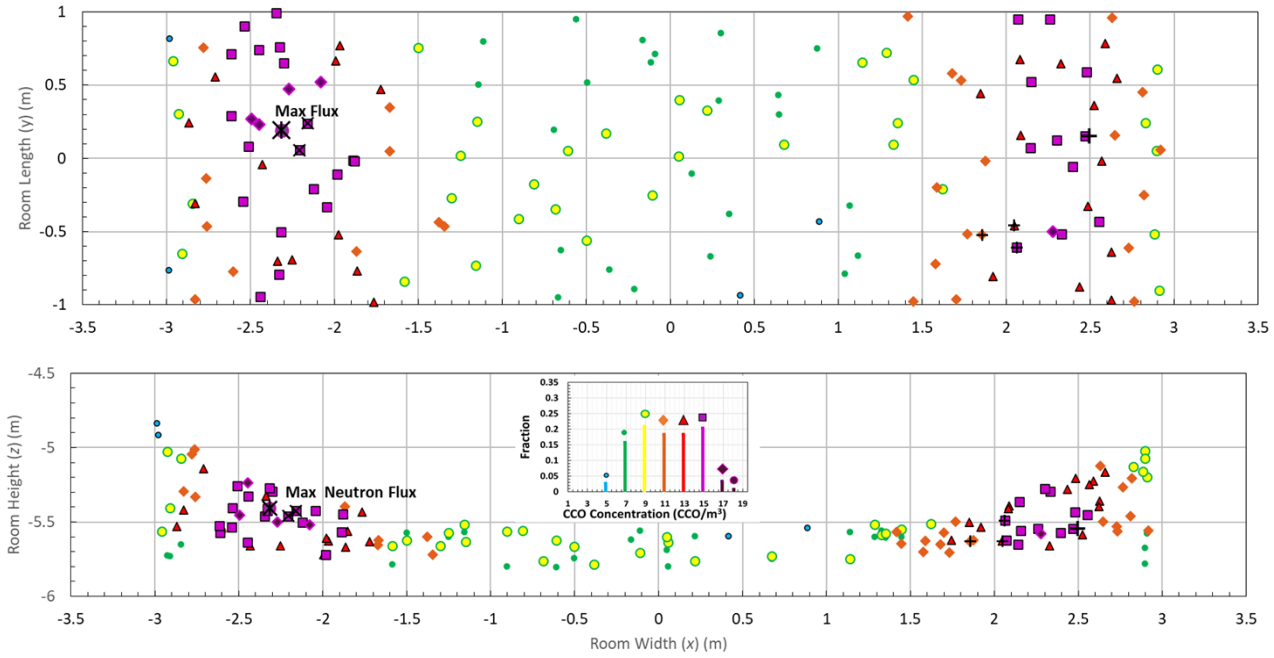

Fig. 35. Plan and side view of spatial distribution of simple concentration within 75-cm radius sphere at 1000 years for CCOs emplaced in a hexagonal array in lower repository horizon; maximum neutron flux overlays maximum simple concentration.

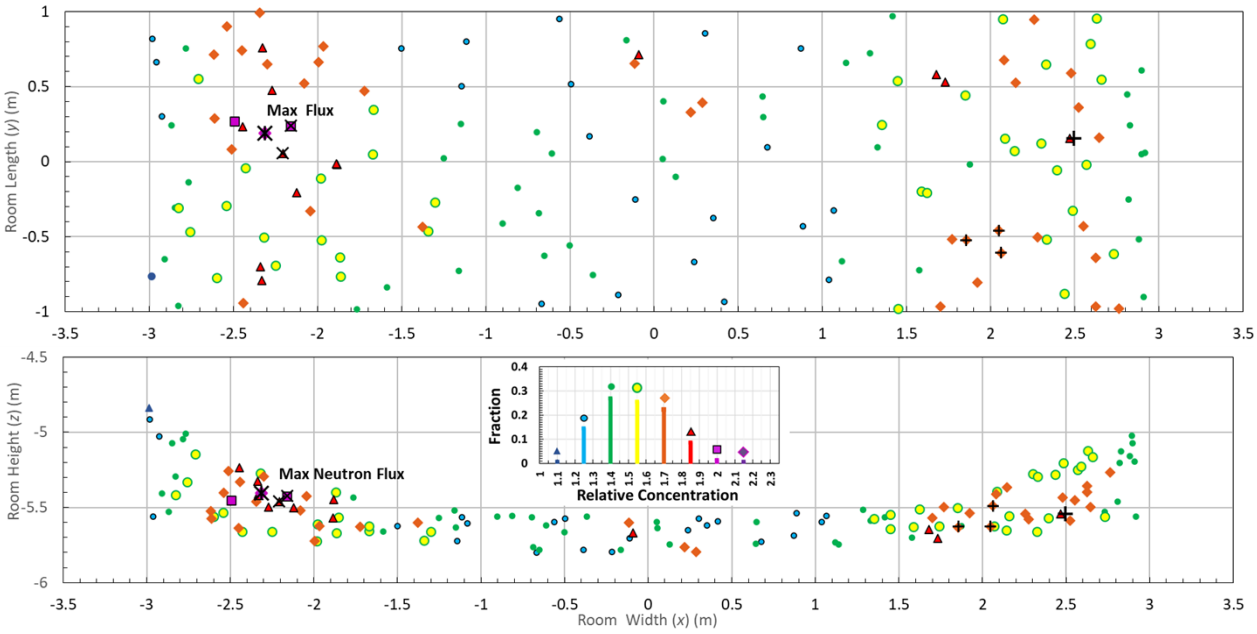

Fig. 36. Plan and side view of spatial distribution of relative weighted concentration at 1000 years for CCOs emplaced in a hexagonal array in lower repository horizon; maximum neutron flux overlays maximum relative weighted concentration.[65, Fig. 27]

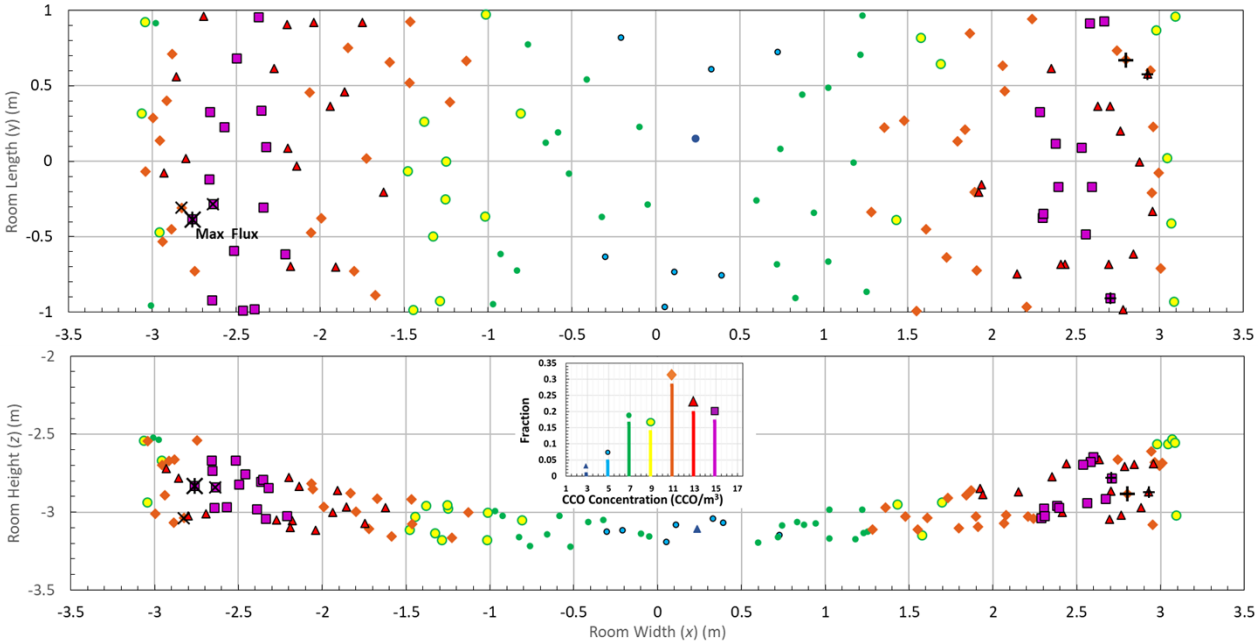

Fig. 37. Plan and side view of spatial distribution of simple concentration at 1000 years for CCOs emplaced in a hexagonal array in upper repository horizon; maximum neutron flux at edge of region with highest simple concentration.

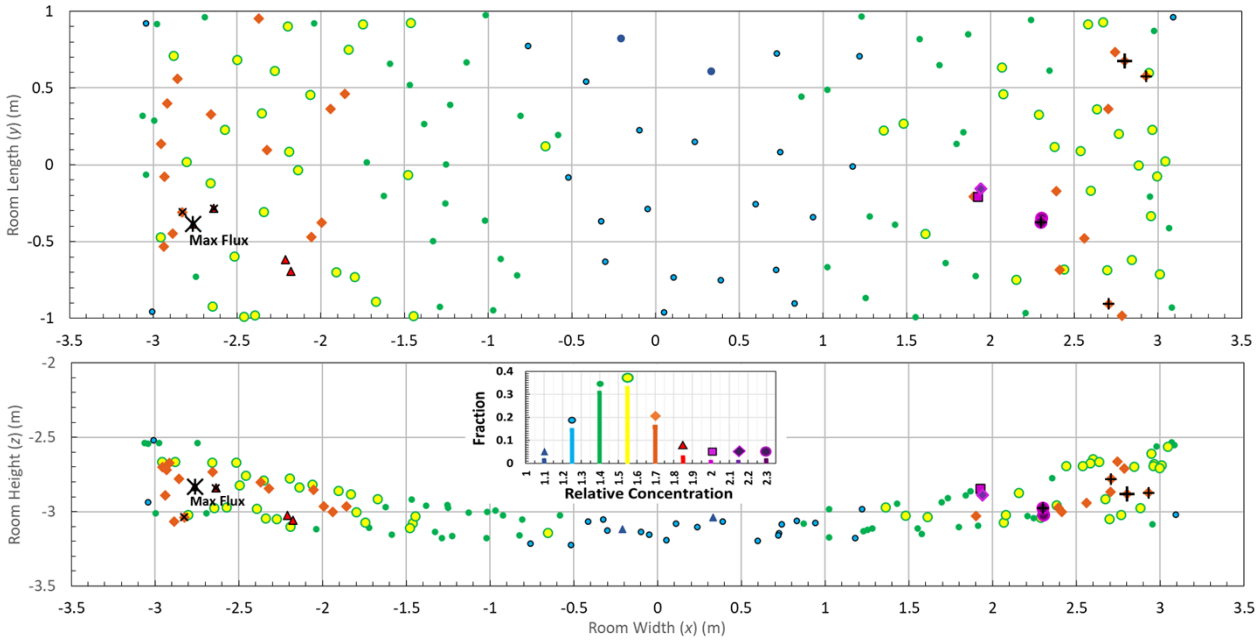

Fig. 38. Plan and side view of the spatial distribution of relative weighted concentration at 1000 years for CCOs emplaced in a hexagonal array in upper repository horizon; maximum neutron flux at edge of region with high relative weighted concentration.[65, Fig. 29]

VII. CRITICALITY EVALUATION OF COMPACTED ARRAYS WITH BORON CARBIDE

A criticality evaluation was also conducted to set the mass of boron carbide (B_4C) neutron poison necessary to prevent criticality if hydrogenous material is not limited. Other neutron poisons such as gadolinium, which forms insoluble compounds, would likely be acceptable but are not considered here.

VII.A. CCO Conceptual Model with B_4C

The criticality evaluation with B_4C uses the same irregular array compaction, based on the salt-creep calculation, but includes B_4C where natural boron is considered (19.9 wt. % ^{10}B and 80.1 wt. % ^{11}B).

VII.B. Results with B_4C

Between 10 g and 50 g of B_4C and up to 6 kg of polyethylene moderator was added to the fissile Region 1 in the criticality evaluation. Only 10 g of B_4C is necessary to stay below k_{eff} of unity if the moderator mass remains <3.9 kg (which is a factor of 2.3 above the 1.69 kg allowed without B_4C —Fig. 39).[24, App. M]

VII.C. Comparison with Previous B_4C Analysis

The initial criticality evaluation with B_4C in 2018, modeled a uniform array configuration rather than the irregular array configuration (Fig. 6).[62;67] Furthermore, an unrealistic, intact 63.5-cm layer of MgO was set above the CCOs rather than mixed in the reflector Region 2 (Fig. 17). However, the fissile Region 1 (Fig. 17) contained a cement filler of SiO_2, MgO, Al_2O_3 and H_2O rather than the more reactive carbon/graphite filler (3.5% more reactive—§V.D.1).

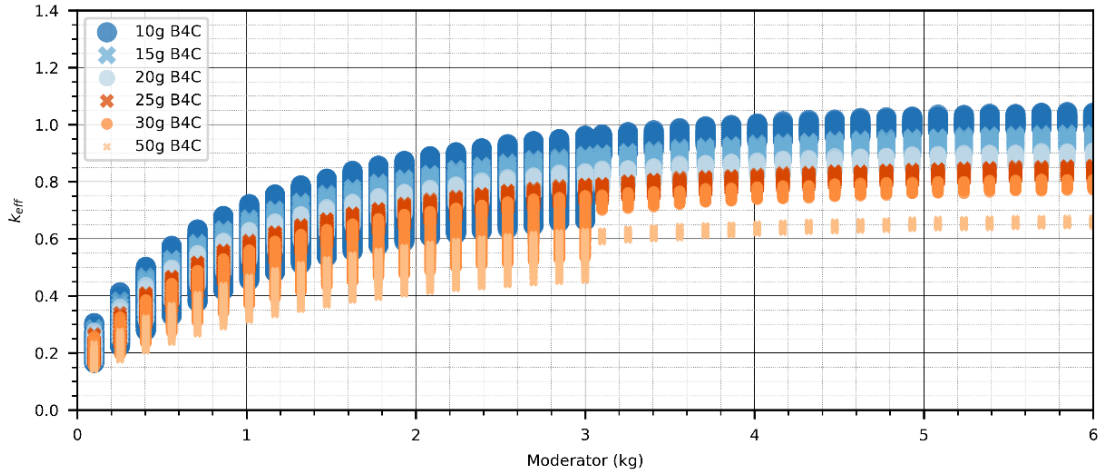

(a) Full range of variation

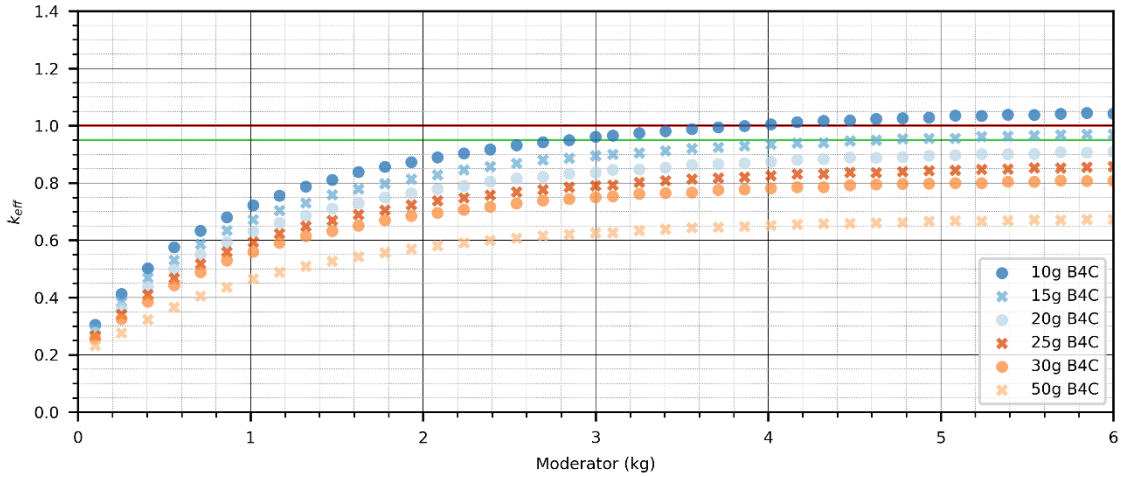

(b) Maximum values

Fig. 39. Reactivity of irregular array with between 10 g and 50 g B_4C and up to 6 kg moderator (data from Brickner et al. [24]).

VII.C. Longevity of B_4C in Disposal Room

For B_4C to remain effective as a neutron poison, it must remain in sufficient quantity in the CCO. The two feasible methods to deplete the B_4C, dissolution and consumption in radiation field, will not reasonably occur within the WIPP repository.

VII.C.1 Insolubility of B_4C

B_4C is the third hardest material after boron nitride and diamond; it has a high absorption cross section of neutrons, without forming radioactive isotopes; and it is insoluble in water and acids.[n] If brine dissolved Pu in degraded CCOs, the B_4C would be left behind as insoluble products of the CCO.[o]

VII.C.2. B_4C Consumption in Radiation Field

The minimal neutron flux from surplus Pu (which permits humans to be next to CCOs without shielding) is insufficient to deplete boron placed in the CCO over 10^4 years of isolation at WIPP, as demonstrated below.

Neutrons are potentially produced from three natural sources: (1) cosmic rays (i.e., protons, alpha particles, heavy element nuclei, and free electrons) colliding with atmospheric matter; (2) spontaneous fission of Pu and U radioisotopes; and (3) alpha particles produced from decay of Pu and U colliding with Be. Within the repository, only the latter two sources are feasible since cosmic rays cannot penetrate beyond the top 10 m of the surface. Furthermore, the latter two sources would normally only produce a small flux of neutrons.

For the demonstration, we make four very conservative assumptions: (1) all Pu isotopes decay; (2) abundant Be is present to produce neutrons from every Pu isotope decay (thus dominating over the neutrons produced by spontaneous fission); (3) the production of neutrons from all Pu isotopic activity is 10^7 neutrons/s-Ci, which bounds the neutron conversion for ^{238}Pu interacting with Be of 2×10^6 neutrons/s-Ci; and (4) every neutron produced is absorbed by ^{10}B.

The 10^7 neutrons/s-Ci is equivalent to 2.7×10^{-4} neutrons per decay from alpha particle (or 3700 ^{239}Pu atom decays per neutron since 3.7×10^{10} decays/s-Ci. If every produced neutron is absorbed by ^{10}B, then 3700 ^{239}Pu atom decays for every ^{10}B atom absorption. Converting from atoms to grams of ^{239}Pu and ^{10}B through the Avogadro constant yields 88 389 g ^{239}Pu/g ^{10}B. For a CCO containing 380 g ^{239}Pu, 0.0043 g of ^{10}B would be consumed. For 10-g B_4C placed in a CCO there are 7.8 g of B of which 19.75% is ^{10}B, or 1.53 g ^{10}B. Thus, only 0.28% of the 1.53 g ^{10}B is consumed even for exceedingly conservative assumptions (i.e., all Pu isotopes fully decay, and all neutrons produced from abundant Be are absorbed by ^{10}B.)

VIII. WIPP WASTE ACCEPTANCE CRITERIA

The representative geomechanical analysis of compaction of CCOs and the corresponding criticality evaluation of the irregular array are used to define three disposal options in the WIPP WAC[20] for CCOs with different waste forms (Table III).

VIII.A. Conservative Bias in Supplemental WAC Limits for CCOs

The supplemental WAC criteria do not relate to nuclear criticality safety when humans are present during transportation or WIPP facility operations. Rather, the supplemental WAC criteria ensure that the post-closure criticality after 300 or more years has low-probability and can be excluded from performance assessments for WIPP. Therefore, only an administrative margin of 0.05 is included here for USL to allow for (1) CCO configuration and geologic uncertainty, and (2) use of acceptable knowledge rather than measurements, to define contents and configuration of fissile material in CCO (e.g., configuration of reflective metals in CCO, such as a handling container). Furthermore, the $2\overline{\sigma}_{SCALE}$ offset for k_{eff} is omitted.

Hence, for the post-closure criticality results, a representative assembly of fissile material in a geologic setting is subcritical when the criticality index $k_{eff} \leq 0.95$ (Table III). Granted most post-closure criticality evaluations at WIPP sets the subcriticality limit at unity because the uncertainty in geologic processes dominates uncertainty. However, we do not want uncertainty in CCO contents, based on acceptable knowledge, to unwittingly dominate uncertainty when defining WAC limits.

VIII.B. Supplemental WAC Limits for CCOs

Based on a conservative bias for the criticality index $k_{eff} \leq 0.95$, the allowable moderator is (1) 2800 g per CCO when 10 g B_4C is included in Option A, (2) 1300 g per CCO without filler in Option B, and (3) 1500 g per CCO when the miscellaneous, non-hydrogenous filler mass is >2000 g per CCO in Option C (Fig. 20, Table II).[p] The filler mass is expressed as six times the amount of ^{239}Pu FGE (Table III) to facilitate spreading the filler between several inner convenience cans (i.e., internal

[n] https://m.chemicalbook.com/CASDataBase accessed 12/15/2021

[o] Similarly, boron and carbon in borated stainless steel does not go into solution as the stainless steel degrades but rather is left as separate chromium boride particles, with a composition of $(B,C)_6(Cr_2Fe)_{7.66}$.[95]

[p] Limits are reported in grams to match the specification used in the WIPP WAC.[20]

handling container) that contain a portion of the maximum 380 g of Pu in a CCC.

The general conditions of waste packaged in a CCO are as follows: First, waste shall adhere to criteria in Table 1 of WIPP WAC (e.g., ≤ 380 ^{239}Pu FGE and ≤ 1 wt. % Be/BeO). Second, optional B_4C shall be well mixed with the ^{239}Pu FGE and shall include placing ≥ 10-g B_4C in each convenience container in the CCC that contains ^{239}Pu FGE.[q]

Third, the mass of hydrogenous material in CCC shall include the mass of all organic material (e.g., mass of polyethylene plastic wrap) and the mass of water associated with all inorganic material (e.g., adsorbed moisture on zeolite, water of hydration in clay, or water in hydrated metal ion such as $CoCl_2{\cdot}6H_2O$). Fourth, optionally credited miscellaneous, non-hydrogenous filler shall be well mixed with ^{239}Pu FGE, which may be divided between any convenience containers inside the CCC in proportion to their ^{239}Pu FGE contents. The three option requirements are for an individual CCO; any combination of CCOs using different options may be placed in a room.

The only neutron poison considered in this analysis is B_4C; however, other neutron poisons, such as gadolinium that forms insoluble compounds, would likely be acceptable provided a technical justification is developed.

The requirement for well-mixed B_4C for Option A and well-mixed miscellaneous filler for Option C is not equivalent to requiring a homogeneous or uniform mixture. Rather, what is implied is that the B_4C or the credited miscellaneous filler have particle sizes relative to the fissile material such that (1) the B_4C or the miscellaneous filler may occupy interstitial spaces between the fissile material, and (2) separate regions of B_4C or credited miscellaneous filler do not form.[r]

The hydrogenous limits are based on 100% polyethylene (CH_2), which bounds most material potentially present in TRU waste (e.g., organic material and water associated with other contents).[88] This approach has been used for including the effects of compaction in other payload containers. Nonetheless, less stringent requirements are possible for most other hydrogenous material. For example, the allowable moderator mass substantially increases from 1600 g polyethylene moderator to 2500 g water moderator for each CCO in an irregular array, a 50% increase (§VI.A.1). However, establishing increased limits for specific moderator materials requires the CCO user provide justification for type of hydrogenous material present and the equivalence to CH_2.

Table III. Supplemental WIPP Waste Acceptance Criteria for CCO[1;20]

Option(1)	Boron Carbide (B_4C)(2) (g)	Hydrogenous Content(3) (g)	Miscellaneous Filler(4) (g)
A	≥10	≤2800	—
B	—	≤1300	—
C	—	≤1500	≥6×FGE

(1) Waste packaged in each CCO shall adhere to limits in Table 1 of WIPP Waste Acceptance Criteria in addition to limits specified under Options A, B, or C.

(2) The B_4C shall be well mixed with the ^{239}Pu fissile gram equivalent (FGE) and remain so during transportation, storage, and handling operations. The B_4C mass is based on the natural abundance of ^{10}B (i.e., 19.9 wt. % ^{10}B). The B_4C mass requirement shall apply to (a) each CCC that contains directly loaded TRU waste with ^{239}Pu FGE, or (b) any convenience containers used to load a CCC that contain ^{239}Pu FGE. For example, if a CCC is directly loaded with TRU waste containing ^{239}Pu FGE and also loaded with two cans containing ^{239}Pu FGE, the directly loaded TRU waste in the CCC and each can in the CCC shall include at least 10-g of well mixed B_4C.

(3) Mass of hydrogenous content shall include mass of any organic material (e.g., mass of plastic, cellulose, foam) and mass of water associated with any inorganic material (e.g., mass of adsorbed water on zeolite, water of hydration in concrete and clay, or water in hydrate such as hydrated metal ion).

(4) Only the non-hydrogenous portion of miscellaneous filler mass well mixed with ^{239}Pu FGE shall meet the miscellaneous filler mass requirement. The miscellaneous filler shall remain well mixed with ^{239}Pu FGE during transportation, storage, and handling operations. If several convenience containers are used to load a CCC, then each convenience container shall independently meet the miscellaneous filler criteria. For example, if a CCC is loaded with two convenience containers, where the first contains 100 ^{239}Pu FGE and the second contains 280 ^{239}Pu FGE, at least 600 g and 1680 g of miscellaneous filler shall be present within each respective convenience container.

VIII.C. Use of Acceptable Knowledge

Acceptable knowledge can be used to determine presence of B_4C, graphite/cement filler, and allowable hydrogenous material (primarily water and plastic) present in CCCs to determine compliance with Table III. Compliance with WAC limits for many TRU waste stream characteristics are established via acceptable

[q] A generator site could properly apportion 10-g B_4C between handling/convenience containers but ensuring well mixing of such small amounts of B_4C with ^{239}Pu FGE might not be able to rely upon acceptable knowledge. Thus, this approach is not considered here.

[r] The term well-mixed is as used for soils: a well-mixed soil has a distribution of particles sizes such that interstitial spaces are readily filled. In soils engineering, well mixing is specified to improve soil compaction density. Here, well mixing is specified to ensure adequate neutron interaction with the B_4C or miscellaneous filler.

knowledge, where the WAC defines acceptable knowledge as follows:[96]

> Acceptable knowledge –Any information about the process used to generate waste, material inputs to the process, and the time period during which the waste was generated, as well as data resulting from the analysis of waste, conducted prior to or separate from the waste certification process authorized by the EPA's Certification Decision, to show compliance with Condition 3 of the certification decision (Appendix A of this part) (40 CFR §194.2 and §194.67).

Option A in Table III (placing 10 g of B_4C in each CCC) may be useful for TRU waste that can be well mixed with B_4C and has high plastic and water content or contains hydroscopic salts that may theoretically increase water content. In the latter case, a technical evaluation of the water adsorbed by a hygroscopic material might be used to show that greater than 2800 g requires free water.

Option B assesses only the mass of hydrogenous material in a CCC (usually water and plastic), which may be useful for TRU waste that cannot be well mixed with B_4C (or miscellaneous filler material in Option C) and/or has existing limits on water and plastic content, such as planned surplus Pu disposal at WIPP.

For diluted surplus Pu from Savannah River Site, for example, acceptable knowledge based on procurement and process controls can demonstrate that the diluted surplus plutonium will meet Option B since the hydrogenous material is <700 g. First, the manufactured PuO_2 has an initial moisture content <10 g. Second, the adulterant used to dilute the PuO_2 is not hydroscopic, and the moisture content is easily bound by 240 g (~6% of total mass of diluted surplus Pu). Third, the plastic bagging used to limit contamination in the two handling convenience cans is <400 g.[62, App. A] Adherence to process controls (i.e., verification of packaging configuration) could be verified by routine radiography, if desired.

Option C assesses both the mass of non-hydrogenous, well-mixed filler and mass of hydrogenous material in a CCC. Option C may be useful for waste forms with defined amounts of miscellaneous filler that could benefit from the marginal increase in allowable moderator. Acceptable knowledge from process controls could also show that the diluted surplus Pu from Savannah River Site meets the requirements of Option C, if desired, since the adulterant filler is ~3480 g.[62, App. A]

IX. SUMMARY OF LOW-PROBABILITY OF CRITICALITY IN COMPACTED CCO

Room closure from salt creep beneficially encapsulated and isolates TRU waste as containers lose structural integrity; however, the change in container configuration influences the potential for criticality. Here, we present a qualitative low-probability rationale that room closure from roof fall and salt creep cannot sufficiently compact an array of emplaced CCOs containing up to 380 fissile gram equivalent ^{239}Pu to form a critical assembly provided (a) sufficient boron carbide (B_4C) neutron poison is well mixed with the fissile material, or (b) a constraint is placed on the mass of hydrogenous material present in CCOs (primarily water and plastics), which, in turn, depends upon the mass of non-hydrogenous filler well mixed with the fissile material (Table IV).

The criticality scenario has been screened out from consideration in performance assessments for WIPP compliance certification applications based on combining this finding with the rationale that (1) arrays of drums, boxes, and POCs are also insufficiently compacted within WIPP disposal rooms, and (2) hydrologic and geochemical conditions cannot sufficiently concentrate ^{239}Pu and ^{235}U elsewhere within the WIPP disposal system, as presented in companion reports.[11;12]

The rationale for the low probability of the disrupted CCO array depends upon constraints developed from (1) geomechanical phenomenological modeling of roof fall and salt creep, and (2) criticality modeling of neutron transport. High-fidelity, geomechanical modeling establishes a reasonable configuration of CCOs for subsequent criticality evaluation during two representative repository phases: (1) early large salt block fall onto CCOs, and (2) later gradual salt compaction of a room filled with CCOs. The rockfall and room closure models represent a segment in disposal Room 4 (middle of a panel of 7 rooms) halfway down the 91-m room axis where the ratio of horizontal to vertical compaction is likely the greatest.

IX.A. Roof Fall in Room Filled with CCOs

In simulations of roof-fall (§III), a rigid, trapezoidal, salt block detaches from the roof, similar in size and shape to the largest roof fall observed at WIPP that separated at a clay seam in the lower repository horizon. Whether the salt block suddenly detaches along the entire length or progressively detaches from the roof (to impart more rotation) the salt block bounces slightly and settles on top of an array of CCOs. CCOs are jostled but mostly return to the disposed configuration, without noticeably causing collapse or clustering.

Because of the bounding conditions selected, roof falls shortly after WIPP closure are not likely to cause extensive deformation, collapse, or clustering and, thereby, produce a critical assembly of CCOs prior to later room closure from salt creep.

IX.B. Compaction of CCOs from Salt Creep

In the geomechanical analysis, care is taken to demonstrate that the disrupted CCO array is reasonable and representative by examining the influence of four cases on the final configuration. The cases are based on the combination of two situations: the horizon of the room in the salt strata, and the initial configuration of the emplaced CCO array.

The room is modeled at both horizons of the bedded salt repository (designated simply as upper and lower horizons) to consider the influence of differing arrangements of geologic strata, particularly the interspersed clay seams where slippage occurs, which subtly influence room closure.

The salt compaction analysis also includes results where the CCOs start as a hexagonal array and where the CCOs start as a more compact triangular array. Although a room full of 7-packs of CCOs would initially be placed in a hexagon configuration, the 7-packs are held together with plastic wrapping that will allow CCOs to readily shift once the walls contact the emplaced containers.

To expand the pool of situations modeled, past geomechanical analyses are reevaluated using conditions consistent with the current analysis to examine room closure with different clay friction coefficients, CCOs with different strengths, and rooms filled with different containers (i.e., 6-inch and 12-inch POCs—§IV.E).[19;22;65;68]

Finally, several conservative assumptions are used that promote more compaction: (a) any gas pressure from cellulose degradation and metal corrosion that would normally arrest compaction is not included; (b) container elements are deleted from the analysis once they become severely distorted or the material fractured thereby reducing material volume in room (e.g., plywood quickly splintered and thus not much of the plywood elements remain at 1000 years); (c) plywood failure strength is reduced 80%; (d) the stainless steel CCCs are empty; thus, structural stiffening from TRU waste is omitted; and (e) MgO bags are omitted thereby reducing material volume in a room by ~5%.

Shortly after the room ceiling contacts the CCO drums (in the room center by ~40 years and along the entire length after ~60 years), the outer CCO shell crumples and the plywood spacers rapidly fail. By 100 years, the inner CCCs have begun to topple over, and by 200 years, most CCCs are on their side. By 300 years, most room closure has occurred. Yet, the room closure asymptotically approaches a maximum at 1000 years. The greater closure at the room center displaces much of the top tier of CCCs toward the room sides. The center is mostly a single layer, which consists primarily of the bottom tier of CCCs. CCCs are not clumped or bunched together down the axis of the room in the *y*-direction.

The CCO concentration measure of the container spacing shows that the geomechanical simulations produce a wide range in the distribution, but the concentration distributions remained similar both in terms of range and shape in the upper and lower horizon and when starting with either a triangular or hexagonal array. The concentration distributions also remain similar even when varying clay friction coefficients, CCO strength, and changing to 6-inch POC construction. Only the 12-inch POC, is noticeably different.

IX.C. Criticality Evaluation of Compacted Arrays without Boron Carbide

The coordinate positions of the CCC centers from the four geomechnical cases are used in two criticality evaluations: (1) criticality evaluation without boron carbide (B_4C) mixed with CCC contents (discussed here),[67] and (2) analysis with B_4C, (discussed below in §IX.D).[24] In both cases, the analysis examines the potential for criticality in CCOs with generic waste forms to avoid specifying a specific waste form.

Whether a fissile region (or assembly of fissile regions) is critical depends upon the generation and interaction of neutrons with matter within and outside the assembly, which for a finite heterogenous system, depends upon four general categories of parameters (1) type, mass, and form of fissile material (i.e., 380 g FGE ^{239}Pu as PuO_2); (2) material mixed with the fissile material and its overall concentration (e.g., special reflector Be/BeO, moderating hydrogenous material such as water and plastics, non-hydrogenous filler modeled as graphite, cement material, and stainless steel components); (3) nearby material and its concentration outside the fissile array (e.g., reflecting stainless steel, MgO, salt, and brine); and (4) shape of individual CCOs and array configuration of fissile regions and, thereby, neutron leakage (e.g., spherical and cylindrical fissile region, uniform CCO array, and four geomechanical simulation cases for irregular array—upper/lower horizon and hexagonal/triangular emplacement). In the criticality evaluation here, the parameters in the first category are fixed and parameters in the latter three categories are varied to determine relative importance.

IX.C.1. Allowable Hydrogenous Moderator with and without Filler in Fissile Region

The modeled system remains subcritical (i.e., k_{eff} ≤0.95—§VIII.B) when the allowable hydrogenous moderator in the CCO is ≤1.3 kg/CCO for the representative irregular, non-uniformly compacted array without B_4C (Table IV). Including ≥2 kg of a non-hydrogenous filler material in the fissile region reduces the reactivity of the CCO array, whether the filler material is conservatively modeled as graphite or represented as a cement mixture of SiO_2, MgO, and Al_2O_3.

IX.C.2. Other Material in Fissile Region

Based on varying other parameters, additional factors are not necessary to control to ensure improbability of post-closure criticality. As expected, using water as the sole moderator in the fissile region is much less reactive than polyethylene: k_{eff} is reduced by 0.125 and the allowable moderator mass increases by ~50% for the irregular, non-uniformly compacted CCOs (§VI.A.1).

The influence of excess MgO surrounding CCOs (which may act as a reflector) is small. The model includes ~3.7 times the amount of MgO that would be necessary in the room full of CCOs, yet the reactivity with 100% salt is only slightly less (k_{eff} decreases by 0.025) (§VI.A.2).

Finally, including 585-g beryllium (Be) or beryllium oxide (BeO) special reflector material in the fissile region (7% more than allowed in WIPP Waste Acceptance Criteria—WAC[20]) has little influence on reactivity (k_{eff} decreases by <0.01 near k_{eff} of unity) for irregular array (§VI.A.3).[24]

IX.C.3. CCC Stainless Steel Around Fissile Region

For the irregular array base case, a 0.71-cm discrete stainless-steel reflector is set around the fissile region, which is the thickness of the CCC (§VI.B). The stainless-steel reflector increases reactivity by reflecting neutrons back into the fissile region. The allowable moderator mass is 1.3 kg ($k_{eff} \leq 0.95$—§VIII.B). A 1.41-cm thick discrete stainless-steel reflector around the fissile region of the CCC, which is twice the thickness of the CCC, slightly increases k_{eff} by 0.03 near k_{eff} of unity. The corresponding allowable moderator mass decreases 5%.[24, App. O] If the stainless-steel reflector is removed, k_{eff} decreases by 0.05 and the allowable moderator mass increases 11%.

A reflective thickness twice the thickness of the 0.71-cm CCC considers the possibly of reflective metal inside the CCC. While the allowable moderator is reduced 5%, it is not excessive. Furthermore, modeling conservative compensate for this reduction. For example, a sphere with unconstrained diameter was used for the irregular array, which increases moderator mass ~5% over a more realistic sphere constrained by the CCC diameter (§V.D.4). Furthermore, the administrative margin on k_{eff} of 0.05 adds an additional ~12% margin.

IX.C.4 Uncertainty from Geologic Strata

The compacted configuration of CCOs in the upper repository horizon is slightly more reactive than in the lower repository horizon (§VI.C); Δk_{eff} is ~0.025 larger a k_{eff} near unity, which translates to an allowable moderator mass of 1.3 kg/CCO. In the less reactive lower horizon, the allowable moderator mass is 1.4 kg/ CCO (9% increase in allowable moderator mass for lower horizon).

IX.C.5. Minor Influence of Initial CCO Configuration and Boundary Conditions

The slightly wider range in closure and concentration of CCOs initially emplaced in a hexagonal array translates into a slightly wider range of reactivity than CCOs initially emplaced in a triangular array (§VI.D). In turn, the maximum allowable moderator mass is 1.69 kg per CCO for a hexagonal array with mirror boundary conditions and increases 3% to 1.74 kg for a triangular array with periodic boundary conditions. For the situation with filler, the maximum moderator mass is 2.02 kg per CCO for a hexagonal array and increases 3% to 2.08 kg for a triangular array with filler (§VI.D).

IX.C.6. Reduced Reactivity from Brine around Fissile Region

The introduction of brine around the fissile region reduces reactivity as occurred previously when analyzing the behavior of pipe overpack containers. The presence of brine about CCOs reduces the room k_{eff} by 0.15 to the point that 3 kg of moderator per CCO is allowable (§VI.E), which is about the same effect as adding 10 g B_4C.

IX.D. Criticality Evaluation of Compacted Arrays with Boron Carbide

A criticality evaluation of compacted CCOs containing B_4C neutron poison establishes that 10 g of B_4C mixed with the contents prevents criticality provided the moderator mass is 2.8 kg ($k_{eff} \leq 0.95$), as controlled by the WIPP WAC (§VIII.B). The criticality evaluation uses the previous assumptions and the same irregular array configuration, based on the salt-creep calculation, but includes B_4C where natural boron is considered (19.9 wt. % ^{10}B and 80.1 wt. % ^{11}B).

IX.E. Uniform Array Analysis Provides Additional Understanding

Criticality evaluation of a regular, uniformly compacted array is also conducted to more fully explain behavior observed in the irregular, non-uniformly compacted array. The supporting uniform analysis assumes that the CCO array remains intact (i.e., CCOs remain vertical and in three tiers); only the spacing between the CCC decreases. The uniform criticality evaluation uses a 25% and 50% reduction in a uniform horizontal spacing (§V.C.5). The latter value corresponds to early criticality evaluation using uniformly compacted CCO arrays.[62;67]

The reactivity of the uniformly array always bounds the reactivity of the irregular array, and in many cases

the trends observed in the uniformly compacted follows those of the irregular compacted array. For example, behavior for a bounding regular, uniformly compacted array follows the trend of the irregular, non-uniformly compacted array: (1) when water is the sole moderator the allowable moderator mass increases by 50% for the both the irregular and uniform array; (2) when influence of beryllium special reflector is small near k_{eff} of unity; and (3) when both a graphite and cement filler increase the maximum allowable moderator mass.

When differences in behavior occur between irregular and regular arrays, the differences in neutron leakage and reflection in the configuration explain the different behavior. Two specific examples are as follows.

First, adding 2-kg filler to the fissile region of the CCC for uniformly compacted array provides a large benefit (37% increase in allowable moderator mass), but only provides a modest benefit for the irregular compacted array (18% increase in allowable moderator mass). For the uniformly compacted array, the disk-like cylinders of the fissile region (which are most reactive) are stacked on top of each other to form essentially a single stub cylinder (with similar height to diameter ratio) that is very reactive with essentially the ^{239}Pu mass of three CCOs. The reactivity greatly decreases (leakage greatly increases) for the uniformly compacted array as the height of the cylinder is increased to include the graphite/cement filler. In contrast, the irregular non-uniformly compacted array with spheres (or cylinders) are scattered about the room and the reactivity does not change much (i.e., leakage in the system does not greatly increase) as the fissile region size increases to accommodate the filler.

Second, adding a discrete reflector in around the CCC, decreases the reactivity of a uniformly compacted array but increases the reactivity of the irregular compacted array. The stainless-steel CCC increases reactivity of the irregular array by reflecting neutrons back into the fissile region. Any isolation is fissile regions is less important because the fissile are spread out. The stainless-steel CCC also increases neutron reflection in the uniform array, but the increased isolation of the fissile regions provided by the stainless-steel CCC is more important, because the proximity of fissile regions in the uniformly compacted array promote neutron interactions.

Table IV. Rationale that rockfall and salt-creep compaction of CCO containers has low probability of causing criticality at WIPP.

Feature *Event* Process	Rationale that Roof Fall and Salt-Creep Compaction of Disposal Rooms Does Not Promote Criticality in CCO Array
Room/CCO *Undisturbed* Roof Fall	**Roof Fall Does Not Cause Clustering and Create a Critical Assembly** A large, rigid trapezoidal shaped salt block that either separates suddenly or progressively along the salt block length from the roof jostles the emplaced CCO array but does not cause collapse or clustering and, thereby, assemble a critical configuration prior to later closure of room from salt creep (§III).
Salt Creep	**Limiting Hydrogenous Material to ≤1.3 kg Sufficient to Prevent Criticality after Compaction** An irregular, non-uniformly compacted CCO array at 1000 years with 380 ^{239}Pu FGE as spheres of unconstrained diameter at center of CCO centerline mixed with ≤1.3 kg of water and plastics (as bounded by polyethylene and controlled by supplemental criteria in the WIPP Waste Acceptance Criteria) is subcritical ($k_{eff} \leq 0.95$—§VIII.B). 1. Room reactivity of the CCO array with hydrogenous material <1.3 kg is not strongly sensitive to (a) excess magnesium oxide (MgO) (§VI.A.2), or (b) presence of beryllium (Be or BeO) (§VI.A.3). A more reactive uniformly compacted array follows these trends. 2. Adding additional reflective material around the fissile region beyond the 0.71-cm thick CCC somewhat increases reactivity and decreases the moderator limit 5% but the assumed spherical fissile region with unconstrainted diameter (~5% effect) and administrative margin of 0.05 on k_{eff} (~11% effect) easily compensate (§VI.B). CCO concentration measure shows that geomechanical simulations in upper/lower horizon with hexagonal/triangular emplacement produce a wide range in CCO spacing, but the resulting concentration distributions remain similar. Consequently, the coordinate positions of CCOs in the irregular, non-uniformly compacted array reasonably represent conditions in the WIPP disposal room (§IV.E). Specifically, 3. Different arrangements of clay seams in geologic strata as represented in upper/lower horizon have only minor influence (§VI.C). 4. Initial CCO configuration only has minor influence (i.e., hexagonal versus triangular configuration, including mirror or periodic boundary conditions down room axis to represent room of infinite extend) (§VI.D). 5. Room reactivity generally increases monotonically as room creeps closed (§VI.F).
	Accounting for ≥ 2 kg Miscellaneous, Non-Hydrogenous Filler and Limiting Hydrogenous Material to ≤1.5 kg Sufficient to Prevent Criticality in CCOs after Salt-Creep Compaction Representative irregular, non-uniformly compacted array with ≥2 kg of miscellaneous, non-hydrogenous carbon or cement (SiO_2, MgO, and Al_2O_3) filler material and ≤1.5 kg polyethylene plastic mixed with 380 g of ^{239}Pu as spheres at center of CCO centerline in most reactive upper horizon is subcritical ($k_{eff} \leq 0.95$—§VIII.B). A more reactive bounding uniformly compacted array follows this trend: reactivity decreases when adding non-hydrogenous filler (§VI.A.1)
	10-g B_4C Sufficient to Prevent Criticality in CCOs after Salt-Creep Compaction when Moderator Mass Limited to ≤2.8 kg The k_{eff} is reduced by 0.18 when 10 g of B_4C is added to each CCO with 1.5 kg of moderator. Furthermore, the irregular, compacted array of CCOs remains subcritical if the moderator mass is limited to ≤2.8 kg ($k_{eff} \leq 0.95$—§VIII.B).
Human Intrusion Salt Creep	**Brine around CCOs reduces reactivity** Brine in the reflector region around CCOs reduces k_{eff} by 0.15 at 1.5 kg moderator and increases the allowable moderator mass to 2.5 kg (factor of 1.9 increase over 1.3 kg at $k_{eff} \leq 0.95$—§VI.E), which is about the same effect as adding 10 g B_4C.

REFERENCES

[1] R.P. Rechard, B.A. Day, B. Reedlunn, and J.E. Bean, Jr. 2022. Improbability of nuclear criticality in criticality control overpacks after salt creep compaction at Waste Isolation Pilot Plant, SAND2022-0952. Albuquerque, NM: Sandia National Laboratories.

[2] R.P. Rechard, L.C. Sanchez, H.R. Trellue, and C.T. Stockman. 2001. Unfavorable conditions for nuclear criticality following disposal of transuranic waste at the Waste Isolation Pilot Plant. *Nuclear Technology,* **136** (1) 99–129.

[3] R.P. Rechard. 2015. Probability and consequences of nuclear criticality at a geologic repository--I: conceptual overview for screening. *Nuclear Technology,* **190** (2) 97–126.

[4] DOE (US Department of Energy). 2016. Surplus plutonium disposition, record of decision. *Federal Register,* **81** (65) 19588–19594.

[5] R.P. Rechard. 2019. Improbability of transuranic waste compaction by salt creep causing criticality in bedded salt repository; Memorandum to Paul E. Shoemaker, 8880; Todd Zeitler, 8863; Ross Kirkes, 8883; November 2019, Albuquerque, NM: Sandia National Laboratories.

[6] DOE (US Department of Energy). 2019. Title 40 CFR Part 191 Compliance Recertification Application for the Waste Isolation Pilot Plant, DOE/WIPP-10-3609. Carlsbad, NM: Carlsbad Area Office, US Department of Energy.

[7] S. Brunell, J. Bethune, P. Docherty, D.C. Kicker, S. Kim, S. King, J. Long, and T.R. Zeitler. 2023. Summary report for the 2023 replacement panels planned change request performance assessment, ERMS 579729. Carlsbad, NM: Sandia National Laboratories.

[8] DOE (US Department of Energy). 2024. Notice of availability of final environmental impact statement for surplus plutonium disposition program. *Federal Register,* **89** (13) 3642–3644.

[9] DOE (US Department of Energy). 2024. Record of decision for the final Environmental Impact Statement for the Surplus Plutonium Disposition Program. *Federal Register,* **89** (77) 28763–28767.

[10] DOE (US Department of Energy). 1996. Final programmatic environmental impact statement, EIS-0229. Washington, DC: US Department of Energy.

[11] R.P. Rechard, B. Reedlunn, J.E. Bean, Jr., B.A. Day, and L.C. Sanchez. 2025. Improbability of post-closure criticality in array of transuranic waste containers after compaction by salt creep at Waste Isolation Pilot Plant, SAND2025. Albuquerque, NM: Sandia National Laboratories.

[12] R.P. Rechard, S. King, and P.V. Brady. 2025. Hydrologic and geochemical constraints on post-closure criticality in geologic media near Waste Isolation Pilot Plant, SAND2025. Albuquerque, NM: Sandia National Laboratories.

[13] R.P. Rechard. 2025. Low risk of post-closure criticality at Waste Isolation Pilot Plant SAND2025. Albuquerque, NM: Sandia National Laboratories.

[14] R.P. Rechard. 2025. Fissile mass and concentration necessary for post-closure criticality in geologic media near bedded salt repository Memorandum to Steve Wagner, 8880; ; Ross Kirkes, 8883; October 2025, ERMS. Albuquerque, NM: Sandia National Laboratories.

[15] R.P. Rechard, L.C. Sanchez, P.J. McDaniel, J. Hunt, and G. Broadous, Fissile mass and concentration criteria in geologic media near bedded salt repository presented at the International High-Level Radioactive Waste Management Conference, April 14-18, 2019, Knoxville, TN, 2019.

[16] AREVA. 2012. Criticality control overpack criticality analysis for TRUPACT-II and HalfPACT, 01937.01.M009-1, Revision O. AREVA Federal Services.

[17] NWP (Nuclear Waste Partnership). 2021. Nuclear criticality safety evaluation for contact-handled transuranic waste containers at the Waste Isolation Pilot Plant, WIPP-016, Revision 6. Carlsbad, NM: Nuclear Waste Partnership.

[18] B.A. Day. 2013. Calculation of CH and RH payload container waste volumes, PLD-CAL-0001, Rev. 1. Carlsbad, NM: Nuclear Waste Partnership.

[19] B. Reedlunn, J.E. Bean, Jr., J. Wilkes , and J. Bignell. 2023. Simulations of criticality control overpack container compaction at the Waste Isolation Pilot Plant, SAND2023-10477. Albuquerque, NM: Sandia National Laboratories.

[20] DOE (US Department of Energy). 2022. Transuranic waste acceptance criteria for the Waste Isolation Pilot Plant, DOE/WIPP-02-3122, Revision 11. Carlsbad, NM: US Department of Energy, Carlsbad Field Office.

[21] SNL (Sandia National Laboratories). 2018. Sierra/Solid Mechanics user's guide. 4.50, SAND2018-10673. Albuquerque, NM: Sandia National Laboratories.

[22] B. Reedlunn and J.E. Bean, Jr. 2019. Simulations of pipe overpack container compaction at the Waste Isolation Pilot Plant SAND2019-12111. Albuquerque, NM: Sandia National Laboratories.

[23] ORNL (Oak Ridge National Laboratory). 2018. SCALE Code System, ORNL/TM-2005/39, Version 6.2.3. Oak Ridge, TN: Oak Ridge National Laboratory. Most recent version available from Radiation Safety Information Computational Center as CCC-834.

[24] B.D. Brickner, R. Cumberland, and R. Reed. 2022. Post-closure nuclear criticality safety evaluations for disposition of criticality control overpacks at the Waste Isolation Pilot Plant, ORNL/TM-2021/2046. Oak Ridge, TN: Oak Ridge National Laboratory.

[25] Pub. L. 97-425. 1983. Nuclear Waste Policy Act of 1982, 96 Stat. 2201; 42 U.S.C. 10101 et seq.

[26] EPA (US Environmental Protection Agency). 1985. 40 CFR Part 191: Environmental standards for the management and disposal of spent nuclear fuel, high-

level and transuranic radioactive wastes: final rule. *Federal Register,* **50** (182) No. 182, 38066–38089.

[27] EPA (US Environmental Protection Agency). 1993. 40 CFR Part 191: Environmental radiation protection standards for the management and disposal of spent nuclear fuel, high-level and transuranic radioactive wastes, final rule. *Federal Register,* **58** (242) 66398–66416.

[28] R.P. Rechard. 2000. Historical background on performance assessment for the Waste Isolation Pilot Plant. *Reliability Engineering and System Safety,* **69** (1-3) 5–46.

[29] S. Kaplan and B.J. Garrick. 1981. On the quantitative definition of risk. *Risk Analysis,* **1** (1) 11–27.

[30] EPA (US Environmental Protection Agency). 1996. 40 CFR Part 194: Criteria for the certification and re-certification of the Waste Isolation Pilot Plant's compliance with the 40 CFR Part 191 disposal regulations; final rule. *Federal Register,* **61** (28) 5224–5245.

[31] EPA (US Environmental Protection Agency). 2005. 40 CFR Part 197: Public health and environmental radiation protection standards for Yucca Mountain, Nevada; proposed rule. *Federal Register,* **70** (161) 49014.

[32] EPA (US Environmental Protection Agency). 2008. 40 CFR Part 197: Public health and environmental radiation protection standards for Yucca Mountain, Nevada; final rule. *Federal Register,* **73** (200) 61256:61289.

[33] F.W. Bingham and G.E. Barr. 1979. Scenarios for the long-term release of radionuclides from a nuclear-waste repository in the Los Medanos region of New Mexico, SAND78-1730. Albuquerque, NM: Sandia National Laboratories.

[34] F.W. Bingham and G.E. Barr, Development of scenarios for the long-term release of radionuclides from the proposed Waste Isolation Pilot Plant in southeastern New Mexico, presented at the Scientific Basis for Nuclear Waste Management, Proceedings of the International Symposium, Boston, MA, November 27–30, 1979, 1980

[35] D.G. Brookins. 1978. Geochemical constraints on accumulation of actinide critical masses from stored nuclear waste in natural rock repositories, ONWI-17. Office of Nuclear Waste Isolation, Battelle Memorial Institute.

[36] Pub. L. 96-164. 1979. Department of Energy National Security and Military Applications of Nuclear Energy Authorization Act of 1980. (93 Stat. 1259).

[37] R.L. Hunter. 1989. Events and processes for constructing scenarios for the release of transuranic waste from the Waste Isolation Pilot Plant, Southeastern New Mexico, SAND89-2546. Albuquerque, NM: Sandia National Laboratories.

[38] D.A. Galson and P.N. Swift, Recent progress in scenario development for the WIPP, presented at the High-Level Radioactive Waste Management 1995. Proceedings of the Sixth Annual International Conference, Las Vegas, NV, April 30–May 5, 1995, 1995.

[39] D.A. Galson, P.N. Swift, D.R. Anderson, D.G. Bennett, M.B. Grawford, T.W. Hicks, and R.D. Wilmot. 2000. Scenario development for the Waste Isolation Pilot Plant compliance certification application. *Reliability Engineering and System Safety,* **69** (1-3) 129–149.

[40] R.P. Rechard, L.C. Sanchez, C.T. Stockman, and H.R. Trellue. 2000. Consideration of nuclear criticality when disposing of transuranic waste at the Waste Isolation Pilot Plant, SAND99-2898. Albuquerque, NM: Sandia National Laboratories.

[41] DOE (US Department of Energy). 2008. Yucca Mountain repository license application, safety analysis report, DOE/RW-0573, Rev. 1. Washington, DC: Office of Civilian Radioactive Waste Management, US Department of Energy.

[42] GAO (Government Accountability Office). 2019. Surplus plutonium disposition: NNSA's long-term plutonium oxide production plans are uncertain, GAO-20-166. Washington, DC: US Government Accountability Office. Accessed: accessed 25 February 2021. [Online]. Available: https://www.gao.gov/assets/710/702239.pdf

[43] DOE (US Department of Energy). 2014. Report of the plutonium disposition working group: analysis of surplus weapon-grade plutonium disposition options, Washington, DC: US Department of Energy. Accessed: February 24, 2021. [Online]. Available: http://fissilematerials.org/library/doe14a.pdf

[44] DOE (US Department of Energy). 2012. Draft surplus plutonium disposition supplemental environmental impact statement, DOE/EIS-0283-S2. Washington, DC: Office of Environmental Managment, US Department of Energy.

[45] DOE (US Department of Energy). 2015. Final surplus plutonium disposition supplemental environmental impact statement--Summary, EIS-0283-S2. Washington, DC: US Department of Energy. Accessed: 24 February 2021. [Online]. Available: https://www.energy.gov/sites/prod/files/2015/04/f22/EIS-0283-S2_SPD_Summary.pdf

[46] GAO (Government Accountability Office). 2017. Plutonium Disposition: Proposed dilute and dispose approach highlights need for more work at the Waste Isolation Pilot Plant, GAO-17-390. Washington, DC: US Govenment Accountability Office.

[47] R.D. Carter. 1973. Appendix N, criticality calculations. Nuclear reactivity evaluations of 216-Z-9 enclosed trench, ARH-2915. Atlantic Richfield Hanford Company.

[48] M.H. Lipner and J.M. Ravets. 1980. Nuclear criticality safety analyses for the Waste Isolation Pilot Plant project, WAES-TME-3025. Advance Energy Systems Division, Westinghouse Electric Corporation.

[49] W.A. Blyckert and R.D. Carter. 1980. Criticality parameters of 55-gallon waste drum arrays, RHO-SA-183; CONF 801107-58. Rockwell Hanford Operations, Rockwell International Corporation.

[50] W.R. Stratton. 1983. The myth of nuclear explosions at waste disposal sites, LA-9360. Los Alamos, NM: Los Alamos National Laboratory

[51] C.D. Bowman and F. Venneri. 1996. Underground supercriticality from plutonium and other fissile material. *Science and Global Security,* **5** (3) 279–302.

[52] G. Taubes. 1995. News & comment: Blowup at Yucca Mountain. *Science* **268** (5219) 1826–1839.

[53] W.E. Kastenberg, P.F. Peterson, J. Ahn, J. Burch, G. Casher, P.L. Chambré, E. Greenspan, D.R. Olander, J.L. Vujic, B. Bessinger, N.G.W. Cook, F.M. Doyle, and L.B. Hilbert. 1996. Considerations of autocatalytic criticality of fissile materials in geologic repositories. *Nuclear Technology* **115** (3) 298–310.

[54] R.A. Van Konynenburg. 1996. Comments on the draft paper 'Underground supercriticality from plutonium and other fissile material'. *Science and Global Security,* **5** (3) 303–322.

[55] W.L. Meyers, W.R. Stratton, R.H. Kimpland, R.G. Sanchez, and R.E. Anderson. 1996. The myth of an exploding excess nuclear material repository. *Transactions American Nuclear Society* **75** (214).

[56] G.H. Canavan, S.A. Colgate, O.P. Judd, G.H. McCall, A.G. Petschek, J.C. Solem, T.F. Stratton, W.R. Stratton, and P.P. Whalen. 1995. Comments on 'nuclear excursions' and 'criticality issues', LA-UR-95-0851. Los Alamos, NM: Los Alamos National Laboratory.

[57] R.P. Rechard, M.S. Tierney, L.C. Sanchez, and M.-A. Martell. 1997. Bounding estimates for critical events when directly disposing highly enriched spent nuclear fuel in unsaturated tuff. *Risk Analysis* **17** (1) 19–35.

[58] DOE (US Department of Energy). 1996. Title 40 CFR Part 191: Compliance certification application for the Waste Isolation Pilot Plant, DOE/CAO-1996-2184. Vol. I-XXI. Carlsbad, NM: DOE Carlsbad Area Office.

[59] R.P. Rechard and M.S. Tierney. 2005. Assignment of probability distributions for parameters in the 1996 performance assessment for the Waste Isolation Pilot Plant, Part 1: Description of process. *Reliability Engineering and System Safety* **88** (1) 1–32.

[60] B.Y. Park and F.D. Hansen. 2005. Determination of the porosity surfaces of the disposal room containing various waste inventories for WIPP PA, SAND2005-4236. Albuquerque, NM: Sandia National Laboratories

[61] NA/NRC (National Academies/National Research Council). 2020. Review of the Department of Energy's plans for disposal of surplus plutonium in the Waste Isolation Pilot Plant, Washington, DC: The National Academies Press.

[62] E.M. Saylor and J.M. Scaglione. 2018. Nuclear criticality safety assessment of potential plutonium disposition at the Waste Isolation Pilot Plant, ORNL/TM-2017/751/R1. Oak Ridge, TN: Oak Ridge National Laboratory.

[63] B. Reedlunn. 2018. Enhancements to the Munson-Dawson model for rock salt, SAND2018-12601. Albuquerque, NM: Sandia National Laboratories.

[64] B. Reedlunn, G. Moutsanidis, J. Baek, T.-H. Huang, J. Koester, E. Matteo, X. He, K. Taneja, H. Wei, Y. Bazilevs, J.-S. Chen, C. Mitchell, R. Lander, and T. Dewers. 2019. Initial simulations of empty room collapse and reconsolidation at the Waste Isolation Pilot Plant, SAND2019-15351. Albuquerque, NM: Sandia National Laboratories.

[65] B. Reedlunn and J.E. Bean, Jr. 2021. Additional simulations of criticality control overpack and pipe overpack container compaction at the Waste Isolation Pilot Plant SAND2021-11268 CTF. Albuquerque, NM: Sandia National Laboratories.

[66] B.D. Brickner. 2019. Post-closure nuclear criticality evaluations involving 6- and 12-inch pipe overpack TRU waste containers at the Waste Isolation Pilot Plant, ORNL/TM-2019/1222. Oak Ridge, TN: Oak Ridge National Laboratory.

[67] E.M. Saylor. 2020. Nuclear criticality safety assessment of criticality control containers without moderation control at Waste Isolation Pilot Plant, ORNL/TM-2020/1713. Oak Ridge, TN: Oak Ridge National Laboratory.

[68] B. Reedlunn and J.E. Bean, Jr. 2020. Further simulations of criticality control overpack container compaction at the Waste Isolation Pilot Plant, memorandum, SAND2020-5105 CTF. Albuquerque, NM: Sandia National Laboratories.

[69] Savannah River Nuclear Solutions. 2018. Surplus plutonium disposition program dilute and dispose approach: life cycle cost estimate summary report, SRNS-RP-2018-00570. Aiken, SC: Savannah River Nuclear Solutions.

[70] DOE (US Department of Energy). 2021. Supplement analysis for the Waste Isolation Pilot Plant Site-Wide Operations, DOE/EIS-0026-SA-12, Revision 0. Carlsbad, NM: US Department of Energy.

[71] AIB (Accident Investigation Board). 2014. Radiological release event at the Waste Isolation Pilot Plant on February 14, 2014, Phase 1, Washington, DC: Office of Envirnmental Management, US Department of Energy.

[72] Pub. L. 102-579. 1992. *Waste Isolation Pilot Plant Land Withdrawal Act*, 106 Stat. 4777.

[73] B. Reedlunn, J.G. Arguello, and F.D. Hansen. 2022. A reinvestigation into Munson's model for room closure in bedded rock salt. *International Journal of Rock Mechanics and Mining Sciences,* **151** 105007, doi: doi.org/10.1016/j.ijmms.2021.105007.

[74] B. Reedlunn and J.E. Bean, Jr. 2024. More simulations of criticality control overpack container compaction at the Waste Isolation Pilot Plant, SAND2024-07834CTF. Albuquerque, NM: Sandia National Laboratories

[75] NWP (Nuclear Waste Partnership). 2021. CH waste downloading and emplacement technical procedure, WP 05-WH1025, Rev. 30. Carlsbad, NM: Nuclear Waste Partnership.

[76] B. Reedlunn and J.E. Bean, Jr. 2020. Impact of properly specifying the Clay F and Clay G friction coefficients in disposal room closure simulations at the

Waste Isolation Pilot Plant. Memorandum, SAND2020-3537 CTF. Albuquerque, NM: Sandia National Laboratories.

[77] NRC (US Nuclear Regulatory Commission). 2020. Certificate of complicance for radioactive material packages, TRUPACT-II, Certificate 9218, Rev 25, Docket 71-9218. Washington, DC: US Nuclear Regulatory Commission.

[78] NRC (US Nuclear Regulatory Commission). Packaging and transporation of radioactive material. *Title 10 Code of Federal Regulations,* **Part 71**.

[79] ANSI (American National Standards Institute). 2014. An American national standard for nuclear criticality safety in operations with fissionable materials outside reactors, ANSI/ANS-8.1-2014. La Grange Park, IL: American National Standards Institute.

[80] J.J. Duderstadt and L.J. Hamilton, *Nuclear Ractor Analysis*. New York, NY: John Wiley & Sons, 1976.

[81] DOE (US Department of Energy). 2013. TRUPACT-II safety analysis report, Revision 23. Carlsbad, NM: Us Department of Energy, Carlsbad Field Office.

[82] NRC (US Nuclear Regulatory Commission). 2003. Yucca Mountain review plan, final report, NUREG-1804, REV 2. Washington, DC: Office of Nuclear Material Safety and Safeguards, US Nuclear Regulatory Commission.

[83] DOE (US Department of Energy). 2016. Waste Isolation Pilot Plant documented safety analysis, DOE/WIPP 07-3372. Carlsbad, NM: US Department of Energy, Carlsbad Field Office.

[84] G.D. Van Soest. 2022. Performance assessment inventory report - 2022, INV-PA-22, Revision 0. Carlsbad, NM: Los Alamos National Laboratory.

[85] G.D. Van Soest. 2018. Performance assessment inventory report - 2018, INV-PA-18, Revision 0. Carlsbad, NM: Los Alamos National Laboratory.

[86] DOE (US Department of Energy). 2022. CH-TRAMPAC, Revision 6. Carlsbad, NM: Carlsbad Field Office, US Department of Energy.

[87] J.K. Thompson. 1977. Minimum critical mass of plutonium-polyethylene system found to be significantly lower than plutonium-water system. *Nuclear Technology,* **33** (2) 235–236.

[88] G.W. Neeley, D.L. Newell, S.L. Larson, and R.J. Green. 2004. Reactivity effects of moderator and reflector materials on a finite plutonium system, SAIC-1322-001 Rev. 1. Science Applications International Corporation.

[89] R.P. Rechard, L.C. Sanchez, M. Olgvun, and G. Ryba. 2019. Fissile mass and concentration necessary for criticality in geologic media near bedded salt repository, Memorandum to Paul E. Shoemaker, 8880; Todd Zeitler, 8862; Ross Kirkes, 8883; November 2019, Albuquerque, NM: Sandia National Laboratory.

[90] H.C. Paxton, J.T. Thomas, D. Callihan, and E.B. Johnson. 1964. Critical dimensions of systems containing ^{235}U, ^{239}Pu and ^{233}U, TID-7028. Los Alamos National Laboratory; Oak Ridge National Laboratory.

[91] C. Vignes, J.E. Bean, Jr., and B. Reedlunn. 2023. Improved modeling of Waste Isolation Pilot Plant disposal room porosity, SAND2023-04826. Albuquerque, NM: Sandia National Laboratories.

[92] Y. Wang and L.H. Brush. 1996. Estimates of gas-generation parameters for the long-term WIPP performance assessment, memorandum to M.S. Tierney, January 26, 1996, ERMS 231943. Albuquerque, NM: Sandia National Laboratories.

[93] Y. Wang and L.H. Brush. 1996. Modify the stoichiometric factor y in the BRAGFLO to include the effect of MgO added to WIPP repository as a backfill, memorandum to M.S. Tierney, February 23, 1996, ERMS 232286. Albuquerque, NM: Sandia National Laboratories.

[94] J. Reyes. 2008. Letter to D.C. Moody (5 Enclosures). 11 February 2008., ERMS 549331. Washington, DC: US Environmental Protection Agency, Office of Radiation and Indoor Air.

[95] D.A. Moreno, B. Molina, C. Ranninger, F. Montero, and J. Izquierdo. 2004. Microstructural characterization and pitting corrosion behavior of UNS S30466 borated stainless steel. *Corrosion,* **60** (6) 573–583.

[96] DOE (US Department of Energy). 2018. Transuranic waste acceptance criteria for the Waste Isolation Pilot Plant, DOE/WIPP-02-3122, Rev. 9. Carlsbad, NM: Carlsbad Field Office, US Department of Energy.

DISTRIBUTION

E-mail—Internal

James E. Bean, Jr.	01554	jebean@sandia.gov
Benjamin Reedlunn	01558	breedlu@sandia.gov
Emily R. Stein	01864	ergiamb@sandia.gov
Joshua Rutkowski	06817	jerutko@sandia.gov
R. Chris Camphouse	08842	rccamph@sandia.gov
Heeho D. Park	08844	heepark@sandia.gov
Brad A. Day	08881	baday@sandia.gov
G. Ross Kirkes	08881	grkirke@sandia.gov
Technical Library	01977	sanddocs@sandia.gov

E-mail—External

Bret D. Brickner	bricknerbd@ornl.gov	Oak Ridge National Laboratory
Riley M. Cumberland	cumberlandrm@ornl.gov	Oak Ridge National Laboratory
Ron Livingston	ronald.livingston@srs.gov	Omega Technical Services



Sandia National Laboratories

Sandia National Laboratories is a multimission laboratory managed and operated by National Technology & Engineering Solutions of Sandia LLC, a wholly owned subsidiary of Honeywell International Inc. for the U.S. Department of Energy's National Nuclear Security Administration under contract DE-NA0003525.